

CR 73246

AVAILABLE TO THE PUBLIC

TRANSPIRATION COOLING SYSTEM DEVELOPMENT FOR REENTRY VEHICLES

D2-114181-1

Prepared by

C.L. Jaeck, R.T. Torgerson, and V. Deriugin

Space Division
THE BOEING COMPANY
Seattle, Washington

GPO PRICE \$ _____

CFSTI PRICE(S) \$ _____

July 1968

Hard copy (HC) _____

Microfiche (MF) _____

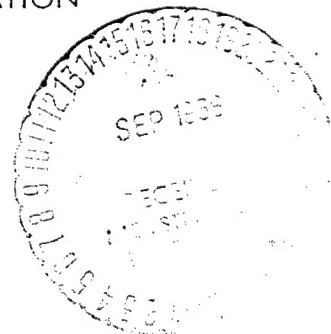
653 July 65

NATIONAL AERONAUTICS AND SPACE ADMINISTRATION
Ames Research Center
Moffett Field, California

NASA Contract No. NAS2-3443

FACILITY FORM 602

1	144	1
(PAGES)	(CODE)	
CR-73246	33	
(NASA CR OR TMX OR AD NUMBER)	(CATEGORY)	



DISTRIBUTION STATEMENT A
Approved for Public Release
Distribution Unlimited

DMC QUALITY INSPECTED 4

Reproduced From
Best Available Copy

20000712 064

TRANSPIRATION COOLING SYSTEM DEVELOPMENT FOR
REENTRY VEHICLES

D2-114181-1

Prepared by

C.L. Jaeck, R.T. Torgerson, and V. Deriugin

Space Division
THE BOEING COMPANY
Seattle, Washington

July 1968

NATIONAL AERONAUTICS AND SPACE ADMINISTRATION
Ames Research Center
Moffett Field, California

NASA Contract No. NAS2-3443

PRECEDING PAGE BLANK NOT FILMED

PREFACE

This report was prepared by the Space Division of the Aerospace Group of The Boeing Company, Seattle, Washington, under Contract NAS 2-3443 with NASA/Ames Research Center, Moffet Field, California. The NASA Contract Monitors were Mr. Pat Peterson and Mr. Nick S. Vojvodich.

Mr. Vladimir Deriugin was the Program Manager, Mr. Carl L. Jaeck was the principal investigator, and Mr. Ronald T. Torgerson was the materials and processes specialist.

ABSTRACT

This report describes the design, fabrication, and test of a transpiration system test panel module for reentry vehicles. The transpiration system was designed with the objectives of light weight, reusability, minimum refurbishment cost, and mission flexibility.

The module development program consisted of four phases; materials evaluation, component analysis and development, fabrication of hardware, and test of the module in a plasma facility.

This study demonstrated the feasibility of a transpiration system for reentry vehicles.

KEY WORDS

Transpiration system

Reentry vehicles

Material

Automatic control

CONTENTS

	<u>Page</u>
SUMMARY	1
INTRODUCTION	2
SYMBOLS	3
TRANSPIRATION SYSTEM DEVELOPMENT	4
Module Design Concepts	5
Materials Considerations	7
System Components	8
MODULE FABRICATION	8
Surface Screen	9
Sensor Installation	10
Thermocouple Installation	11
Module Assembly	11
Plasma Tunnel Module Holder Assembly	12
TRANSPIRATION SYSTEM TEST	12
Test of Inconel Module 1	13
Test of Inconel Module 2	15
Test of Columbium Module 1	16
SUMMARY OF PLASMA TEST RESULTS AND THEIR IMPACT ON TRANSPIRATION SYSTEM TEST PANEL DESIGN	17
CONCLUDING REMARKS	18
APPENDIX A---MATERIALS EVALUATION	21
APPENDIX B---MODULE AND COMPONENT ANALYSIS AND DEVELOPMENT	28
APPENDIX C---TEST FACILITIES	39
TABLES	41-49
FIGURES	50-136
REFERENCES	137

ILLUSTRATIONS

<u>Figure</u>		<u>Page</u>
1	Schematic of the transpiration cooling system	51
2	Transpiration system baseline design	52
3	Final module	54
4	Screen component	55
5	Detail of module attachment loops and support clips	56
6	Wire screen tile	57
7	Detail of forming and welding fixture for screen component	58
8	Forming and welding fixture for screen component	60
9	Columbium module 2 after disilicide coating showing coating fixture	61
10	Inconel module 3 with sensor, thermocouple, and Q-felt insulation installed	62
11	Chromel/Alumel thermocouple and ceramic sensor tube installed on screen for Inconel module 1	63
12	Silicone sponge installed in the backplate	64
13	Backplate for Inconel module 1	65
14	Backplate assembly for Inconel module 2	66
15	Attachment frame for module during plasma tests	67
16	Keeper pins	67
17	Inconel screen and holder frame mounted in copper holder	68
18	Inconel module 1 mounted in plasma test holder	70
19	Inconel module 1 in copper fixture subsequent to testing in the Boeing arc plasma facility	71
20	Close-up of Inconel module 1 in copper holder	72
21	Close-up of Inconel module 1 and frame showing gaps in insulation and damage to wire loops	73
22	Frame and keeper pins	74
23	Layup of Inconel module 1	75
24	Inconel module 1	76
25	Post test examination of Inconel module 1 components	77
26	Design changes to correct for coolant channeling	78
27	Inconel module 2 subsequent to testing in the Boeing arc plasma facility	79
28	Columbium module 1 subsequent to testing in the Boeing arc plasma facility	80
29	C-103 columbium wire screen with a thin disilicide coating	81
30	C-103 columbium wire screen with a thick disilicide coating	82
31	C-103 columbium wire screen with an optimized disilicide coating	83
32	Two-inch diameter flame test unit design I	84
33	Two-inch diameter flame test unit design II	85
34	Transpiration cooling module pressure drop without sensor or thermocouples	86
35	Transpiration cooling module pressure drop with ceramic sensor tube and thermocouples	87
36	Flame test unit with .025" dia. 20-mesh Inconel screen	88
37	Columbium flame test unit subsequent to 4 hours of flame testing for sensor and controller calibration	89

ILLUSTRATIONS (Continued)

<u>Figure</u>		<u>Page</u>
38	Calibration curve for iridium - 40% rhodium/iridium thermocouple	90
39	Properties of Inconel	91
40	Properties of columbium	92
41	Properties of aluminum oxide	93
42	Effective emissivity of .017" dia. 18-mesh Inconel screen	94
43	Data-theory comparison of the laminar blocking function ψ for the 2" dia. flame specimens	95
44	Examination of discrepancies in flame test data for coolant efficiency	96
45	Calculated coolant flow rates	97
46	Enthalpy of superheated steam	101
47	Percent reduction in flow rate by pulse width modulation of the solenoid valve	102
48	Valve characteristics - Skinner two-way B2 series	103
49	Platinum resistance thermometer calibration curve	104
50	Sensor installation I	108
51	Inconel flame test unit with sensor installation I subsequent to 9 hours of flame testing	109
52	Temperature history of the .017" dia. 18-mesh Inconel screen and sensor with zero coolant flow	110
53	Data-theory comparison of the temperature response of the wire and sensor near time zero and with zero coolant flow	111
54	Data-theory comparisons for the temperature-time derivative of .017" dia. 18-mesh Inconel screen	112
55	Temperature history of .017" dia. 18-mesh Inconel screen and sensor with coolant flow	113
56	Comparison of surface screen temperature measurements from a thermocouple and optical pyrometer	115
57	Calibration of sensor installation I in a flame test unit with .017" dia. 18-mesh Inconel screen	116
58	Controller	117
59	Control panel	118
60	Temperature history of .017" dia. 18-mesh Inconel screen as maintained by the automatic control system	120
61	Sensor and thermocouple installation	123
62	Temperature history of the .020" dia. 18 x 20-mesh disilicide coated columbium screen and sensor with zero coolant flow	124
63	Comparison of the temperature response of the wire and sensor near time zero and with zero coolant flow	125
64	The effective pcr for disilicide coated columbium screen	126
65	Calibration of sensor installed in a flame test unit with .020" dia. 18 x 20-mesh disilicide coated columbium screen	127
66	GN ₂ purge system	128
67	Temperature history of .025" dia. 20-mesh Inconel screen and platinum resistance thermometer to linear heating distribution	129

ILLUSTRATIONS (Concluded)

<u>Figure</u>		<u>Page</u>
68	The amount of coolant required to fully wet the dry module matrix	130
69	Flame test facility	131
70	Water storage tank, flowmeter, and manometer	133
71	Flame temperatures (#8 tip) with fixed $O_2-C_2H_2$ flow rates	134
72	Schematic of turbulent flow duct - Boeing arc plasma facility	135
73	Boeing plasma tunnel calibration for static pressure and heating rate	136

TABLES

<u>Table</u>		<u>Page</u>
1	Summary of test results for Inconel module 2 and columbium module 1	41
2	Evaluation of operation of transpiration system components	42
3	Disilicide coating development	43
4	Oxidation tests of disilicide coated C-103 columbium wire screen	45
5	Cold flow pressure drop tests of 2" dia. test unit I	47
6	Effective emissivity of screens tested during development program	48
7	Module numbers and sensor serial numbers	49

TRANSPIRATION COOLING SYSTEM
DEVELOPMENT FOR REENTRY VEHICLES

By

C. L. Jaeck, R. T. Torgerson, and V. Deriugin

SUMMARY

The baseline design of a transpiration cooling system generated under an earlier study phase of NASA Contract NAS 2-3443 has been applied to the development of a transpiration cooling panel module. This module is a basic building block for a larger (1' x 2') transpiration cooling test panel which was tentatively conceived as a minimum size test bed for the development of a transpiration cooling system for reentry vehicles. As a result of this study such a system has been found desirable and feasible for reentry vehicle application because of its apparent competitiveness in weight with ablation cooling systems with the added advantage of mission flexibility, reusability, and minimum refurbishment cost.

The development of a single 3" x 3" module has been proposed as the first step toward building the larger panel and is considered to be Phase I of the overall program. During Phase I, the system aspects, such as a closed loop automatic temperature-flow control system with a manual override, temperature sensing equipment, and module material components, were studied and checked out. These tasks were accomplished by testing 2" diameter transpiration specimens which contained a matrix of the same material used in the module, in an oxyacetylene flame.

Upon completion of this test series, five modules were fabricated, two of columbium and three of Inconel. All modules included a welded assembly of four supports and screen, insulation, pressure barrier, silicone sponge, backwall with water inlet and distribution tube as well as a temperature sensor. Besides the temperature sensor, the automatic temperature-flow control portion of the modules consisted of an off-on operated solenoid valve with pulse width modulation and an electronic controller with manual override. Also included, but not a part of the module, was an emergency, injection, or film cooling system with a series of holes drilled in the copper block of the module holder upstream of the module (similar to slot cooling).

Three of these single module assemblies were tested in the Boeing Plasma Facility to determine and study operational characteristics. Most of the module components showed good to excellent performance. However, such items as coolant distribution, surface deformation, and surface temperature variations and measurement require further improvement and development work. Therefore, only approximations of maximum local temperatures of the module screen surface could be made. The maximum local temperatures estimated on the Inconel module were up to the order of 2500 F where local screen melting occurred and of a similar order for the columbium module which exhibited no failures.

Analysis, flame tests, and tests of the module assemblies have indicated that the size of the module prevents it from being a true indicator of the transpiration system performance due to the presence of edge and size effects. This is especially true for arranging module insulation, locating instrumentation, and determining the cooling effectiveness of the module. Although good qualitative information was obtained, the conclusions drawn from the analysis and the tests were that quantitative performance data and more conclusive system information are required.

The work on Phase I has shown that with some refinement of the single module, the capability exists to proceed with Phase II of the transpiration cooling panel development program and that significant new design and performance information can be expected to result.

INTRODUCTION

Radiation and ablation cooled structures and heat shields have found use on various kinds of reentry vehicles and have been accepted as feasible and reliable thermal protection devices. For glide reentry of manned vehicles these techniques were applied to the Gemini and Mercury vehicles and most recently have undergone successful flight tests on the Apollo flights.

However, in the search for more efficient refurbishable design and performance of vehicles and vehicle systems, an effort was made to reevaluate the effectiveness of the various possible thermal protection systems and techniques and it was decided to look again into the feasibility and desirability of transpiration and/or injection cooling protection systems. The ensuing study as applied to the NASA M2-F2 vehicle resulted in a baseline design concept and showed that transpiration protection may be weight competitive with ablation systems and offers the additional advantages of multiple use and considerable reduction in refurbishment requirements. In order to substantiate and verify the conclusions derived from the design study and the analytical results it was suggested to design, build and test a prototype transpiration cooling test panel which would contain all ingredients and aspects of transpiration and yield design and performance data for the development of transpiration and/or injection cooling protection systems for reentry vehicles. Beyond providing improved vehicle mission flexibility, this is of particular importance for cases where the vehicle contour has to remain inviolate and/or where local heating conditions do not permit other cooling schemes.

Thus, the objective of the present contract was to make the first step in designing, building, and testing such a transpiration test panel. The approach adopted was to first build a 3" x 3" transpiration test panel module using a previously developed baseline design and modifying it where necessary to satisfy manufacturing and testing requirements.

This document reports on the work done under Phase I of the contracted task and provides the required background information for estimating the effort required on Phase II and for the final step of building and testing the full size transpiration cooling test panel.

SYMBOLS

A	Area
c	Specific heat of sensor or wire
$c_{60^{\circ}\text{F}}$	Specific heat of screen material at 60°F
c_{T_w}	Specific heat of screen material at temperature T_w
i	Enthalpy
l	Length of sensor
\dot{m}	Coolant mass flow rate per unit area
r	Radius of wire mesh
T	Temperature
T_w'	Controller setting
ΔT	Controller bandwidth or range
t	Time
\dot{q}_r	Radiation heat flux per unit area
\dot{q}	Convective heat flux per unit area with no coolant flow
ϵ	Emissivity
ϵ_p	Emissivity of total radiation pyrometer when used with a black body
σ	Stefan-Boltzmann constant
ρ	Density of wire or sensor material
ψ	Blocking function (defined by eq. B7)

Subscripts:

c	Coolant
cw	Cold Wall
bw	Backwall
hw	Hot Wall

which can be used both as a purging and cooling medium through the main solenoid valve as well as for emergency use through the emergency valve. Starting the cooling with gaseous nitrogen will prevent freezing of the coolant under space entry and under plasma jet testing conditions.

Design concepts, component and materials considerations, as well as aspects of module fabrication are briefly described in the following sections. A more detailed description of the analysis, testing, and development work conducted under the present contract is presented in the respective appendices.

Module Design Concepts

Several design concepts were investigated in reference 1. The result of that study was the development of a baseline design concept which would be applicable to manned space reentry vehicles and would be weight competitive with an ablation protection system with the additional advantage of reusability. The vehicle used for that study was the NASA developed M2-F2.

Baseline design.- The original baseline design concept is shown in schematic form in figure 2.

On the basis of the earlier study the most convenient basic building unit of the thermal protection blanket on the vehicle surface with compound curvature was found to be a 1' x 2' panel. This panel would consist of modules 3" x 3" in size. Each panel was composed of a structural and a control portion.

Structural portion.- The structural portion consisted of:

1. Modules with 3" x 3" disilicide coated .02 inch diameter 20-mesh C-103 columbium alloy screen at the surface.

The module screens or tiles could be divided into "support tiles" or tiles with support clips and "supported tiles" without clips. The tiles are mechanically joined together by keeper pins to form the surface of the panel.

The 3" x 3" size was selected to accommodate flexing of the support clips due to thermal growth and to minimize surface waviness.

Columbium C-103 alloy was selected as the screen material because it is weldable, ductile, and has good strength at temperature. The disilicide coating provides oxidation resistance with controlled emissivity.

2. An outer layer of 1/2" of heat stabilized Dyna-Quartz (Q-felt) insulation (located immediately behind the surface screen). This insulation has a use temperature limit of about 3000°F and provides a low resistance to coolant flow.
3. A layer of close-weave refrasil cloth under the outer layer of insulation to develop a pressure drop and a smooth coolant flow through the surface screen.

4. An inner layer of 1/4" of Q-felt insulation.
5. A compressed layer (1/4") of silicone sponge to keep the screen taut and to keep the insulation under compression.
6. An aluminum alloy tube backwall.

Control portion.- In addition, one module per panel was to contain a surface temperature sensor as shown in figure 2b. The proposed sensor was a platinum resistance thermometer, installed on a metal post or rod midway between front and back surfaces and insulated from the coolant. The surface temperature was to be inferred from the resistance readings. The signal generated would be fed into the controller, thus determining the coolant (water) flowrate. A controller would provide pulse width modulation of the valve, that is the width of the pulse in proportion to the temperature sensor output. Provision for using slot cooling for emergencies was to be included.

Performance.- The targeted performance of the baseline system was:

1. Ten fifteen minute cycles at heating rates up to $100 \text{ Btu/ft}^2 \text{ sec}.$
2. Heating rate transients to be between $3-5 \text{ Btu/ft}^2 \text{ sec}^2.$
3. A maximum surface temperature of $2700^\circ \text{F}.$

This original baseline design of the transpiration cooling protection system formed the basis and the starting point for the work on the program described in the present report.

Final design.- The final design of the transpiration system as shown schematically in figure 1 evolved from the baseline design which underwent considerable changes due to a variety of practical systems, design, materials, and fabrication considerations, not the least of which was that the system was to be checked out on a small scale module rather than the originally suggested large scale transpiration cooling test panel. Furthermore, it was decided due to economy and availability considerations, to build both Inconel and columbium screen modules and the respective frames for attachment in the Boeing plasma jet duct. The final design of the transpiration test panel modules is shown in figure 3.

The essential elements of each module are:

- 1a. A 3" x 3" disilicide coated .02 inch diameter 18 x 20 mesh C-103 columbium alloy screen at the surface for the columbium module.
- 1b. A 3" x 3" .025 inch diameter 20 mesh Inconel screen at the surface for the Inconel module.
2. A layer of 3/4 Dyna-Quartz (Q-felt) insulation with a special arrangement of pieces of heat stabilized and unstabilized Q-felt.
3. An outer layer of 1/4 inch compressed silicone sponge.

4. A layup of 3 layers of sailcloth as a pressure barrier.
5. An inner layer of 1/4 inch compressed silicone sponge.
6. A stainless steel backwall.

It is seen here that except for the screen component item (1a) which in itself had only minor design modifications, considerable changes had to be made in the approach to the structural portion which are explained largely by functional and by materials considerations.

The control portion used in the final design consists of a temperature sensor, an automatic controller, and a valve for coolant flow control as described in a later section on system components and in Appendix B.

Materials Considerations

One of the major problems to be investigated which is of particular importance for the structural portion of the system was the judicious application of the most suitable materials for the various components of the transpiration cooling panel. The most attractive feature for using refractory materials on the surface of a vehicle is their high temperature capability and therefore the capability for rejecting a considerable portion of the incoming heat flux by radiation. However, on the other hand, refractory metals are considerably more expensive and a lot more complicated to fabricate and to handle than heat resistant nickel-base alloys whose maximum temperature capability extends only to about 2000°F. Therefore, in the course of this program, two types of materials were used for the surface screen of the module. In the first case a heat resistant nickel-base alloy (Inconel) screen was used to develop the design, to evaluate component materials (except for the columbium parts), and to checkout the control loop. In the second case, in order to achieve and to check out maximum temperature capability, a disilicide coated columbium (C-103) wire screen was used for operation at temperatures up to 2500°F.

Although the initial target temperature fixed on the baseline design was 2700°F, in the course of the development of the best feasible coated columbium wire screen it was found that this temperature limit was too high to permit cycling and reusability and, therefore, it was dropped to 2500°F. Evaluation tests showed that with a particular coating the wire screen could withstand ten cycles at 2500°F in a furnace with air circulation, without significant coating failure. The details of the development program on screen materials are presented in Appendix A.

For the insulation a combination of heat stabilized and unstabilized Dyna-Quartz (Q-felt) was used in order to provide high temperature capability and good contact with the screen wire. In some cases slurry-type Q-felt insulation was applied to the wire screen in order to improve the contact between insulation and screen.

The pressure barrier selected was nylon sailcloth in three layers since no close weave refrasil or other high temperature cloth could be found with

the necessary permeability to permit maintaining a reasonable pressure drop across the pressure barrier.

Behind and in front of the pressure barrier are compressed layers of open-cell silicone sponge to maintain the insulation under some compression, and to permit uniform coolant distribution.

The backwall was made out of stainless steel plate in order to provide material compatibility with the plumbing attachments and strength because of test facility requirements. Weight considerations were considered of less importance on the small scale (module) approach than simplicity and cost effectiveness on this phase of the program.

System Components

In addition to the structural portion, there is a control portion vital to the successful operation of the transpiration system.

Thus, in order to effect proper control, a temperature sensor, an automatic controller, and a solenoid valve for coolant flow control are required. The analysis and the major considerations for the selection, evaluation, and operation of these components are presented in Appendix B.

Originally, as shown in figure 2, it was planned to use a wire post extending from the surface to the backwall and a platinum resistance thermometer for temperature control using a temperature level considerably lower than that of the screen, and a specially designed and built solenoid valve for flow control.

In the course of the present study neither the platinum band around the post nor a thermocouple attached to such a post were workable solutions due to poor thermal response, materials incompatibility and low output. Thus, the original concept had to be changed to using a high temperature platinum resistance thermometer at the screen surface in order to get the required thermal response level at the automatic controller. At the same time, it was found that it would not be necessary to design a special solenoid valve if a certain increase in dimensions and weight could be tolerated, thus permitting the use of off the shelf items.

The automatic controller which is electronically operated was built by Zeltex, Inc., of Concord, California. It provides pulse width modulation for the off-on operated solenoid valve and controls the amount of cooling fluid to the module by controlling the length of time the valve is kept open.

MODULE FABRICATION

Three Inconel and two columbium modules were fabricated in accordance with the design concept and configuration described in a previous section and in Appendices A and B. In order to facilitate plasma testing of a single 3" x 3" module, extensive modification of the baseline design for the backwall

and the fabrication of a module holder were required. The module assembly consisted of the following components:

1. Surface screen with integral attachment loops and welded support clips.
2. Q-felt insulation.
3. Nylon sailcloth pressure barrier.
4. Silicone sponge.
5. Coolant flow baffle.
6. Temperature sensor and ceramic tube.
7. Surface screen and backwall thermocouples.
8. Backwall assembly including pass throughs for sensor and thermocouple leads, coolant inlet and distribution tube, and support for the valve.

The module holder assembly for plasma testing of the modules consisted of the following components:

1. Module holder frame simulating adjacent modules.
2. Keeper pins for attaching surface screen to module frame.
3. Copper module holder for Boeing plasma test.

The fabrication and assembly of the transpiration cooling modules and the module holder assembly are described in the following paragraphs.

Surface Screen

The configuration of the surface screen for the module is shown in figures 4 and 5. The attachment loops are formed from straight wire extensions of the screen and the support clips are welded to these wires.

Screen tile.- To facilitate fabrication of the surface screen component a screen tile was designed with a 2.5" x 2.5" section of the screen with 1.5" of unwoven straight strands around the screen as shown in figure 6.

The Inconel screen tile was prepared by removing strands from 20 mesh 0.025" diameter wire woven screen. The columbium screen tile was woven to the figure 6 configuration using annealed C-103 columbium alloy wire purchased from the Wah Chang Albany Corporation, Albany, Oregon. The weaver experienced difficulties in weaving the .020" diameter columbium wire to 20 mesh square on the largest (48") available hand loom. Therefore, screen tiles 18 mesh by 20 mesh were accepted as the best effort of the weaver. In the event that larger quantities of screen tiles are required, the proper mesh screen and tile configuration can be obtained by weaving on an automatic loom.

Fabrication of screen.- The tooling fixture used for fabrication of the surface screen assembly is shown in figures 7 and 8. This fixture provides for forming of the attachment loops and welding of the wires to the support clips. The entire forming and welding operation can be performed without removal of the screen from the fixture until completed. Both the columbium and the Inconel surface screen components were fabricated using this fixture.

Resistance spot welding was used to join the Inconel screens to the support clips and no difficulties were encountered.

Several techniques for joining the columbium wire screen to the sheet metal support clips were investigated. Resistance welding of wire to sheet gave joints which exhibited good strength and ductility but, after the coating operation, the resistance welded joints showed loss in both strength and ductility due to penetration of the coating into the joint area. For this reason tungsten arc and electron beam welding techniques were investigated for making the columbium joints. A two-operation joining technique was finally developed which consisted of first resistance spot welding of the wire to the clip to hold the wire in place and then rewelding each wire by the electron beam process. Tests of wire to clip welds fabricated using this technique showed good strength and ductility after coating.

Coating of columbium screen assembly.- The columbium screen components were disilicide coated at 1950° F in the fluidized bed facility. Figure 9 shows the screen component in the coating fixture after completion of the coating operation. Some distortion of the screen components occurred during coating, however, these parts were judged usable. The screen for columbium module 1 was coated for 8 hours and a considerable amount of thermal cracking was evident. The screen for columbium module 2 was coated for 7 hours and only minor thermal cracks were observed with the thinner coating. The coating thicknesses as measured on control specimens were as follows:

Module No.	Columbium screen	Coating condition	Coating part growth per side (inches)	Nominal coating thickness (inches)
1	1	8 hours @ 1950° F	.0018	.0030
2	2	7 hours @ 1950° F	.0016	.0027

Sensor Installation

The sensor used in the modules was a platinum resistance thermometer device (RTD) consisting of a platinum wire sensing element mounted in a 0.175" x 0.175" x 0.085" aluminum oxide case. The sensor installations are described in Appendix B. Two types of sensor installations were used: Type I for Inconel module 1 and Type II for the remaining four modules.

Figure 10a is a photograph of the screen surface and figure 10b of the back side of Inconel module 3 showing the Type II sensor installation.

Thermocouple Installation

Chromel/Alumel thermocouples (T/C) with Inconel sheaths were used as the surface T/C for the Inconel test modules and as the backwall T/C for both the Inconel and columbium modules. In the case of the surface T/C for the Inconel module the sheath and insulation were stripped back 1/4" and the wires spot welded to the surface screen (see Appendix A). The sheath was attached to a support clip as shown in figure 11. The length of T/C parallel to the surface screen is designed to reduce conduction effects in the thermocouple wires as well as the channeling of the coolant along the T/C and lowering of the temperature at the hot junction.

The Chromel/Alumel thermocouples for the backwall temperature measurement were the grounded junction type. The thermocouples were sealed in the backwall with epoxy cement and protrude 1/8" into the lower sponge.

The Ir-40Rh/Ir thermocouple used for surface temperature measurement of the columbium module was bonded to the columbium screen with molybdenum disilicide cement as described in Appendix A. An alumina insulator was used to protect the T/C from the coolant and to enable a pass-through for the backwall. For columbium module 1, a two piece insulator was used and a 90° bend made in the wire to permit an installation similar to that for the Inconel module. The insulators at the bend were sealed with a phosphate bonded alumina cement. This design proved unsatisfactory during plasma testing because the coolant penetrated the porous cement and shorted out the T/C. For columbium test module 2, the T/C was run straight from the backwall to the screen. In both installations, the insulator was sealed in the backwall with epoxy cement.

Module Assembly

In addition to sensor and thermocouple installations, assembly of the test modules included installation of insulation, pressure barrier, sponge and backplate. The two types of assemblies used are illustrated in figure 23 for Inconel module 1 and figure 26 for the other four modules.

Insulation.- Stabilized and unstabilized Q-felt described in Appendix A were used for insulation. Inconel module 1 contained three layers of Q-felt parallel to the surface screen: a 1/16" layer of unstabilized Q-felt in contact with the screen followed by 1/2 and 1/4" layers of stabilized Q-felt.

For the remaining modules the parallel layer of unstabilized Q-felt was retained but the remaining insulation was in the form of alternate layers of stabilized and unstabilized Q-felt placed perpendicular to the surface screen. This type of insulation arrangement is shown in figure 10b. The development of this concept to reduce coolant channeling is described in a following section.

Pressure barrier.- Two layers of 1.25 oz nylon sailcloth were used as the pressure barrier on Inconel module 1 and three layers on the other four modules (see Appendix A). The sailcloth was sealed at the sensor tube and thermocouple pass-throughs using epoxy or silicone rubber cement.

Silicone sponge.- Open cell silicone sponge foamed to give approximately an 80% porosity was used for coolant distribution (see Appendix A). A layer of 1/4" was used between the backwall and the pressure barrier. A layer of 5/16" compressed to 1/4" was used between the pressure barrier and the Q-felt insulation. The intent of the compressed sponge is to keep the insulation forced against the surface screen. The silicone sponge was cut to size with a bandsaw after first freezing in liquid nitrogen. Installation of the lower layer of silicone sponge in the base plate is shown in figure 12.

Backplate.- The design of the backplate for Inconel module 1 is shown in figure 13. As a result of coolant channeling and assembly difficulties the backplate was redesigned for the remaining four modules. Figure 14 is a photograph of the redesigned backplate showing the coolant tube and pass throughs for the sensor and the two thermocouples. Installation of the first layer of silicone sponge is shown in figure 12. The backplate with the sponge, sailcloth pressure barrier, and coolant flow baffle installed is shown in figure 14.

Plasma Tunnel Module Holder Assembly

The fixture for holding the transpiration cooling modules during testing in the plasma tunnel consisted of a water cooled copper holder, a metal frame and keeper pins. A sketch of the module holder frame is shown in figure 15 and the keeper pins in figure 16. The function of the frame is to hold the module in the plasma arc test fixture under restraining conditions which simulate those of adjacent modules of multiple module panel assemblies. The keeper pin and wire loop arrangement was intended to allow for thermal expansion and contraction.

Figure 17 is a photograph showing an Inconel surface screen and frame installed in the copper holder. Only one Inconel frame and one columbium frame were fabricated since it was felt the frames would be reusable. However, spare sets of keeper pins were fabricated for both the Inconel and columbium modules in case of warpage or other damage to the pins.

The columbium frame was fabricated from C-103 columbium alloy and the wire loops welded by the two-operation resistance and electron beam welding technique developed for the columbium test module. The columbium frame and 0.040" diameter keeper pins were disilicide coated in the same coating run as columbium module screen No. 1. The distortion encountered with the surface screens caused an assembly problem which made it necessary to fabricate replacement keeper pins from smaller diameter (0.030") columbium wire.

The final installation of Inconel module 1 in the plasma test holder is shown in the photographs in figure 18.

TRANSPIRATION SYSTEM TEST

The complete module assembly was evaluated by a series of tests in the Boeing Duct Plasma Facility which is described in Appendix C. The modules,

when tested in the plasma facility, were mounted in the cavity of a water cooled copper plate (block) as shown in the previous section. The plate was inserted into the tunnel at the exit of the duct section to form the bottom surface of a channel. The upper surface of the module and copper plate was exposed to the plasma, while the back surface was protected and maintained at atmospheric pressure.

Three single module assemblies were tested, two containing Inconel screens and one with disilicide coated columbium screen. All modules were tested at a total enthalpy of 2475 Btu/lb_m and a cold wall heat flux of 30 Btu/ft²-sec. The test conditions were slowly varied so that the applied heating rate was increased over a period of several minutes during the start of each run and slowly decreased at the end of the run.

A thermocouple and a total radiation pyrometer were installed during all tests for measuring the surface temperature. The modules with Inconel screens contained a Chromel/Alumel front surface thermocouple, while the modules with disilicide coated columbium contained an Iridium 40% Rhodium/Iridium thermocouple. The backwall temperature was also monitored during all runs and measured by a Chromel/Alumel thermocouple.

No attempt was made to measure the mass flow of transpirant. This decision was based on the presence of edge effects discussed in Appendix B and the unsteady nature of automatic regulated coolant flow.

The tests of the second Inconel module and the columbium module were monitored visually using a mirror arrangement installed after the first Inconel module test. The objective of this installation was to permit visual observation of hot spots not indicated by the module instrumentation and to allow precautionary measures such as calling in manual override of the controller or auxiliary emergency injection cooling.

Test of Inconel Module 1

Test results and observations.- The first module tested contained an Inconel surface screen and sensor installation I. Three consecutive runs were made of 30, 15, and 15 minutes. The controller setting was varied during the first test to provide surface temperatures of 1500, 1700, and 1900°F. The surface temperature of the second and third runs was 1900°F. A controller bandwidth of 100°F was maintained during all runs.

Examination of the module after the third run revealed that the forward area of the surface screen was destroyed as is shown in figures 19 and 20. In addition, a few of the wire loops of the surrounding frame were destroyed, and the sides of the frame were buckled in toward the module as shown in figures 20, 21, and 22. Q-felt that was hand-rubbed into the areas between the loops was washed out. Joints between the screen component attachment legs and the Q-felt insulation were considerably enlarged as a result of coolant flow. This is shown in figure 21 by the black areas at the edges of the wire mesh (woven section).

Study of color motion pictures (16 mm) which were taken during 11 minutes of each run revealed the following two problem areas:

1. A hot spot developed in the region of the screen failure during the first run. This area of increased heating was believed to be due to the initial predeformation of the surface screen. The surface screen tends to deform due to the pressure of the sponge. This type of surface distortion tends to produce an increase in heating rate forward of the deformation peak, which in turn promotes further deformation and subsequent failure.
2. Problem (1) was made more severe by channeling of coolant along the forward wall and backwall of the copper block, and upward through the cracks between the module support clips and the Q-felt insulation shown in figure 23. Little or no coolant reached the sides of the attachment frame and center surface area of the module.

Although the module screen component was partially destroyed, the following encouraging items were noted:

1. The active control loop performed very well, as is indicated by the survival of the screen downstream of the sensor. Furthermore, the hot spot did not result in destruction of the entire surface, i.e., did not lead to catastrophic failure.
2. Gaseous nitrogen was used to purge the module (see Appendix B) during and following tunnel shutdown to prevent freezing of residual water in the module matrix. This system operation was excellent.
3. The injection ("slot") cooling system was activated at the end of the third run when the module surface was at 1900°F. The "slot" cooling was shown to be a successful emergency feature for a transpiration system.
4. Internal components of Q-felt, sailcloth, sponge, and backwall performed very well. The module assembly and breakdown are shown in figures 24 and 25.

Corrective measures.— The following changes were incorporated into the module design to correct the problems noted above:

1. The sensor was moved forward 1/2" into the region of increased heating and installation II was used.
2. The internal layup of the Q-felt insulation was changed as shown in figure 26. The insulation was placed in the module in vertical layers of heat stabilized (HS) and unstabilized (US) Q-felt to provide channels for coolant flow to the center of the module. At the surface a horizontal layer of Q-felt was used to provide good contact with the screen and aid in the spreading of the coolant. The addition of a metal (.010 stainless steel) coolant baffle further restricted the coolant flow to the center of the module. To allow some coolant flow to the frame and loops, horizontal holes were drilled in the vertical sides of the redesigned backplate. The raised attachment points (figures 13 and 25) on the backplate

were extended around the entire edge to simplify assembly. The horizontal holes were capped at one end with five layers of sailcloth to prevent an excessive flow of coolant.

3. The frame was taped to the copper block to prevent coolant flow through the gap between these two respective components.
4. The gaps between the loops and wire mesh were filled with a slurry of unstabilized Q-felt and Synar (colloidal silica) binder which was then flame cured.
5. The number of layers of sailcloth was increased from 2 layers to 3 layers. The coolant supply pressure in the storage tank was already minimized at 5 psig (19.7 psia) and therefore, the increased pressure drop across the sailcloth would aid in the distribution of coolant.

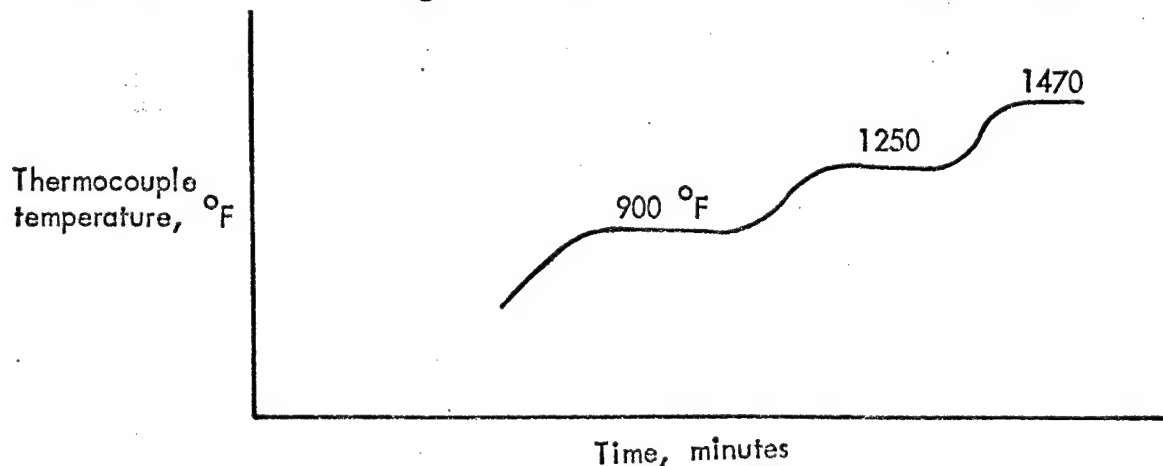
Cold flow test of this design revealed excessive coolant flow around the ceramic sensor tube, such that sensor operation could be impaired. To correct this situation an annular baffle plate and heat stabilized Q-felt were added to the modules.

A mirror set-up was installed in the Plasma Facility in order to permit visual observation.

Test of Inconel Module 2

Test results and observations.- A second module with an Inconel screen component and the design changes discussed above was tested during two 20 minute runs in the Plasma Facility. The controller was adjusted to provide a surface temperature of 1500°F and a bandwidth of 60°F.

During the early part of the first run the screen buckled upward. Visual observation showed the formation of hot spots and the screen was protected during the remainder of the run by using the slot cooling system. Following the run the module was manually deformed to nearly its initial shape. During the second run automatic operation of the controller was achieved. However, the surface temperature as indicated by the thermocouple continued to increase with the controller setting fixed as indicated below and in Table 1.



During the third transient the screen, which was not monitored visually at that time, failed forward of the sensor as shown by the photographs of figure 27. Post-test examination of the module and the viewing of color motion pictures revealed the following:

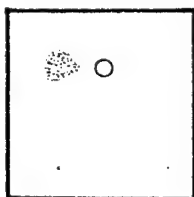
1. The Q-felt slurry and Synar binder performed very well, and was intact after the two runs. The slurry was easily removed after the test to allow removal of the keeper pins and module from the copper block.
2. The frame, wire loops, and keeper pins were not damaged during the test, even though there was insufficient coolant flow to these areas.
3. The ceramic cement holding the temperature sensor level with the surface of the screen broke, allowing the screen to move away from the sensor.
4. In general, the coolant distribution over the module surface was poor. The coolant flow was actually visible only in the downstream half of the module surface.

Test of Columbium Module 1

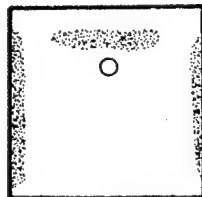
A module containing a disilicide coated columbium screen component and design changes discussed in an earlier section was tested in the Boeing Plasma Facility for four 20 minute runs. The Iridium 40% Rhodium/Iridium thermocouple failed during the first run. The backwall and total radiation pyrometer measurements for this series of test are summarized in Table 1. As shown in this table, the controller setting was increased during the test series. The performance and the temperature distribution over the module varied from test to test. The hot areas during each test are indicated below:

○ Sensor

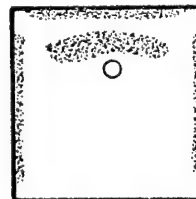
⊗ Hot areas



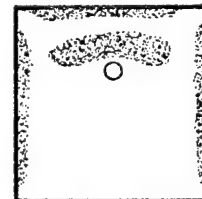
Run 1



Run 2



Run 3



Run 4

The coolant in general appeared around the sensor as liquid in the first and second test, and as steam during the last two tests. Again little coolant reached the wire loops and frame; however, these areas were undamaged. Post-test examination revealed no failures of the columbium parts. In the area of the sensor, and a few of the wire loops, the slurry washed away, as shown in figure 28. Also, the surface screen did undergo some thermal distortion during the test series as shown in figure 28b. This thermal distortion again caused the ceramic cement bond between the sensor and screen to break, and allowed the screen to move away from the sensor.

Visual monitoring of the module was maintained at all times and either controller override or "slot" cooling was called in when danger of overheating was observed.

SUMMARY OF PLASMA TEST RESULTS AND THEIR IMPACT ON TRANSPIRATION SYSTEM TEST PANEL DESIGN

The present program led to the realization of many important factors on the path of investigating the feasibility of developing a working transpiration system usable on reentry vehicles. The vehicle under immediate consideration in the original design of the transpiration system was the NASA/Ames developed M2-F2 vehicle.

In the course of the present study it was found that virtually every design feature adopted previously in the baseline design had to either be defined in more detail or reevaluated, and in most cases, underwent some sort of rearrangement or modification. The prevailing reasons were material choice or compatibility, functional and operational integrity, and fabricability.

The effectiveness of the system and its components also underwent considerable scrutiny such that a largely improved basis for the evaluation of the transpiration system for vehicle application was created.

On the basis of these findings, a better assessment of the feasibility, complexity, effectiveness, and reliability of transpiration systems can be made.

The major findings can be expressed as follows:

1. Failures in the module surface screen do not necessarily lead to system failure and may not be catastrophic. Under certain circumstances it is possible for the damaged screen to withstand repeated heating cycles without catastrophic disintegration.
2. Ways must be found to detect and to deal with hot spots.
3. Screen coating might still be improved with sufficient materials research thus improving the maximum screen temperature capability.
4. The observed module deformation is not necessarily indicative of the panel deformation because of the difference in attachments between adjacent modules which might be less restraining and thus alter the deformation problem. Also different weaving methods might influence the character of deformation.
5. Edge and corner effects on the module are more pronounced than on the larger size panel although some solution of the interface problem between transpiration surfaces and other adjacent structures will have to be provided. At any rate, on a larger scale panel, primarily the edge and corner modules will be influenced by peripheral effects whereas the internal modules can be expected to remain virtually unaffected.

6. Installation of thermocouples as system components for better definition of screen temperature should be given serious consideration.
7. The installation and design of the temperature sensor needs improvement in order to provide a more integrated attachment between sensor and screen and permit improved monitoring of the screen temperature.
8. Improved coolant distribution through the insulation by possible rearrangement and better channeling should be investigated.
9. Instead of using the original concept of utilizing the vehicle pressure wall for attaching the system it may be advisable to add a backwall to the panel for better system integrity and attachment although this would result in a weight increase.
10. Since miniaturization of valves was not attempted in this phase of the task this is an item which must be resolved before building the large scale panel. Although no insurmountable difficulties are foreseen, such valves must be developed and checked out.
11. Slurry-type Q-felt and Synar binder application to the surface screen has shown to be highly effective for better temperature distribution due to better contact with the insulation behind the screen.
12. Coating repairs using molybdenum disilicide were shown to be effective where cracking, spalling, or other coating damage occurred and had to be repaired before exposure to the high temperatures.
13. Injection (film) cooling proved to be highly effective as an emergency cooling feature.
14. Successful design and operation of a transpiration cooling system appears feasible; however, it requires further development work.
15. A summary of the evaluation of the performance of the transpiration system and its components developed under the present program is given in Table 2.

CONCLUDING REMARKS

1. Phase I of the program for developing a transpiration cooling system panel was very successful in supplying significant information for the evaluation of the feasibility and the operational characteristics of a transpiration cooling system applicable to glide reentry vehicles such as, e.g., the NASA/Ames developed M2-F2.
2. In general, the module and systems components checked under simulated reentry conditions showed good to excellent performance. However, some items such as coolant distribution, coolant effectiveness, structural distortion, hot spot formation, and high temperature measurement capability showed up as fair to poor and require further development work. It

was therefore concluded that the basis established in Phase I should be broadened to include solutions to the above problems in order to achieve consistent systems operation in high temperature environments.

3. The most encouraging items observed were the excellent controller and valve operation, the high effectiveness of the manual override, and the injection (slot) cooling system and the excellent automatic operation of the feedback controlled coolant loop. Very good results were observed where two-phase coolant operation occurred. Another important discovery was that a screen failure by itself does not necessarily lead to catastrophic protection system failure.
4. The analysis and the evaluation of the thermal behavior of the developed module and of the system have lead to the conclusion that edge, corner, and scale effects preclude valid direct comparison of the performance of the module with that of a full size system. Also the optimum location of temperature sensors or surface thermocouples (if required to minimize the danger from hot spots) can only be determined on a full scale model.
5. The problems of intermodular, structural interface, and backwall attachment techniques need investigation in order to build a full scale (1' x 2') panel and to permit convenient replacement of worn out or damaged modules.
6. It is therefore believed that Phase II dealing with the fabrication of a multimodule assembly should be initiated as the next step towards building a 1' x 2' transpiration cooling test panel. This phase will be devoted to the solution of the still unsolved problems. The work performed heretofore will provide the basis for design and system improvement. No insurmountable obstacles can be foreseen at the present time, and the program can be expected to be completed successfully.

PRECEDING PAGE BLANK NOT FILMED.

APPENDIX A

MATERIALS EVALUATION

Application of suitable materials for the various components is one of the major problems in development of the transpiration cooled panel. In order to establish performance capabilities of the selected materials, evaluation tests were conducted prior to fabrication of the modules. This section describes the evaluation studies of coated columbium screen, component materials by cold flow and flame tests and thermocouples for screen temperature measurement, which led to the selection of the final module materials.

Coated Columbium Screen Development

Screen.- C-103 columbium alloy (Cb-10Hf-1Ti) with an oxidation protective coating was selected for the surface screen material. The screen size selected was 20 mesh with 0.020" diameter wire. The screen actually used was 18 mesh by 20 mesh which represented the best efforts of the weaver. The satisfactory performance of coated C-103 alloy on conventional sheet metal components has been well established for service temperatures to 2700°F. However, the coating integrity of small diameter wire, faying surfaces at wire intersections, and complex wire to stiffener welded joints required further investigation to confirm the necessary oxidation protection capability.

Coating process.- The disilicide coating applied by the Boeing developed fluidized bed process was selected for oxidation protection of the columbium wire screen. The coating facility used was a 5" diameter fluidized bed reactor with a maximum temperature capability of 2100°F. The composition of the fluidized bed was 100% silicon powder and the fluidizing gas was argon with gaseous iodine added as the activator. Decomposition of silicon tetraiodide (SiI_4) at the surface of the metal part results in conversion of the metal surface layer to columbium disilicide (CbSi_2). The metal parts to be coated are attached to tantalum wire fixtures which are suspended in the fluidized bed.

The thickness of the coating is time, temperature, and activator concentration dependent. Normally, columbium alloys are coated to a thickness in the range 0.002 to 0.004". The part thickness grows by 0.001 to 0.0025" (1.0 to 2.5 mils) per side as a result of the coating formation. With the coating process conditions used for coating of the columbium screen, the wire diameter was increased from 0.020" to about 0.024".

Coating and oxidation tests.- Test specimens of columbium screen, 1.5 by 1.0" were disilicide coated to evaluate coating parameters and oxidation resistance. The initial tests of coated columbium screen revealed several problem areas:

1. Severe oxidation at wire intersections.
2. Excessive thermal cracking with the thicker coatings.
3. Warpage of screens during coating.

Table 3 summarizes the 11 coating runs conducted to develop techniques for coating of the screen components. The 6 hours at 2000°F coating conditions gave satisfactory coating thickness except at wire intersections. Figure 29 is a photomicrograph of a cross-section of the wire screen showing the thin coating at the wire intersections. Figure 29 shows a screen specimen after testing for one hour at 2500°F illustrating the failure initiation at the wire intersections.

Results of furnace oxidation tests of coated screen specimens are summarized in Table 4. Oxidation tests were conducted in an air furnace with flowing air passing over the specimen. Preliminary oxidation tests were conducted at 2500°F, 2600°F, and 2700°F for one-hour cycles. Severe oxidation resulted at 2700°F with all failures initiating at wire intersections and progressing over larger areas apparently due to flow of the molten oxide. At 2600°F the oxidation was much less severe and at 2500°F failures occurred usually after the second cycle and were localized at wire intersections. Control specimens of sheet material were oxidation tested at 2700°F with no failures.

Longer coating cycles at 2000°F were investigated for improvement in coating reliability at faying surfaces (wire intersections). Eight hours gave noticeable improvement over 6 hours, but 12 hours resulted in thermal cracking and spalling of the coating due to excessive coating thickness relative to the cross-sectional area of the wire. Thermal cracks caused by thick coatings are shown in figure 30a. Typical oxidation failures at thermal cracks are shown in figure 30b.

At this point, there appeared to be little hope of obtaining protection at 2700°F on columbium screen without a major coating development effort. It was therefore decided to lower the maximum surface temperature to 2500°F. In order to further define the oxidation behavior of coated columbium screen at this temperature, oxidation tests were conducted for ten 15 minute cycles at 2500°F. The screens were coated for 8 hours at 2000°F which represents the best coating conditions established to date. The oxidation test facility was a muffle furnace with a slowly moving air atmosphere. The test facility and techniques were the same as used in a recent USAF funded coating development program (reference 2). The coated screen specimens were removed after each cycle, cooled to room temperature, and examined at 40X magnification for evidence of coating failure. First evidence of failure was observed after the ninth cycle. There was only slight growth of these failures in the tenth cycle. It is believed that the minor failures observed would not have affected the performance of the part for 10 cycles at 2500°F in this test environment.

The appearance of a 2" diameter screen after oxidation testing for 10 cycles is shown in figure 31a. A typical minor oxidation failure can be seen in the photograph (figure 31b) of this screen taken at higher magnification.

As a result of these test results it was decided to proceed with the best coating conditions currently established and conduct further evaluation of coated screens with the transpiration cooling environment using the flame test units. Upon completion of these tests (discussed in a following section) the decision was made to coat the columbium test modules with a coating cycle of 8 hours at 1950°F which represented the best compromise between thermal cracking due to thick coatings and low coating integrity at wire intersections due to thin coatings.

Screen warpage.- Two-inch diameter screens for the flame test units were used to evaluate screen warpage during coating. Screens were coated in the following conditions: (1) mechanically flattened, (2) flattened and stress relieved, and (3) stress-relief flattened between flat plates. No measurable reduction in warpage during the coating process was achieved from preflattening by these methods. The screens, of course, cannot be flattened after coating due to the brittleness of the disilicide coating. However, the 2" diameter screen did not appear to be a good configuration for evaluation of warpage likely to be encountered during coating of the columbium modules. Therefore, it was decided to wait until coating of the module screen components to evaluate warpage and then try to minimize the problem by use of improved fixtures for holding the parts during the coating operation.

Component Materials Evaluation

A simplified transpiration cooling test unit was utilized in the preliminary stage of development of the transpiration cooled module. A 2" diameter flame test unit was designed to be used for both cold flow tests and flame tests with heating from an oxyacetylene torch. The 2" test unit was used to evaluate materials for components of the transpiration cooling system including the pressure barrier, insulation, surface screen and silicone sponge. Potential materials problems investigated were permeability requirements of pressure barrier, contact between Q-felt and surface screen, thickness and compressibility requirements of silicone sponge and performance capability of coated columbium screen. The flame test unit was also used to calibrate and prove out the temperature sensing and fluid control systems.

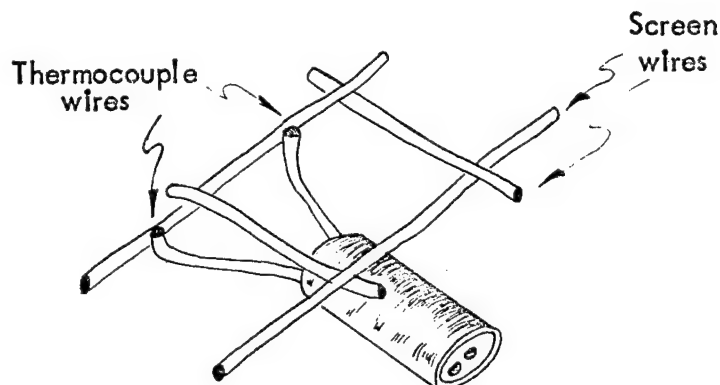
Flame test unit.- The initial test unit design, shown in figure 32, uses a 2" diameter screen and was assembled with Q-felt insulation, pressure barrier, silicone sponge, backwall, inlet tube, and thermocouples. Surface temperature measurements were made initially by optical pyrometer and later by three methods; surface thermocouple, radiation pyrometer, and optical pyrometer. The intention of the test unit design was to have all water channel through the refrasil cloth barrier and thereby simulate the conditions existing in the final module. Further considerations in the design were ease of assembly and disassembly, and cost. Three 2" diameter flame test units were fabricated from Inconel 600 nickel-base alloy. The less costly and easier-to-fabricate nickel-base alloy screens and shells were used for the initial test units. The Inconel units are capable of withstanding surface temperatures to 2000°F.

Initial cold flow and flame tests revealed the following problem areas; (1) the refrasil pressure barrier developed little or no pressure drop; (2) the

pressure barrier prevents the silicone sponge from applying a force on the Q-felt; (3) the Q-felt did not make intimate contact with the wires of the screen resulting in hot spots and buckling of the screen; and (4) the use of a thermocouple positioned under, normal, or parallel to the screen failed to give reliable surface screen temperature measurement.

For these reasons, the 2" diameter flame test unit was redesigned. The new design referred to as Flame Test Unit Design II is shown in figure 33. The following new features were included in the unit:

1. The surface screen is held between the retainer ring and the Q-felt. Holes were drilled in the retainer ring to allow coolant flow through the ring to prevent overheating of the ring.
2. A thin layer of unstabilized Q-felt which provides better contact of insulation with the screen.
3. The addition of a layer of silicone sponge above the pressure barrier to maintain the Q-felt against the screen.
4. The pressure barrier was moved into a lower temperature region and positioned between the two layers of silicone sponge.
5. The thermocouple wires were spot welded to the screen as shown below:



Three Inconel 2" test units were fabricated in accordance with the improved design. In addition three columbium screen and outer shell components were fabricated which could replace the Inconel parts on these units for surface temperatures to 2500°F.

The oxyacetylene torch test facility and the copper holder used for holding the flame test specimen and cooling the shells are described in Appendix C. The transpiration cooling test setup consisted of a water tank with pressure regulator and gages, flowmeters for measuring coolant flow, a mercury manometer for measuring pressure drop, and a needle valve for control of coolant flow. Distilled water was used for all transpiration cooling test

work to eliminate clogging of pressure barrier and insulation materials with water impurities.

Cold flow tests.- In order to find an acceptable pressure barrier, cold flow tests using the initial flame test unit design were conducted on a number of high and low temperature capability cloths. These tests results are summarized in Table 5. The pressure barrier which approaches the 2 psi (4" Hg) requirement is four layers of 0.75 oz per square yard nylon sailcloth. This material was selected for further evaluation. However, nylon has a maximum temperature capability of 400°F which made it necessary to redesign the flame test specimen to keep the temperature of the pressure barrier within the material capability.

Cold flow tests on the redesigned test units indicated that performance of the nylon pressure barrier which was changed to two layers of 1.25 oz sailcloth, silicone sponge, and Q-felt insulation was satisfactory. The substitution was made because the selected two layers showed the same pressure drop as the previously used four layers of lighter sailcloth. The silicone sponge was made from S-5370 RTV silastic foam base and catalyst manufactured by Dow Corning. The silastic was foamed to an open-cell sponge with a porosity of approximately 80%. The unstabilized Q-felt was "Dyna-Quartz" and the stabilized Q-felt was "Micro-Quartz" felt, both produced by Johns-Mansville.

Measurements made of pressure drop and mass flow rate of coolant water are presented in figure 34 for tests conducted without sensor or thermocouples installed. Included are data on units used for flame tests which are described in the following section. Figure 35 shows pressure drop data for flame test units with ceramic sensor tube and thermocouple installed.

Flame tests of Inconel units.- Preliminary flame tests with the initial test unit design revealed problems with screen buckling and unreliable surface screen temperature measurement which resulted in changes to the test unit design as previously discussed. All subsequent tests as described below were performed with a redesigned test unit.

Transpiration cooling tests were conducted using 18 mesh 0.017" diameter wire Inconel screen and operating with a nominal surface temperature of 2000°F. The heat flux was in the range of 30 to 50 Btu/ft²-sec. Temperature measurements were made with Chromel/Alumel thermocouples spot welded to the screen and an optical pyrometer. Good correlation was obtained between the two sensing devices at surface temperatures to 2100°F.

In addition to bare wire screens, tests were conducted on screens with unstabilized Q-felt pressed between the mesh and with the mesh filled with a slurry of Q-felt and binder. The screen containing the wet slurry was dried with a torch prior to flame testing. Screens filled with Q-felt performed more effectively than the plain screens and enabled higher heat fluxes and lower coolant flow. Although less pronounced for the screens with Q-felt, all screens bulged outward due to thermal expansion. This resulted in a hot spot at the center of the screen and greatly decreased cooling efficiency. It was believed that this is characteristic of the localized uneven heating encountered with flame testing.

The Q-felt insulation, sailcloth pressure barrier, and silicone sponge components were reused repeatedly for flame test cycles of 15 minutes minimum duration. Performance of these components was satisfactory for a total of 13 flame test cycles. The Inconel screens generally were replaced after three cycles due to the bulging of the screen which reduced effective cooling due to the gap between the insulation and the screen. Performance of the Q-felt filled Inconel screens was superior to plain screens although eventual bulging occurred with extended operation at temperatures near 2000°F.

In view of the thermal deformation problem with the 18 mesh 0.017" Inconel wire screen, it was decided to proceed with the development of the transpiration cooling modules with 20 mesh, 0.025" diameter Inconel wire screen. The heavier screen significantly reduced the thermal distortion and this type screen was used in fabrication of the Inconel modules. A flame unit containing the larger diameter wire is shown in figure 36.

Flame tests of columbium units.— Transpiration cooling tests were conducted with the disilicide coated columbium test units for cycles of 15 minutes each at a surface temperature of 2500°F. The oxyacetylene torch was adjusted for a slightly oxidizing flame. The surface flux was 40 to 72 Btu/ft² sec. Temperature measurement was made with an optical pyrometer with correction for a coated columbium surface emittance of 0.8.

Performance of the columbium screen was satisfactory with no buckling or bulging away from the insulation as encountered with the Inconel screen. The superior performance of coated columbium screen is attributed to the better strength and thermal properties of columbium compared to the Inconel at their respective maximum test temperatures.

Examination of the columbium screen after 5 cycles at 2500°F revealed no oxidation failures. Some sticking of the unstabilized Q-felt to the back of the screen was observed and microscopic examination revealed some fusion of the Q-felt in contact with the screen and a localized glossy layer on the coated wire. No apparent detrimental effect on screen performance resulted from these reactions. The sailcloth pressure barrier, stabilized Q-felt insulation, silicone sponge, and columbium outer shell performed satisfactorily, and examination after assembly revealed no detrimental effects on these components.

Further flame tests of columbium test units in connection with controller and sensor development (see Appendix B) have compiled sufficient test data to demonstrate successful performance of screen, insulation, pressure barrier, and sponge for 10 transpiration cooling cycles of 15 minutes at 2500°F in the oxyacetylene torch facility. A columbium test unit is shown in figure 37 which was used for 4 hours of flame testing for sensor and controller checkout.

Thermocouple Investigation

Chromel/Alumel thermocouples were used for measuring the surface temperature of Inconel screens and performed satisfactorily. However, Chromel/Alumel are not compatible with disilicide coated columbium at 2500°F due to

chemical reactions with the coating. The Pt/Pt-Rh thermocouple is also incompatible with disilicide coated columbium at this temperature. As a result of work on the X-20 program, Iridium is known to be compatible with disilicide coated columbium at temperatures up to 2700°F. For this reason, the Ir-40Rh/Ir thermocouple appeared to offer the best solution for measurement of surface temperatures of columbium surface screens.

Studies were conducted of thermocouple compatibility and attachment techniques for positive surface temperature measurement of coated columbium screen. Tests were conducted with Chromel/Alumel, Pt/Pt-13Rh and Ir-40Rh/Ir thermocouples. Since T/C wires cannot be spot welded to disilicide coated refractory metals, a cement composed of molybdenum disilicide plus Synar (colloidal silica) binder was used to bond the thermocouples to the coated columbium. Specimens with bonded thermocouples were exposed in an air furnace and the response measured at temperatures from 2000°F to 2600°F. Results of this investigation are described below.

Chromel/Alumel.- Performance was satisfactory at 2000°F but response became unsatisfactory within a few minutes at 2200°F due to thermocouple/coating reactions. The Chromel/Alumel readings were 400° to 500°F low at 2200°F.

Pt/Pt-13Rh.- Performance was satisfactory at 2200°F and 2400°F but the Pt/Pt-13Rh thermocouple response became unsatisfactory after 50 minutes at 2400°F due to thermocouple/coating reactions. These reactions caused the thermocouple to read from 400° to 600°F high at 2400°F. When tested at 2500°F, the T/C failed almost immediately.

Ir-40Rh/Ir.- The thermocouple performed satisfactorily for 2 hours at 2500°F and 1 hour at 2600°F. Fabrication of Ir-40Rh/Ir thermocouples is difficult in comparison to the other T/C materials. Resistance welding of the T/C junction is unsatisfactory due to low strength and brittleness. Fusion welding of the bead can be accomplished although the joint is brittle and extreme care must be exercised in handling. Bend forming of the thermocouple wire is difficult due to high work hardening of the iridium and its inherent low ductility. Exposure to high temperatures further degrades the T/C wire ductility.

The calibration chart for the Ir-40Rh/Ir thermocouple is presented in figure 38. Comparison of Ir-40Rh/Ir T/C bonded to coated columbium screen with a Pt/Pt-13Rh control thermocouple adjacent to the screen showed a maximum deviation of 10°F at 2500° and 2600°F. Since Ir-40Rh/Ir is the only T/C material found to be compatible with disilicide coated columbium, it was selected for use in the columbium test modules in spite of its obvious shortcomings in fabricability and ductility.

APPENDIX B

MODULE AND COMPONENT ANALYSIS AND DEVELOPMENT

In Appendix A various materials were evaluated and final materials selected. Analytical methods and calculations were used to determine performance requirements of the module and its components and were the basis for the selection of such components as temperature sensor, valve, and controller. Flame tests were also conducted on the 2" diameter specimens to confirm analytical calculations, check out system components, and determine the system performance. The selection of the valve requires a knowledge of the coolant flow rates or system efficiency, while the selection of a temperature sensor must consider the thermal response of the screen. In turn, the performance and operating characteristics of these two components determine the design of the controller. The reasons leading to the selection of these components are embodied in the tasks listed below and discussed in detail in the following paragraphs.

1. Determine the effective emissivity of the exposed insulation and screen surface.
2. Establish the efficiency of the transpiration system.
3. Obtain the coolant flow rates for the transpiration module.
4. Measure the thermal response of both Inconel and disilicide coated columbium screen.
5. Determine the thermal response of the selected temperature sensor as installed in the module.

Check out the automatic temperature-coolant control system.

Emissivity of the module surface. - The surface of the transpiration system radiates part of the heat input and affects the coolant flow rate required. The amount of heat radiated is determined by the surface temperature and the effective emissivity of the module surface.¹ Since the module surface is composed of insulation and screen, an effective emissivity of the surface may be calculated from the radiation heat balance,

$$\dot{q}_{r,wire} + \dot{q}_{r,insulation} = \dot{q}_{r,total} \quad (B1)$$

assuming that the screen and insulation each radiate as grey bodies with different temperatures. The left side of equation (B1) can be written as

$$\sigma \epsilon_w A_w T_w^4 + \sigma \epsilon_I A_I T_I^4 = \dot{q}_{r,total} \quad (B2)$$

¹ View factors were not considered.

Since the temperature of the surface screen is critical, but readily measured, it is convenient to define the total surface radiation as

$$\dot{q}_{r, \text{total}} = (A_I + A_w) \epsilon_{\text{eff}} T_w^4 \quad (\text{B3})$$

The effective emissivity can therefore be obtained from equations (B2) and (B3) as follows:

$$\epsilon_{\text{eff}} = \epsilon_w \left[\frac{A_w}{A_w + A_I} \right] + \epsilon_I \left[\frac{A_I}{A_w + A_I} \right] \left[\frac{T_I}{T_w} \right]^4 \quad (\text{B4})$$

The emissivities of oxidized Inconel and disilicide coated columbium are well known² but the values for Q-felt are not available. Also unknown is the temperature difference between the insulation and screen.

The effective emissivity can be obtained with a measurement of surface temperature, such as by a thermocouple or optical pyrometer, and a total radiation pyrometer as follows:

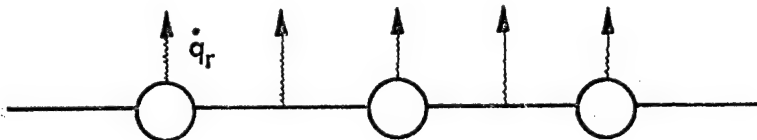
$$\sigma (A_w + A_I) \epsilon_{\text{eff}} T_w^4 = \sigma (A_w + A_I) \epsilon_p T_{\text{total rad}}^4 \quad (\text{B5})$$

$$\epsilon_p = 1.0$$

or

$$\epsilon_{\text{eff}} = \left[\frac{T_{\text{total rad}}}{T_w} \right]^4 \quad (\text{B6})$$

A summary of flame test results of ϵ_{eff} for .017" dia., 18 mesh Inconel screen is presented in figure 42. The data are compared with the first term of equation (B4), Table 6, assuming the wires of the screen are one half imbedded in the insulation as follows:



²The specific heat, density, and normal emissivity of aluminum oxide, Inconel and C-103 columbium alloy are specified in figures 39 to 41. The normal emissivity, for Inconel given in figure 39 was measured after the metal had been exposed (oxidized) at 2000°F for 15 minutes. The values of emissivity of columbium are for disilicide coated specimens tested at ambient pressure.

An average of the data presented in figure 42 indicates that the approximate value of $\epsilon_I (T_I/T_W)^4 (A_I/A_W + A_I)$ is .2.

Efficiency of the transpiration system.- With the effective emissivity of the surface now estimated, the efficiency of the transpiration system can be determined with

$$\psi = \frac{\dot{m} (i_{c,w} - i_{c,bw}) + \sigma \epsilon_{eff} T_w^4}{\dot{q}_{hw}} \quad (B7)$$

where ψ is the blocking function.

A comparison of the laminar blocking function for data obtained during flame tests of 2" dia. specimens and an empirical relationship of reference 6 are presented in figure 43. Since all data shown are greater than the maximum value of ψ , which is 1.0, a further discussion of the results is required.

Since the empirical relationship shown by the curve in figure 43 indicates ψ for the range of the data to be very nearly one, the reasons for the discrepancies can be illustrated by replotting the data as shown in figure 44. Figure 44 indicates that there may be two basic causes of the disagreement. Of the four parameters shown in figure 44, \dot{q}_r was well established in the previous section and mass flow was measured, therefore, the problem must rest in the values of \dot{q}_{hw} and $i_{c,w}$.

The hot wall heat flux was then calculated with the approximation

$$\dot{q}_{hw} \approx \dot{q}_{cw} \frac{T_\infty - T_w}{T_\infty - T_{w,0}} \quad (B8)$$

The smooth body, cold wall heat flux with zero coolant mass flow, \dot{q}_{cw} , was measured with slug calorimeters as discussed in Appendix C. The free stream or flame temperatures were obtained from thermocouple measurements and calculations as described in Appendix C.

The resulting heat flux, however, does not include the possible effect of surface roughness and the heat conducted into the metal shell from the top ring and hot gas gap between the shell and copper block. These effects would increase \dot{q}_{hw} and tend to raise the data of figure 44.

The second problem area may be due to the assumption that the coolant leaves the system at an enthalpy corresponding to the screen temperature and pressure. A low coolant exit temperature would explain some of the discrepancies of figures 43 and 44, but is in itself a disadvantage since the transpirant is not being utilized in the most efficient manner.

A third cause of the discrepancy could be a nonuniform mass flow and temperature distribution over the surface of the flame units, which is not accounted for in the calculations.

Mass flow rate of coolant.- In light of the strong edge effects present in both the flame test specimen and the single module and the requirement to know the coolant flow rates, the system flow rates have been estimated with the empirical relationships of Woodruff (reference 6). The empirical equations have been observed to be in good agreement with theoretical calculations of reference 7.

The transpirant flow rates are presented in figure 45 for flow of water, nitrogen, and helium into a turbulent boundary layer composed of arc heated air. The flow rates for water are presented for test conditions in the Boeing Duct Plasma Facility and a high enthalpy condition representing that for the NASA/Ames arc jet. The nitrogen and helium flow rates are presented only for the Ames Arc Jet condition. The figures 45a to 45d present the coolant flow rates per unit surface area as a function of surface temperature and unblocked heating rate. Trades between surface temperature and coolant mass flows are also indicated.

The flow rates for the two gaseous coolants are presented for comparison purposes and will be of interest in relation to a later section.

These calculations for water were based on the enthalpy of superheated water vapor as presented in figure 46. The calculated enthalpy presented in figure 46 assumes the water vapor acts as an ideal gas and the reference condition is 32°F. The calculations for nitrogen and helium are based on the properties presented in reference 10.

Solenoid valve.- A simple on-off operated solenoid valve was selected to meter the coolant flow because of the required rapid response and high reliability. To meter the small but wide range of coolant flow rates, the valve is operated at a fixed frequency with pulse width modulation.

A two way normally closed subminiature, series B2, valve manufactured by the Skinner Electric Company was selected for the module development program on the basis of size, weight, power consumption, ability to operate in a vacuum, and in any position.

A valve with a 1/16" diameter orifice size was selected on the basis of system pressure drop, steady state flow rate requirements of the single module and the flow rates required to saturate the dry module matrix when heating is initially impressed on the transpiration system. To assure that these requirements are satisfied, the valve was cold flow tested with water.

Presented in figure 47 is reduction in maximum (wide open) coolant flow by pulse width modulation of the valve with different frequencies and coolant supply pressures. The data are observed to be higher than the square wave prediction because of opening and closing transient of the valve as shown in the sketch below:



SQUARE WAVE

ACTUAL

The manufacturer's specification (reference 5) for the nominal valve characteristic with the valve continuously open is presented in figure 48. A few cold flow data points confirm this nominal valve characteristic. On the basis of the cold flow test results and the maximum frequency capability of the valve, a frequency of 5 cps was selected for the valve operating condition.

Description of temperature sensor.- The baseline design for the sensor consisted of a resistance thermometer mounted on a metal rod, and positioned midway between the front and back surfaces. The sensor and rod are insulated and shielded from the coolant. Further analysis of this baseline concept during this program indicated a poor thermal response in comparison to that of the screen. This combined with the large size of available torus shaped sensors indicated that a direct measurement of surface temperature using a resistance temperature device (RTD) or a thermocouple would be a more direct and simpler approach. The incompatibility of platinum thermocouple materials with disilicide coated columbium and the low output per degree change in temperature are the primary disadvantages of a thermocouple sensor. A platinum RTD provides a higher output per degree with less amplification required, and therefore, simplifies the design, decreases the cost, and increases the reliability of the electronic controller.

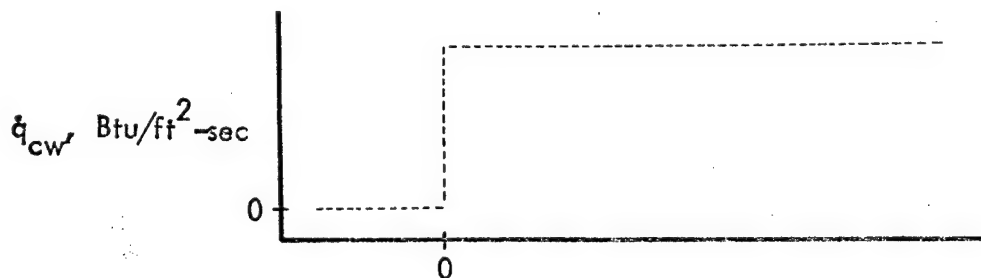
A platinum RTD, Model 118MB, manufactured by the Rosemount Engineering Company, was selected for this program. This sensor can operate at temperatures up to 2732°F (1500°C) and has an acceptable thermal response. The sensor consists of a platinum wire sensing element mounted in a .175" x .175" x .085" aluminum oxide case. Further details and data on this sensor may be found in references 12 and 13.

Each RTD as received from Rosemount Engineering was calibrated at 0°C (ice bath), 200°C (oil bath), and 370°C (oil bath), and a resistance-temperature curve then calculated up to 800°C. The calibration curves for the individual sensors used in the five transpiration modules are presented in figure 49. The sensor serial numbers and module numbers are tabulated in Table 7.

Temperature response of Inconel screen and sensor installation I.- A sensor installation using the Model 118MB RTD should include the following ground rules in order to obtain an effective and reliable surface temperature sensor.

1. The sensor and lead wires should be protected from the coolant. The resistance-temperature characteristic of the sensor element will change with time if directly exposed to steam and water.
2. The sensor should be attached to the screen, so the sensor can move up or down with thermal distortion of the surface.
3. The sensor should be constrained so as to prevent movement or vibration in the horizontal plane.
4. The sensor should be directly exposed to the aerodynamic heating rate and surface screen temperature in order to obtain good thermal response and a sensor temperature as close as possible to the screen temperature.

The first installation design evolved, consisted of holding the sensor vertical between .02" thick metal plates which in turn are welded to the screen. The sensor and plates were installed into a ceramic tube, as shown in figure 50, to shield the sensor from excessive contact with the coolant. The ceramic tube is attached to the screen using two attachment wires which were spot welded to the sides of the metal plates. A 2" dia. flame unit was fabricated which contained a front and backwall Chromel/Alumel thermocouple and the RTD installed as shown in figure 51. The front surface thermocouple wires were spot welded to the screen as discussed in Appendix A. Tests on this specimen were first conducted with the unit dry, and later with coolant flow to study the temperature response of the Inconel screen and sensor. These results are presented in figures 52 through 54. A typical set of temperature-time traces for the Inconel screen and sensor are shown in figure 52 for a step heat input as indicated below:

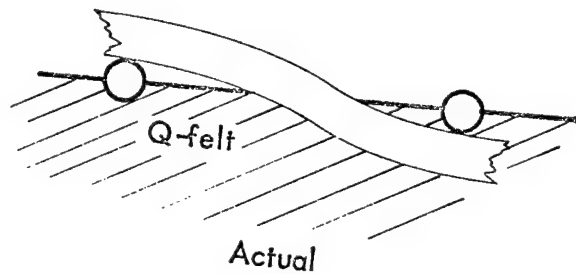
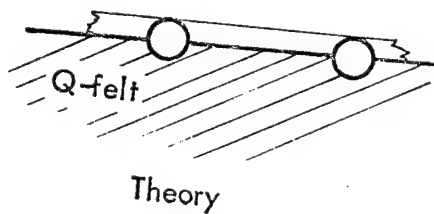


The theoretical thermal response for the screen and sensor for such a step change in heating rate and an "infinite" thermal conductivity is given by the following heat balances:

$$(\rho cr)_w \frac{dT_w}{dt} = \dot{q}_{cw} \frac{T_\infty - T_w}{T_\infty - T_{w,0}} - \sigma \epsilon_w T_w^4 \quad (B9)$$

$$(\rho c l)_s \frac{dT_s}{dt} = \dot{q}_{cw} \frac{T_\infty - T_w}{T_\infty - T_{w,0}} - \sigma \epsilon_s T_w^4 \quad (B10)$$

Equations (B9) and (B10) also include the assumption that heat transfer occurs on the upper one-half of the screen and on one side of the sensor. The remaining surfaces are assumed to be perfectly insulated. The temperature time derivatives near time zero for the screen and sensor are shown in figure 53. The theoretical prediction for the screen, shown in figure 53, does not agree with the data due to a larger mass of wire than that assumed as shown below:



The sensor response is faster than the theory prediction as a result of heat transfer into the sides of the sensor. Each of these effects can be accounted for in equations (B9) and (B10) by the use of an effective $(\rho c r)$ and $(\rho c l)$, and can be established from figure 53.

The results of figures 52, 53, and 54, indicate the response of the screen and sensor without coolant flow can be given as follows:

.017" dia. 18 mesh Inconel

$$\frac{dT_w}{dt} = 12.75 \frac{c_{60^\circ F}}{c_{T_w}} \left[\dot{q}_{cw} \frac{T_\infty - T_w}{T_\infty - 60} - \sigma \epsilon_w T_w^4 \right] \quad (B11)$$

Sensor Installation I

$$\frac{dT_s}{dt} = 2.5 \left[\dot{q}_{cw} - \epsilon_s \sigma T_w^4 \right] \quad (B12)$$

The sensor response is observed to be nearly 1/5 that of the screen. However, these results are for a dry module, which would be of importance during startup or the initial heating transient. Of equal importance is the response and operation of the unit with coolant flow. Two such cases are presented in figure 55. The front surface thermocouple during these wet tests yielded temperature measurements well below that of the optical and total radiation pyrometers. A comparison of optical pyrometer and thermocouple measurements is presented in figure 56. The thermocouple may well be measuring the

temperatures at the surface of the insulation or the coolant exit temperature due to conduction along the thermocouple wires. Only qualitative results could be obtained from these tests; however, the difference in response, with coolant flow, between the screen and sensor seemed to be less than the dry unit values. This can be illustrated qualitatively for the case of the screen by use of equation B9 with the addition of the mass transfer term, as shown in equation B13.

$$(\rho c_r)_w \frac{dT_w}{dt} = \dot{q}_{cw} \frac{T_\infty - T_w}{T_\infty - T_{w,0}} - \dot{m} (i_{c,w} - i_{c,bw}) - \sigma \epsilon_w T_w^4 \quad (B13)$$

The mass transfer term will have less of an effect on the sensor since it is shielded from the coolant.

The flame tests were also used to determine the relationship between screen and sensor temperatures, which constitutes the calibration of the sensor installation. These results are presented in figure 57.

Controller.— The controller provides pulse width modulation at the solenoid valve input as a function of a temperature signal. The signal is a comparison of the difference between the sensor output and controller setting (T'_w), and the controller bandwidth (ΔT). The controller then maintains the screen temperature between T'_w and $T'_w + \Delta T$ and provides zero coolant at T'_w and maximum flow at $T'_w + \Delta T$. The T'_w surface temperature (T'_w) and bandwidth (ΔT) are control variables. The control device was fabricated by Zeltex, Inc., and is shown in figure 58.

The controller ("black box") was installed into a control panel, external to the module as shown in figure 59. The coolant flow through the valve can be controlled automatically or with the manual override. The override bypasses the controller and will operate the valve, either full open or full closed.

The operation of the valve is indicated by center (brown) light, which directly indicates the pulse width or duration the valve is open.

Both the surface temperature (BALANCE) and temperature bandwidth (RANGE) of the controller are variable and set with the respective labeled potentiometers.

The BALANCE and RANGE settings are arrived at by the selection of a desired surface temperature and a temperature bandwidth as indicated in the following example.

EXAMPLE

1. Inconel module II sensor S/N 627 and Installation I
2. Desired surface temperature = 1900°F
3. Desired surface temperature bandwidth = 50°F. Therefore, the controller should maintain the surface temperature between 1900 and 1950°F.

4. From figure 57 the sensor temperatures are $1370 \rightarrow 1400^{\circ}\text{F}$.
5. From figure 49c the sensor resistances are $36.4 \rightarrow 37.2$ ohms.

If there were .5 ohms resistance in the leadwires, .5 ohms must be added to the values in 5., then

6. The sensor resistances to keep T_w between 1900 and 1950°F are 36.9 and 37.7 ohms.
7. The BALANCE potentiometer is set at 36.9 ohms.
8. The RANGE potentiometer is set in the following manner.

Connect the power supply ($24\text{V DC } 0-1$ amp) and valve to the controller. In place of the sensor (RTD) input connect a decade resistance box. Now with the power supply turned on, the controller switch set at AUTO, the balance pot set at 36.9 and the decade box set at 37.7 , dial the range pot until the valve indicator light is lit continuously.

9. Shut off the power supply, disconnect decade box and connect sensor input to controller. The temperature and bandwidth are now set, but during a test the BALANCE potentiometer setting can be changed³. However, the maximum temperature of the screen material must not be exceeded.

Tests were conducted to check out the sensor, controller, and solenoid valve with the previously described 2" diameter transpiration specimen with an Inconel screen and sensor Installation I. Some sample results from these tests are shown in figure 60. The initial test was conducted with coolant tank supply pressure of 15 psig and a controller bandwidth of 40°F . The controller begins to operate the solenoid valve at the lower side of the band and provides for maximum coolant flow rate at the high side of the band. As shown in figure 60a, the screen (thermocouple) temperature was maintained for periods of 60 seconds. However, the controller would then overcorrect and the screen temperature would drop to 130°F . In order to remedy this situation, the supply pressure was decreased to 7.5 and 3.6 psig and the controller bandwidth increased to 60°F . These results are presented in figures 60b and 60c, and indicate a reduction in both the width and depth of the temperature depressions.

The bandwidth was further increased to 200°F on subsequent tests. However a temperature bandwidth of 100°F seemed to yield the optimum system operation. In general, these tests with the controller showed that the sharp difference between the screen and sensor response is not a problem. Further, these tests indicated that rate control would not be required as part of the regulation system.

³If a module is tested in an arc heated plasma facility, consideration must be given to the effect of space charge on the controller. The controller and power supply must be "floated" with the test facility to prevent destruction of these two components.

Flame test of columbium and sensor design II.- Flame tests were conducted on a 2" diameter transpiration specimen containing a second sensor installation and thermocouple attachment technique. The second sensor installation was required for columbium because its thermal response is approximately twice that of Inconel (specific heat of columbium is one-half that of Inconel). A sketch of this new sensor installation is shown in figure 61 and consists of laying the sensor horizontal with one of two large faces exposed to the boundary layer. The sensor is held in a horizontal position and is attached to the screen with a ceramic cement. In addition, the ceramic tube is attached to the screen with the use of external attachment wires.

Since columbium requires a coating to prevent oxidation, thermocouple wires could not be spot welded to screen wires as was the case for Inconel. The Chromel/Alumel thermocouple wires were wrapped around the coated columbium and spot welded together as shown in figure 61. A Chromel/Alumel T/C was used during this test series, since long life and high temperature operation were not key objectives.

The objectives of these flame tests were:

1. To measure the thermal response of the columbium screen and sensor.
2. To obtain the relationship between the screen and sensor temperatures.
3. To check out the transpiration system operation with automatic temperature and flow control.

The thermal response of the screen and sensor for two heating rates and zero coolant flow are presented in figures 62 and 63. As described earlier in this report, the response of the screen and sensor at low temperatures can be given by

$$(\rho_{cr})_{eff} \frac{dT_w}{dT} \approx \dot{q}_{cw} \frac{T_{\infty} - T_w}{T_{\infty} - T_{w,0}} \quad (B14)$$

By considering only the temperature response near time zero, the effective ρ_{cr} can be evaluated, as shown in figure 63 and presented in the following table.

		Source	
1.	.017" dia. Inconel screen	12.75	Flame tests
2.	.025" dia. Inconel screen	$\frac{1}{(\rho_{cr})_{eff}}$	Ratioed from (1)
3.	.020" dia. columbium screen		
4.	.020" dia. columbium screen		
5.	Sensor Installation I	2.5	Flame tests
6.	Sensor Installation II	4.2	Flame tests
		$1/(\rho_{cl})_{eff}$	

By comparing (5) and (6) it can be seen that the sensor response has been nearly doubled, but that of the columbium screen (4) has increased by almost a factor of five (compared to .025" dia. Inconel). Further attempts to calculate the temperature history shown in figures 62 and 63 using equation B14 and $1/(pc\ell)_{\text{eff}}$ resulted in large discrepancies. The data when calculated and plotted as shown in figure 64 should reflect only the variation of specific heat with temperature, which is nearly 40 percent. The large variation between 60 and 500°F can be attributed to one or both of the following:

1. Increased heating due to thermocouple protruding above the screen surface.
2. Insulating phenomena of the disilicide coating.

A calibration of the sensor is presented in figure 65. The surface temperature was obtained with optical pyrometers, which, on the basis of figure 56, gave more accurate readings. Also presented in figure 65 are the results from the tests with automatic temperature and flow control. The two sets of data are in good agreement.

The new sensor installation with the valve and controller, held the surface temperature nearly constant while the heating rate was varied. The operation of the transpiration system was observed to be much improved with the new sensor.

Starting problems and procedures.— The use of water as the transpiration system coolant requires the use of a backup system to prevent the coolant from freezing in tubing and in the module matrix. The structure of a space vehicle can cool down well below the freezing point of water such that consideration must be given to heating of the tubing, valves and matrix before admitting the coolant. Also residual coolant in the module matrix will freeze when the system is tested in a ground facility at reduced pressure during tunnel start-up, shutdown, and between cyclic tests.

The system adopted to solve the above problems is shown in figure 66 and consists of using gaseous nitrogen or helium to warm the module components and purge the residual coolant from the matrix. With the use of solenoid valves at the water and nitrogen tank outlets and the manual override features of the controller, gas and water flow to the module can be controlled.

A second problem is to fill or wet the module matrix with reasonable flow rate in a short time period during vehicle reentry or wind tunnel startup. An estimate of the minimum time available can be obtained by examination of figure 67, which indicates that the Inconel screen reaches the maximum temperature in approximately 12 seconds for the linear increase in heating rate with time. With this rapid buildup in screen temperature, the depth of heat penetration into the Q-felt is small. Therefore, the entire dry matrix must be filled with coolant, the amount of which is shown in figure 68.

In order to prevent the module screen from exceeding the maximum temperature, the manual override system can be used to initially "flood" the matrix. The valve and tank pressure must therefore be selected with this starting flow-rate requirement in mind.

APPENDIX C

TEST FACILITIES

Flame test facility.- The majority of material evaluation and component check out was accomplished by heating 2" diameter transpiration specimens in an oxyacetylene flame. The 2" specimen was mounted in a 1" thick water cooled copper block as shown in figure 69. The specimen and holder were mounted on a carriage which could be moved along the torch axis to vary heating rates. Also, a total radiation pyrometer was attached to the model carriage as shown in figure 69. Alongside the model was a 1-3/8 inch diameter copper cylinder, which contained three copper slug calorimeters. An injection mechanism allowed rapid movement of the model or calorimeters perpendicular to the torch axis.

Throughout the test program a Victor number 8 multiflame torch tip was used with fixed acetylene and oxygen flowrates, and at a slightly oxidizing condition. Following each test or run a heating measurement was made.

The 2" specimens were supplied with distilled water which was controlled initially by a needle valve. During later tests the coolant flow was controlled by the temperature sensor, solenoid valve, and controller. Water flow and pressure into the specimen were measured by a microflow meter and mercury manometer as shown in figure 70.

Thermocouple, calorimeter, RTD sensor, and total radiation pyrometer outputs were recorded on a strip chart recorder.

In order to interpret heat transfer measurements and temperature response data of the screen and sensor, knowledge of the freestream or flame temperature was required. During one run of the test series, temperature along the centerline of the flame was measured with a 1/16" dia. Inconel sheath, Chromel/Alumel thermocouple. The flame temperature was then calculated from:

$$T_{\infty} = \frac{T_w - T_{w,0} \frac{\sigma \epsilon T_w^4}{\dot{q}_{cw}}}{1 - \frac{\sigma \epsilon T_w^4}{\dot{q}_{cw}}} \quad (C1)$$

The cold wall heat flux was obtained from calorimeter measurements which were corrected for geometric effects with the aid of references 14 and 15. The final calculated flame temperatures are shown in figure 71 as a function of distance from the torch tip.

The Boeing plasma facility.- All tests of the modules were conducted in the Plasma Laboratory of The Boeing Company at Seattle, Washington. This facility (figure 72) is a two-dimensional duct flow facility. It uses a tungsten-copper constricted arc heater as a heat source.

Downstream of the arc heater, in sequence, are a plenum chamber, a two-dimensional Mach 2.3 nozzle, a 1" x 4" rectangular duct, and an open test section capable of accommodating a 4" x 8" flat plate specimen.

Calibration of the facility was completed during contract NAS 9-6288, (reference 16) for a wide range of conditions. A typical cold wall heat flux and wall static pressure profile in the streamwise direction are shown in figure 73. Figure 73 is for turbulent flow of reconstituted air at a mass flow rate of .075 lb_m/sec.

During the calibration runs it was noted that the heating rates of the model were a strong function of the balance between the duct exit pressure and the attitude chamber. As the chamber pressure P_c approached the duct pressure P_D a shock wave formed at the downstream end of the duct section (the upper surface of the duct) and impinged on the model surface. All tests conducted during the present program were run with an expanding flow condition, that $P_c < P_D$.

The above conditions were selected for evaluation of the module, since the condition produces the maximum heating rate. The presence of a turbulent boundary layer and a high total enthalpy represents the most severe heating condition and, therefore, the best condition at which to test the transpiration system.

During all tests conducted in this facility during this program, heat transfer measurements in the duct were made to confirm the calibrations. No heat rate measurements were made in the test section.

TABLE 1
SUMMARY OF TEST RESULTS FOR INCONEL MODULE 2 AND COLUMBIUM MODULE 1

Run No.	Approximate run duration, min	Controller parameters		Time, minutes	Temperature measurements			
		T _w , °F (a)	ΔT, °F		Front T/C, °F (a)	Uncorrected pyrometer °F (a)	Estimated surface temperature °F	Backwall T/C, °F
INCONEL MODULE 2								
1	20	1500	100	3.5	1660	-	1660	75
2	20	1500	100	7.5-10	900	1750	1750	75
		1500	100	10.5-11.5	1250	1875	1875	75
		1500	100	11.5-11.8	1470	2020	2470 (b)	75
COLUMBIUM MODULE 1								
1	20	2000	60	-	-	-	-	100
2	20	2200-2400	60	-	-	1600	1600 } (c)	100
3	20	2520-2650	60	-	-	1820	1820	100
4	20	2650	60	-	-	1820	1820	100

^aThe sensor, pyrometer, and front surface thermocouples were not positioned to read T_w at the same location on the module surface.

^bMelting temperature range of Inconel is 2470 - 2575°F.

^cBased on visual observations, color motion pictures and examinations of the module it is believed that the maximum temperatures were of the order of 2500°F.

TABLE 2
EVALUATION OF OPERATION OF TRANSPIRATION SYSTEM COMPONENTS

ITEM	OPERATION	REMARKS
1. Screen	Good	Except for deformation and coolant efficiency - Inconel deformation more pronounced than that of columbium
2. Screen support	Good	Need attachment flexibility to minimize screen deformation
3. Insulation	Good Poor	As Insulation As coolant distributor - cracks adjacent to walls resulting in local flooding and poor distribution elsewhere
4. Sponge	Good	
5. Pressure barrier	Good	Should be closer to surface, therefore needs higher temperature capability
6. Coolant	Very good Fair	As coolant In effectiveness because of limited two-phase operation
7. Thermocouples	Good Poor	For Inconel screen For columbium screen - need more work - may consider as integral part of system
8. Sensor	Good	Better attachment to screen is required
9. Valve	Excellent	Miniaturization to be considered in the future
10. Controller (black box)	Excellent	Size and weight considered unimportant in the present phase of the program - miniaturization to be considered in the future
11. Manual override	Excellent Poor	With water With GN ₂
12. Injection (film) cooling	Excellent	Used as emergency feature - may consider as routine reentry application
13. Keeper pins	Good	Sizing may be critical because of tolerances and screen deformation during coating
14. Module frame	Good	Will be different for vehicle application depending on structural Interface

TABLE 3
DISILICIDE COATING DEVELOPMENT

Coating n no.	Coating conditions		No. of control specimens	Screen specimen	Test parts	Coating thickness control specimen, mils/side		Total coating thickness measured, mils/side	Remarks
	Temp, °F	Time, hrs							
-1	1950	4	1	1			1.4	Control 2.5 Screen -	Insufficient coating thickness
-10	2000	6	1	6			1.9	-	Adequate coating thickness, but poor oxidation resistance at wire intersections
-17	2000	6	1	5			0.7	-	(a)
-29	2000	6	1	5			2.0 (a)	3.4 3.2	Some improvement of coating at wire intersections
			2	3			1.9	3.3 3.2	
-19	2000	8	2	9			2.0 2.1	-	Satisfactory coating thickness except at wire intersections
-21	2000	8	2	0	3 round screens 2 front shells		1.9	-	"
-26	2000	8	2	0	1 round screen		1.9	-	"
-26A	2000	12 (b)	1	4			2.2	-	Thermal cracking and spalling of coating. Excessive coating thickness
0-5	1950	14	4	5	2 round screens		2.0	-	Thermal cracking and spalling of coating. Excessive coating thickness

TABLE 3.- Concluded
DISILICIDE COATING DEVELOPMENT

Specimen No.	Coating conditions		No. of control specimens	Screen specimen	Test parts	Coating thickness control specimen, mils/side	Total coating thickness measured, mils/side		Remarks
	Temp, °F	Time, hrs					Control	Screen	
9	1925	12	1	1	1 round screen	1.8	-	-	Satisfactory coating except for moderate thermal cracking
	1950	8	1	1	2 round screens	1.7	-	-	Satisfactory coating except for slight thermal cracking

iodine concentration, specimens re-run in 8-29
imens from 9-19 were re-run first half of 9-26

TABLE 4
OXIDATION TESTS OF DISILICIDE COATED C-103 COLUMBIUM WIRE SCREEN

Specimen number	Run number	Coating conditions	Oxidation test		Results
			Temp, °F	Time, hrs	
8-10-3	8-10	6 hrs. @ 2000 °F (a)	2500	1	Multiple failures at wire intersections
				2	Slight additional oxidation
8-10-4	8-10	6 hrs. @ 2000 °F (a)	2500	1	Multiple failure at wire intersections and fusion welded wire ends.
8-10-5	8-10	6 hrs. @ 2000 °F	2500	1	Some failures at wire intersections
				2	Slight increase in oxidation
8-10-6	8-10	6 hrs. @ 2000 °F	2500	1	Some failures at wire intersections
9-19-9	9-19	8 hrs. @ 2000 °F	2500	1	No failure
			2600	1	7 failures at wire intersections, no failure at wire ends.
9-19-11	9-19	8 hrs. @ 2000 °F	2500	1	2 failure spots where specimen was wired to rack
			2600	1	Increased size of two failure spots
9-19-10	9-19	8 hrs. @ 2000 °F	2700	1	5 failure areas. Two are severe but not catastrophic. Heavy thermal cracking
9-19-7	9-19	8 hrs. @ 2000 °F	2700	1	Two failure areas of moderate severity and heavy thermal cracking
				2	Very severe failures at 7 areas.
9-26A-2	9-26A	12 hrs. @ 2000 °F	2700	1	One area of severe oxidation failure
10-5-7	10-5	14 hrs. @ 1950 °F (b)	2500	1	No failure
				2	Several small failures at cracks
				3	About 12 small failures at cracks
				4	Many failures at cracks and wire ends

TABLE 4.- Concluded
OXIDATION TESTS OF DISILICIDE COATED C-103 COLUMBIUM WIRE SCREEN

Specimen number	Run number	Coating conditions	Oxidation test		Results
			Temp, °F	Time, hrs	
10-5-8	10-5	14 hrs. @ 1950 °F	2500	1	No failure
				2	No failure
				3	Several small failures at cracks
				4	Many failures initiating at cracks and wire ends
10-5-10	10-5	14 hrs. @ 1950 °F	2700	1	Two severe failure areas
10-5-11	10-5	14 hrs. @ 1950 °F (b)	2700	1	Severe failures with several wires parted
10-5-6	10-5	14 hrs. @ 1950 °F (b)	2500	1/2	No failure
				1	No failure
				1-1/2	Many failure spots at cracks
9-19-8	9-19	8 hrs. @ 2000 °F	2500 (c)	10 cyc. of 15 min ea.	Very small failure spot after 9th cycle. No significant growth of failure during 10th cycle
9-21-3	9-23	8 hrs. @ 2000 °F	2500 (c)	10 cyc. of 15 min ea	Several very small failure spots after 9th cycle. No significant growth during 10th cycle.

● Heavy etching performed on specimens prior to coating which apparently had adverse effect on coating oxidation resistance.

^b Stress relieved 1 hr. @ 2000 °F before coating

^c Tested in Leco furnace. All other specimens tested in tube furnace. Slowly moving air atmosphere for all tests.

TABLE 5
COLD FLOW PRESSURE DROP TESTS OF 2" DIAMETER
TEST UNIT 1

Flow rate, lb/sec	Tank pressure inches mercury	Pressure drop, inches of mercury										
		①	②	③	④	⑤	⑥	⑦	⑧	⑨	⑩	⑪
2.92×10^{-4}	10	.3	.3	.3	.3	.5	.3	.6	1.2	1.5	3.2	2.8
10.95×10^{-4}	10	.5	.6	.5	.5	1.0	.4	1.7	2.4	3.0	9.8	9.4
20.10×10^{-4}	10	.7	.9	.8	.8	1.2	.7	2.6	3.0	4.7	-	-

- ① No pressure barrier
- ② Refrasil C-100-96, .050", one layer
- ③ Refrasil C-100-28, .012", four layers
- ④ Refrasil C-100-96, .050", one layer, and tissue quartz paper, .005", two layers
- ⑤ Refrasil impregnated with barrite
- ⑥ Fiberglass cloth style 128, .007", two layers
- ⑦ Polyimid fiber felt, .025" compressed, one layer
- ⑧ Dacron sail cloth, 3.25 oz., .005", one layer
- ⑨ Nylon sail cloth, .75 oz., .003", one layer
- ⑩ Nylon sail cloth, .75 oz., .003", four layers
- ⑪ Nylon sail cloth, .75 oz., .003", six layers

TABLE 6

EFFECTIVE EMISSIVITY OF SCREENS TESTED DURING DEVELOPMENT PROGRAM

SCREEN	EQUATION (B4) $\epsilon_{\text{eff}} =$
.017" dia. 18-mesh Inconel	$.63 \epsilon_w + .37 \epsilon_I \left(\frac{T_I}{T_w} \right)^4$
.025" dia. 20-mesh Inconel	$.76 \epsilon_w + .24 \epsilon_I \left(\frac{T_I}{T_w} \right)^4$
.020" dia. 18 x 20-mesh columbium	$.66 \epsilon_w + .34 \epsilon_I \left(\frac{T_I}{T_w} \right)^4$

TABLE 7

MODULE NUMBERS AND SENSOR SERIAL NUMBERS

Module number	Module screen	Sensor installation	Sensor S/N	Maximum surface temperature capability, °F
1	Inconel .025" dia. 20-mesh	I	627	2000
2		II	627	2000
3		II	625	2000
1	Columbium .020" dia. 18 x 20-mesh	II	623	2500
2		II	618	2500

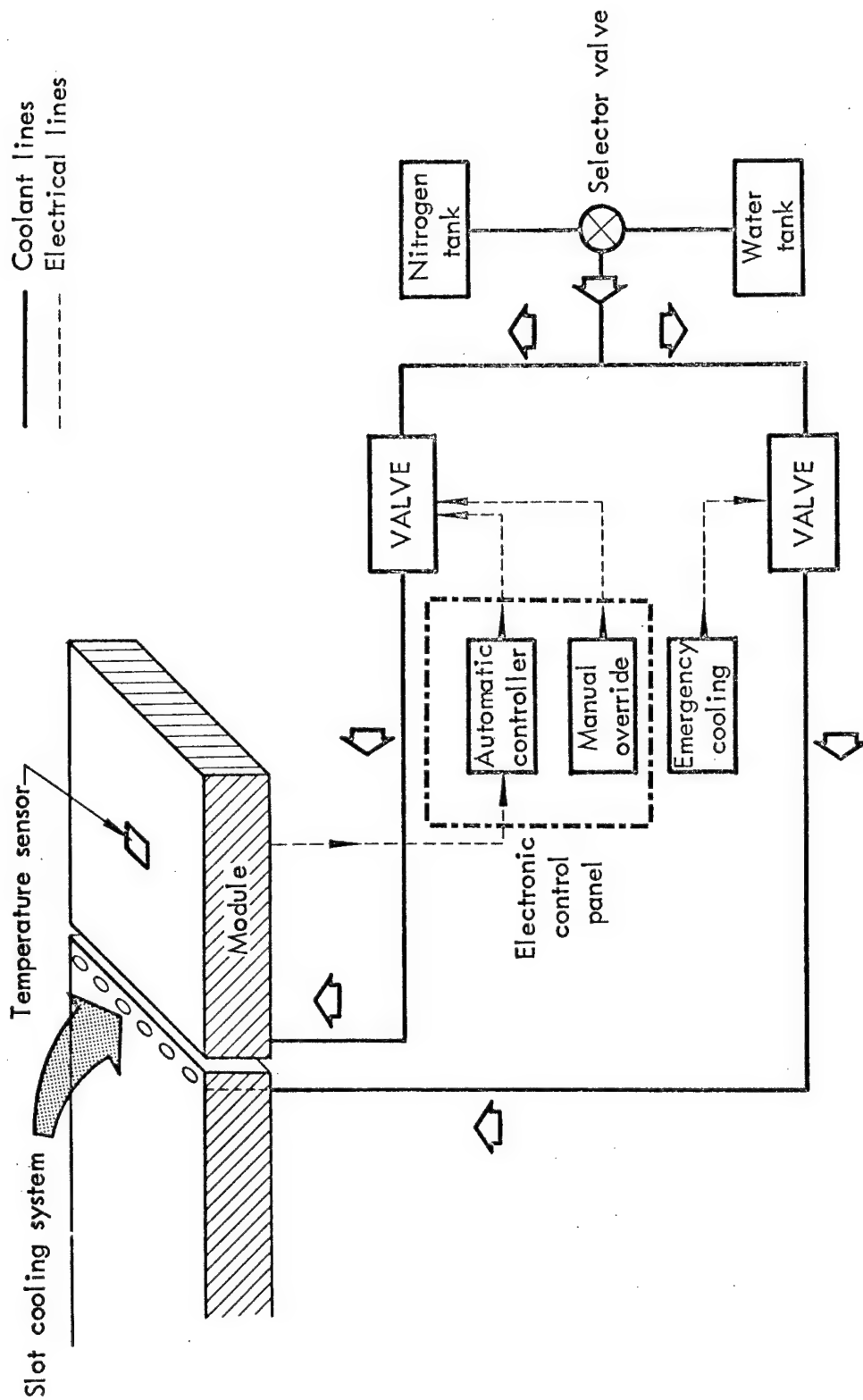
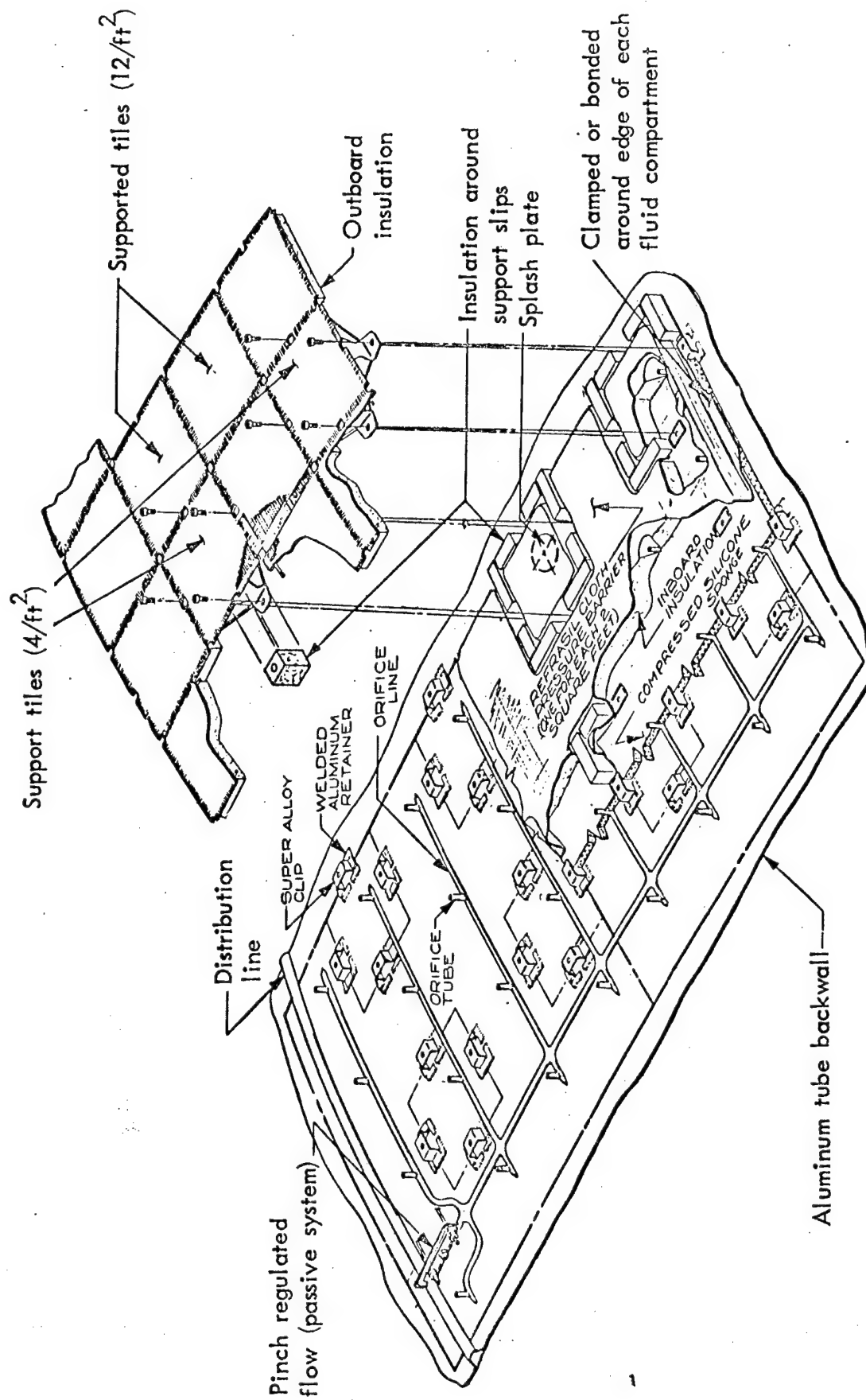
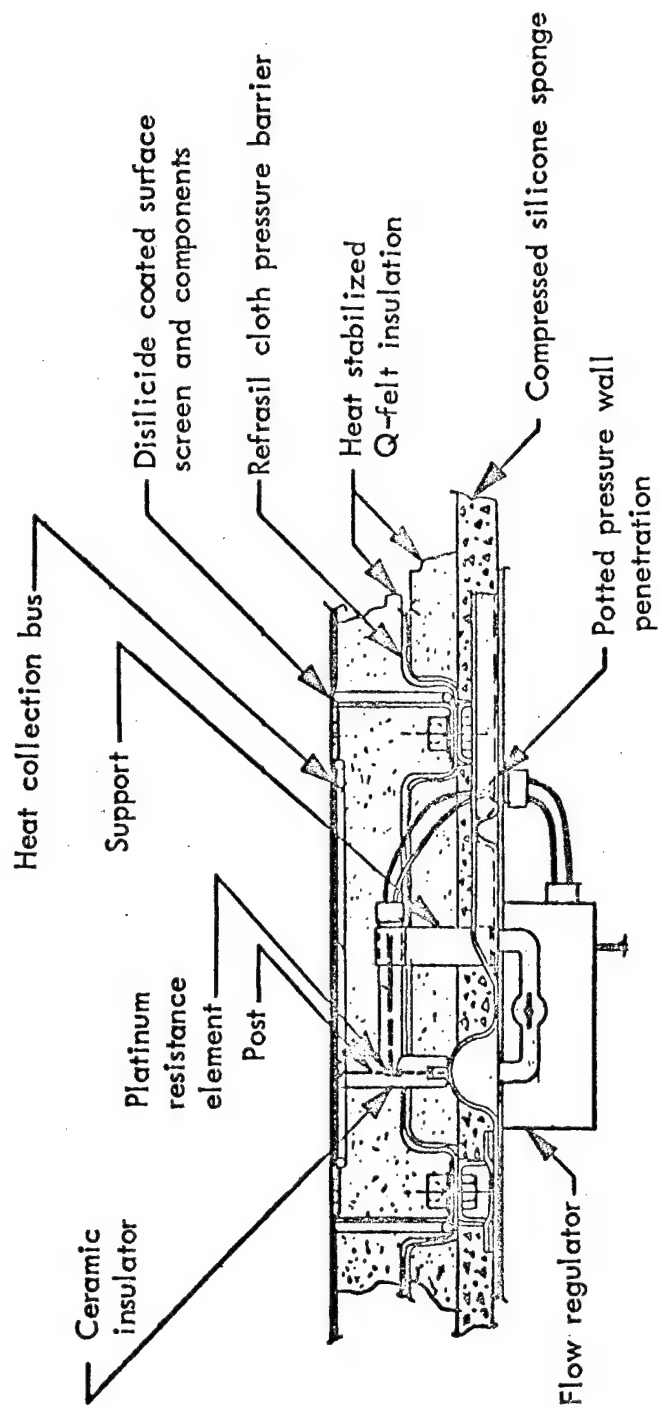


Figure 1.- Schematic of the transpiration cooling system.

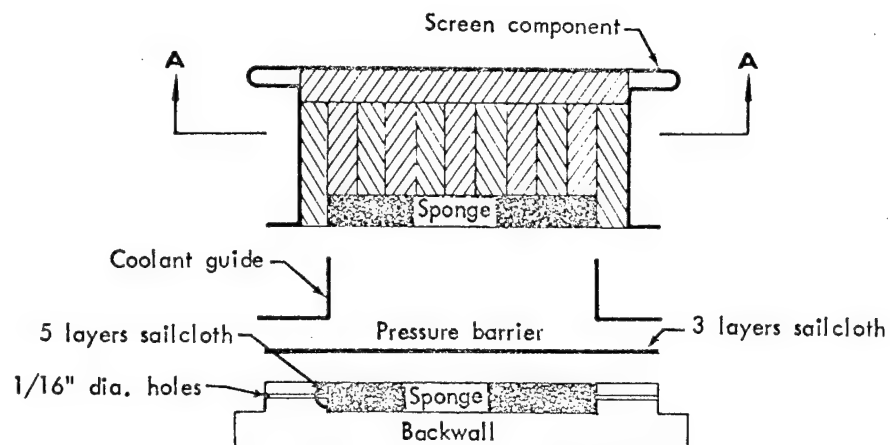




a) Structural portion
Figure 2. - Transpiration cooling system baseline design.

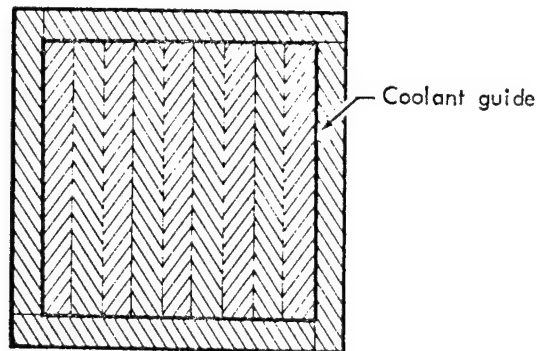


b) Control portion

Figure 2.- Concluded.

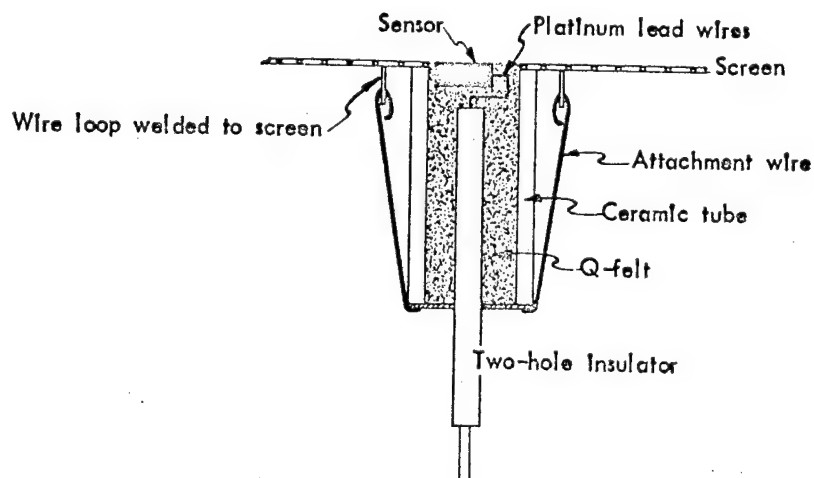


-  Heat stabilized Q-felt
-  Unstabilized Q-felt



Section A-A

a) Structural portion



b) Control portion

Figure 3. - Final module.

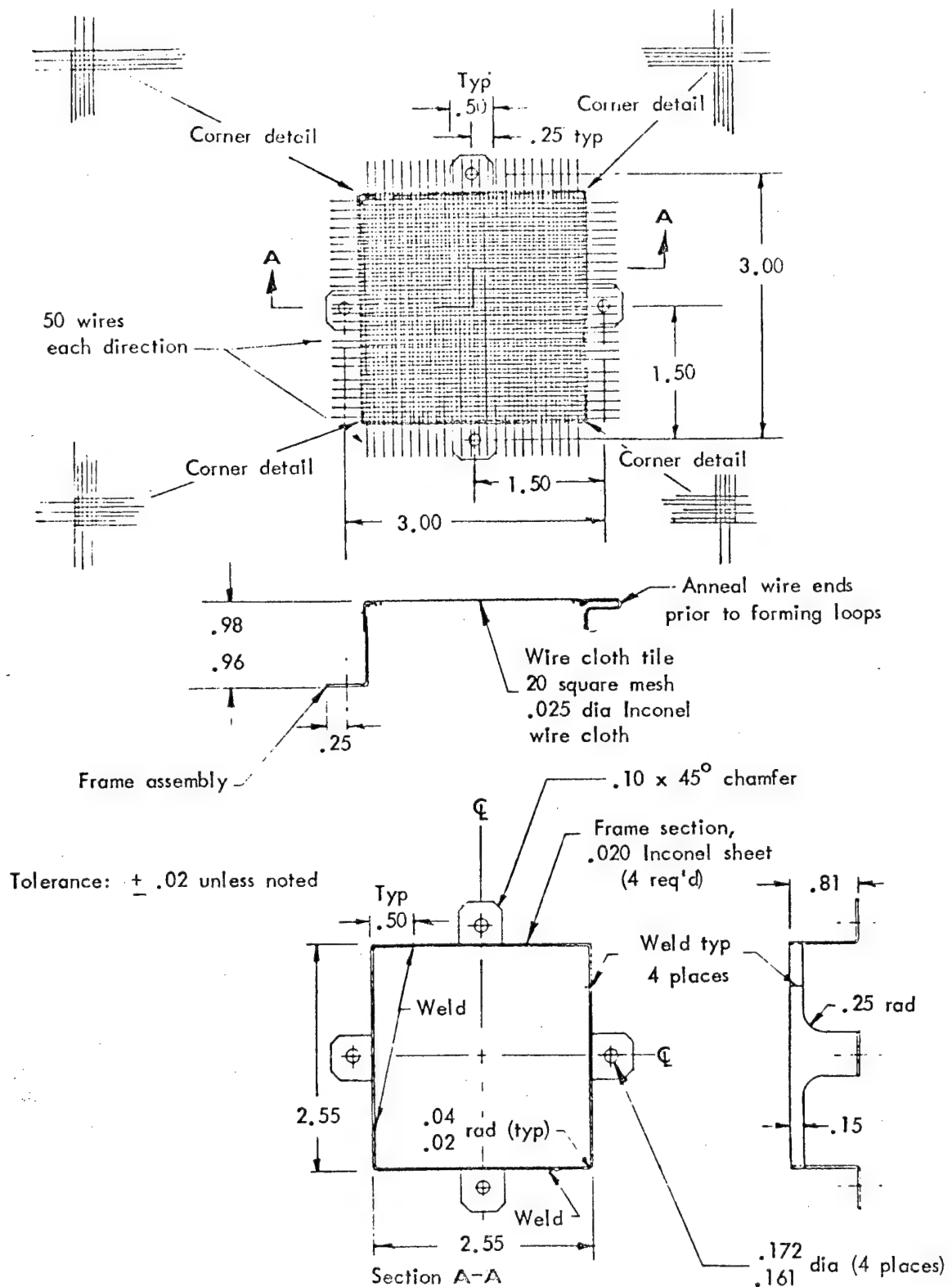


Figure 4.- Screen component.

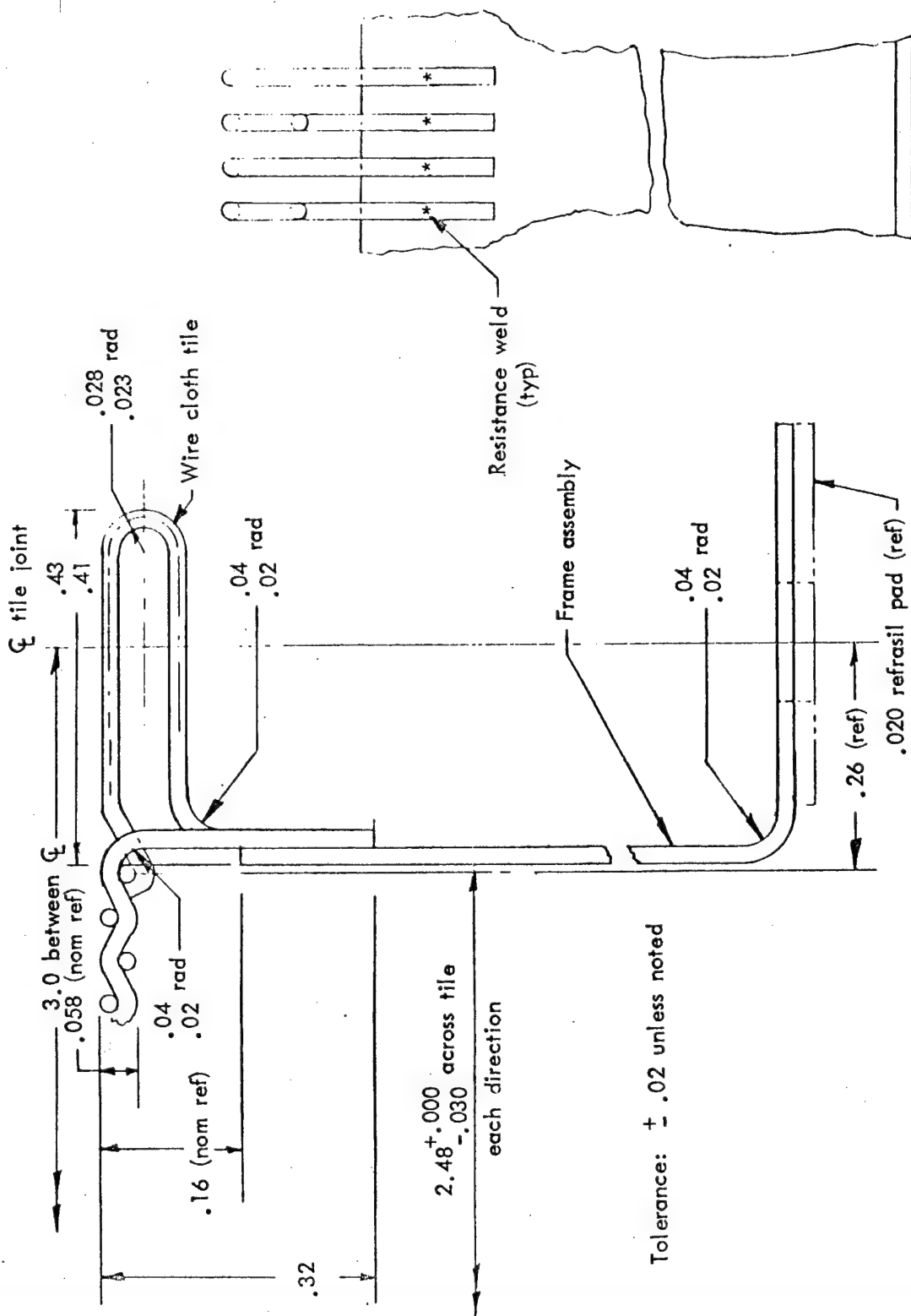
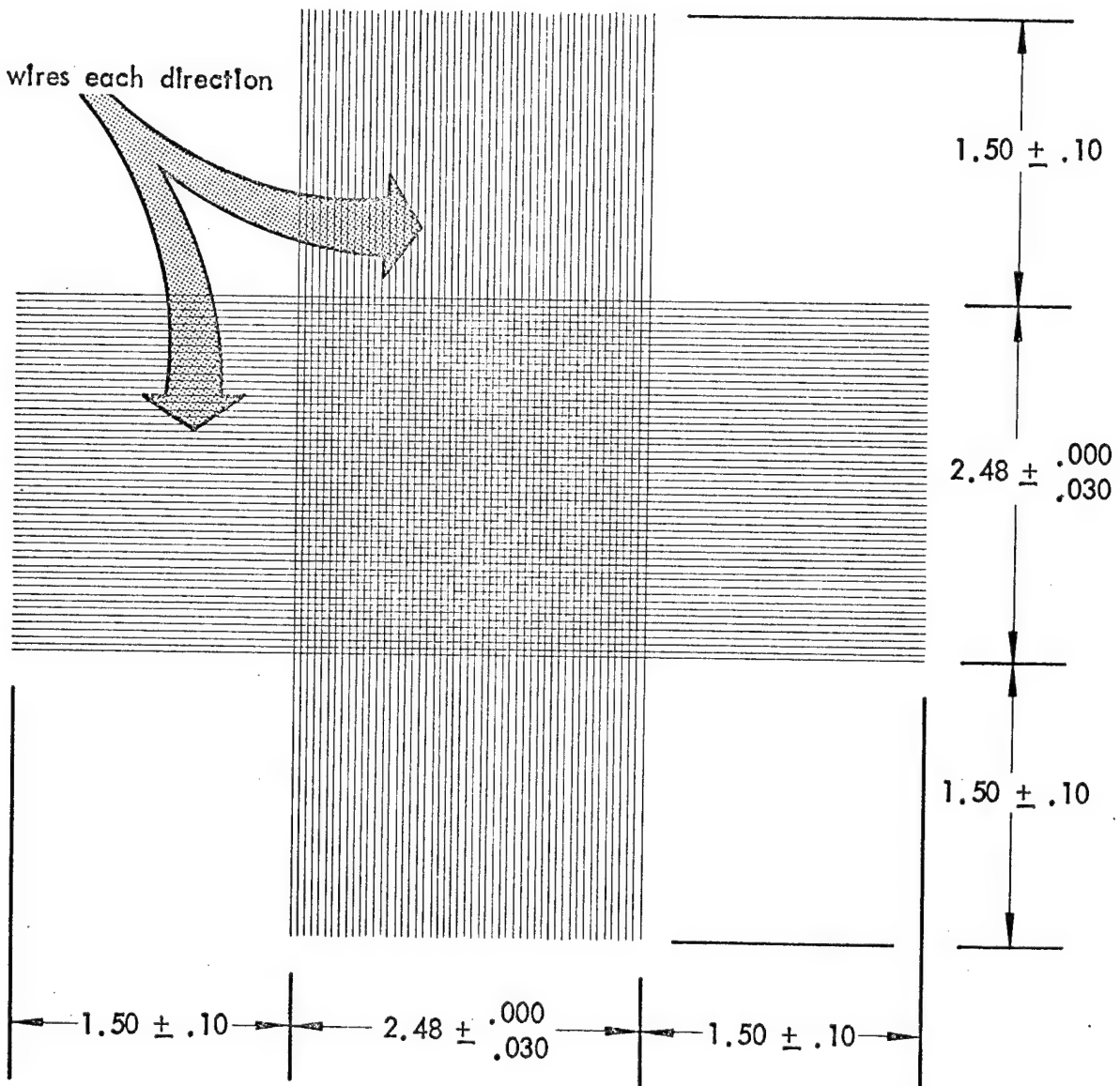


Figure 5.- Detail of module attachment loops and support clips.

~50 wires each direction



20-mesh .020" dia. columbium alloy (C-103) wire

All dimensions are in inches

Figure 6. - Wire screen tile.

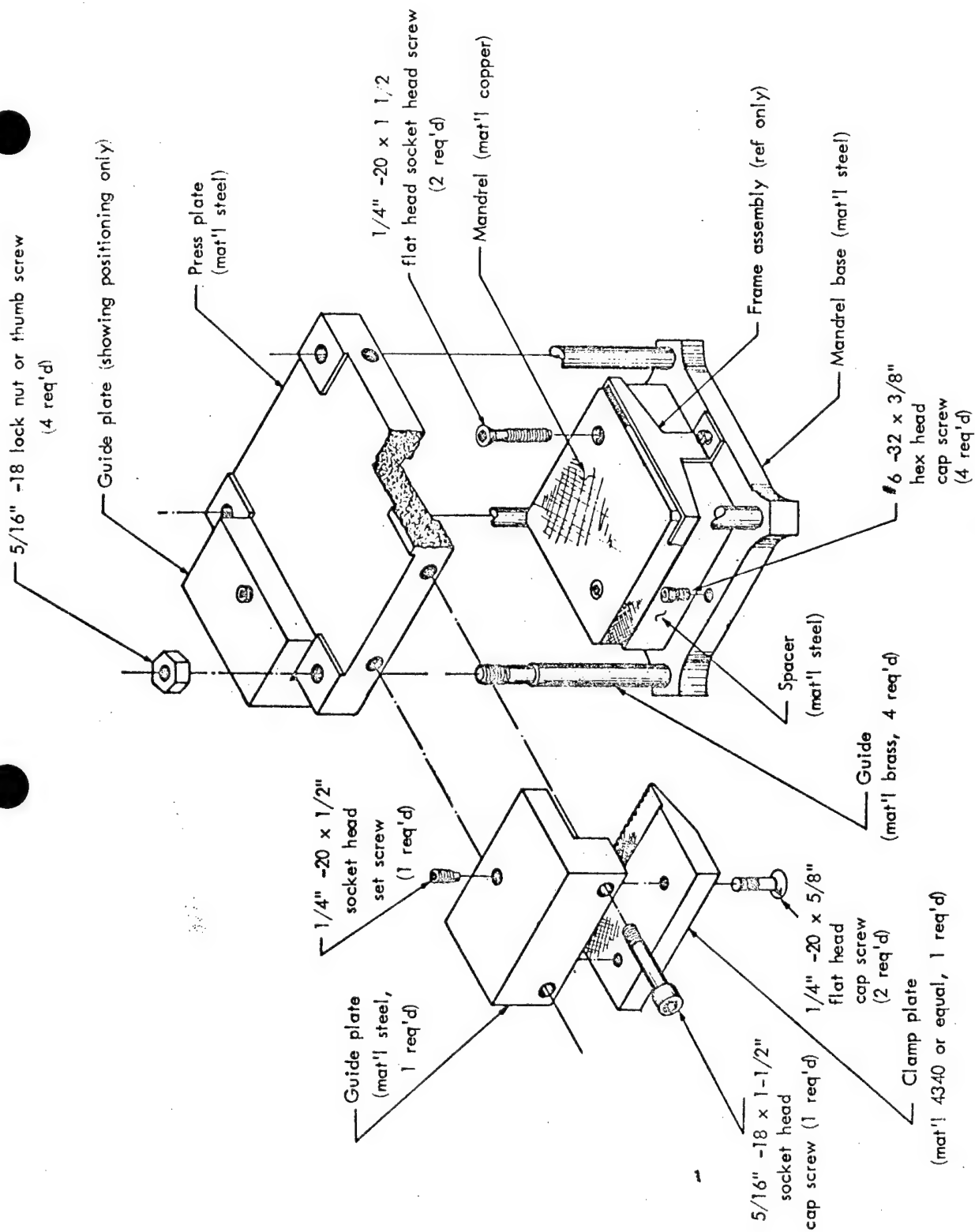


Figure 7.- Detail of forming and welding fixture for screen component.

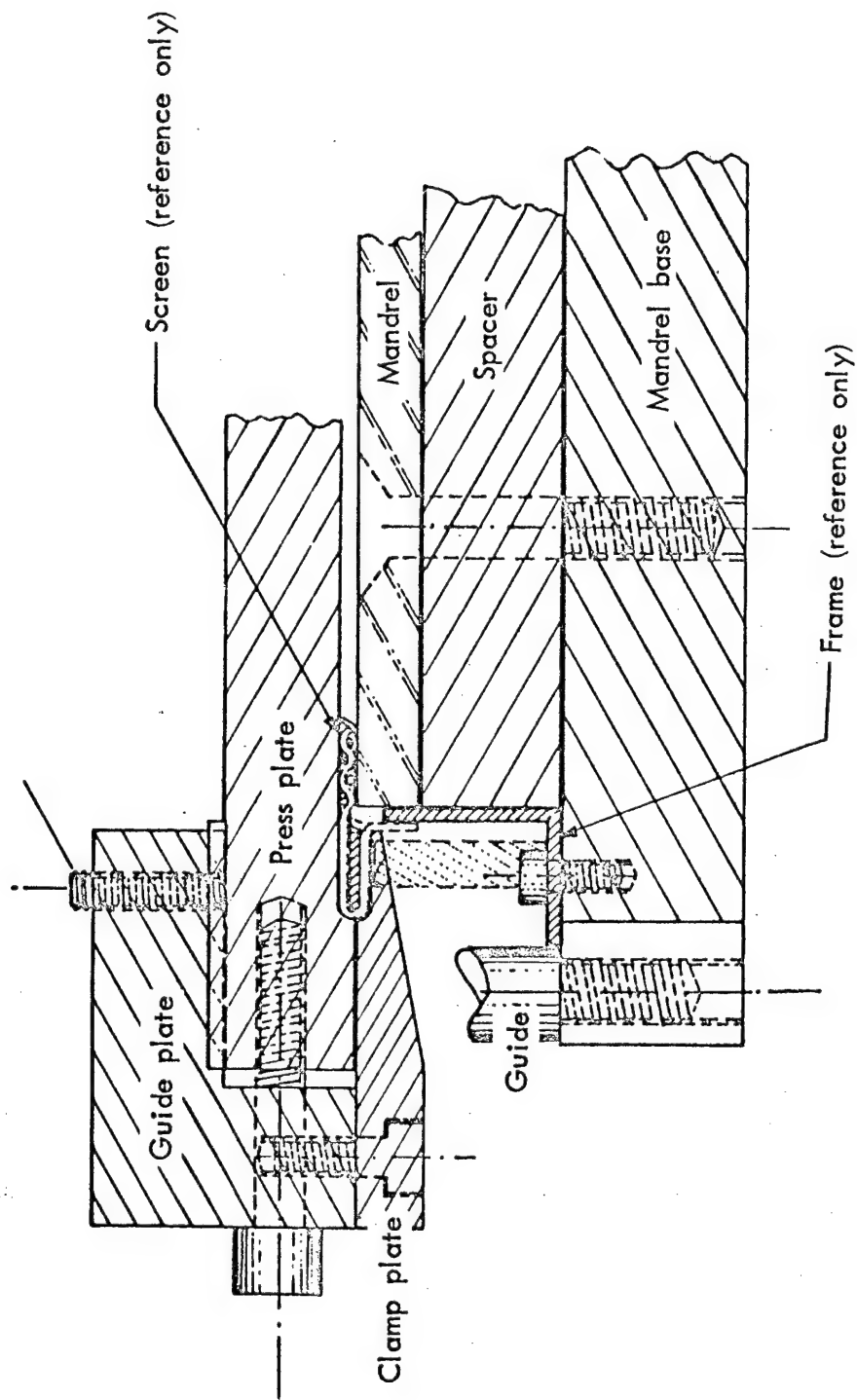


Figure 7.- Concluded.

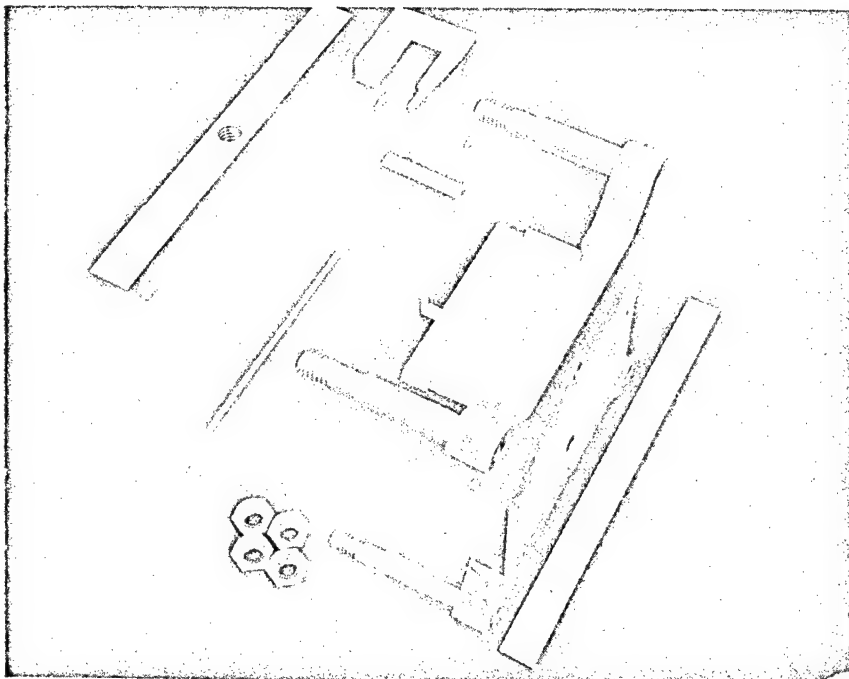


Figure 8. - Forming and welding fixture for screen component.

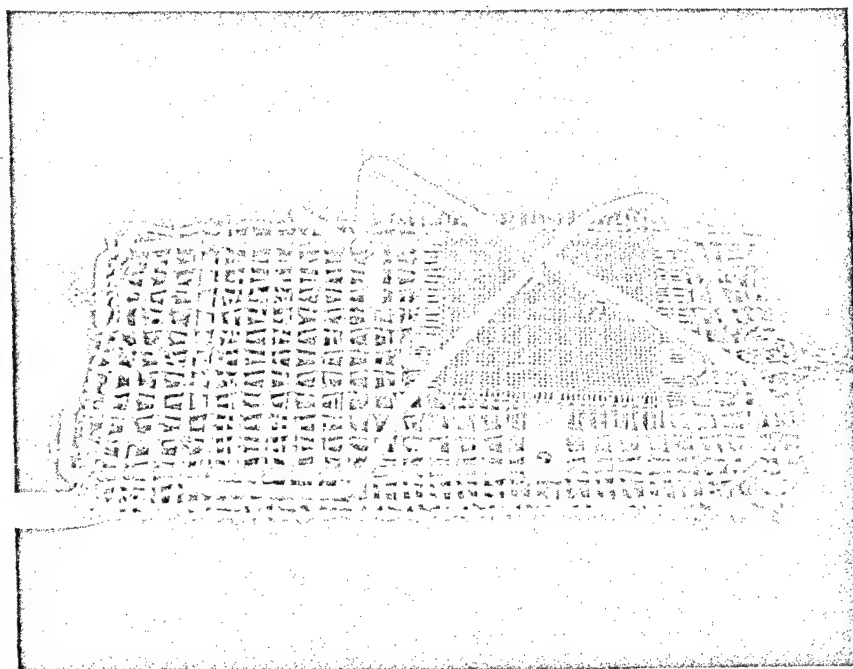
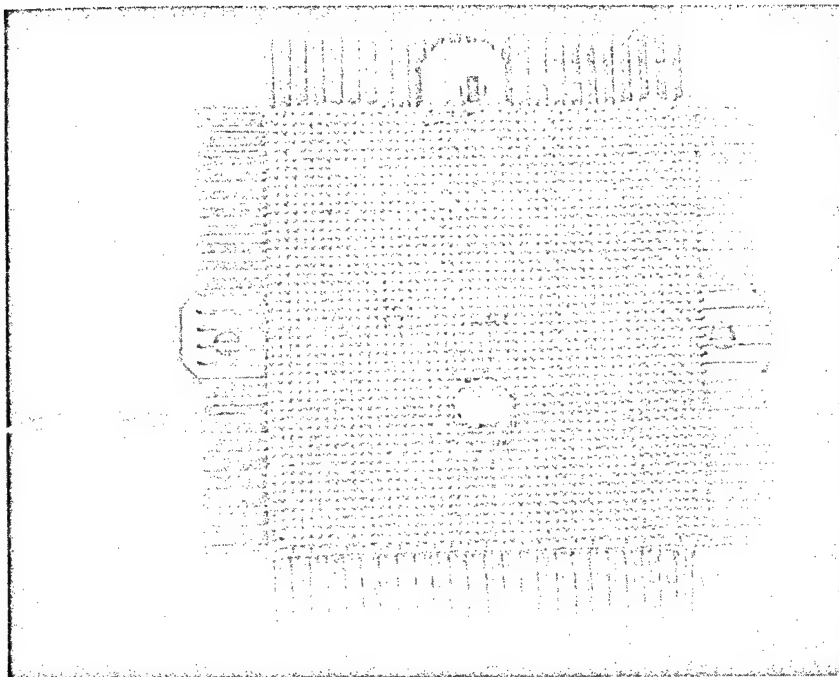
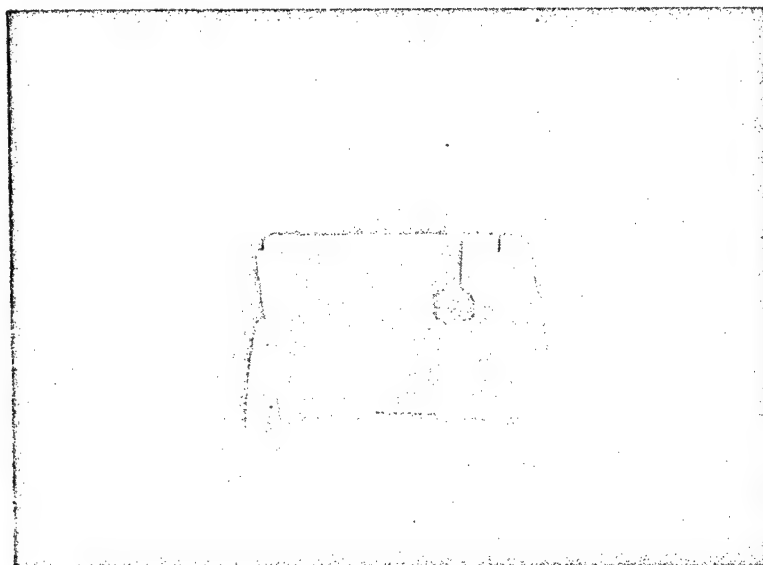


Figure 9. - Columbiuim module 2 after disilicide coating showing coating fixture.



a) Front view



b) Back view

Figure 10.- Inconel module 3 with sensor, thermocouple, and Q-felt insulation installed.

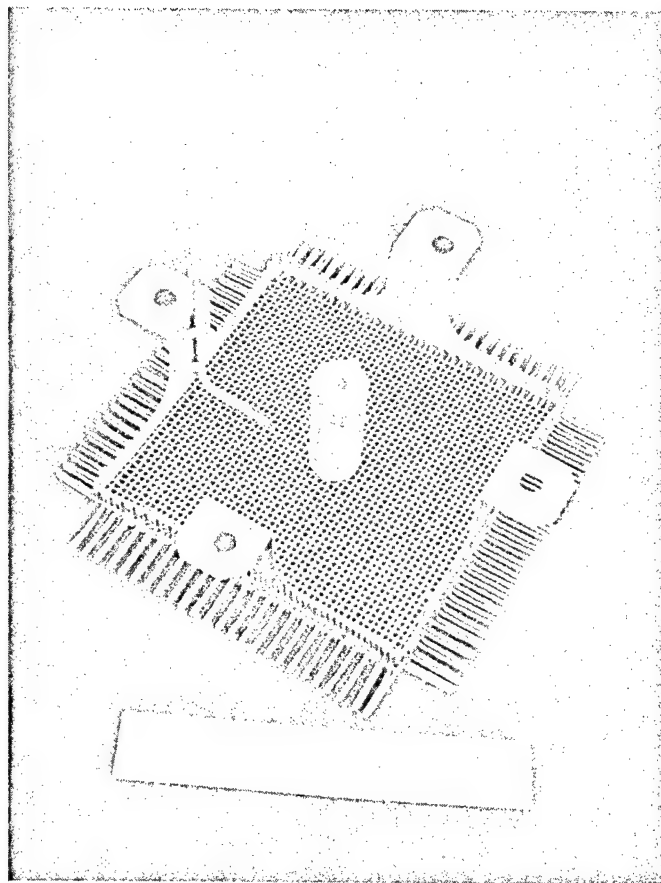


Figure 11.- Chromel/Alumel thermocouple and ceramic sensor tube installed on screen for Inconel module 1.

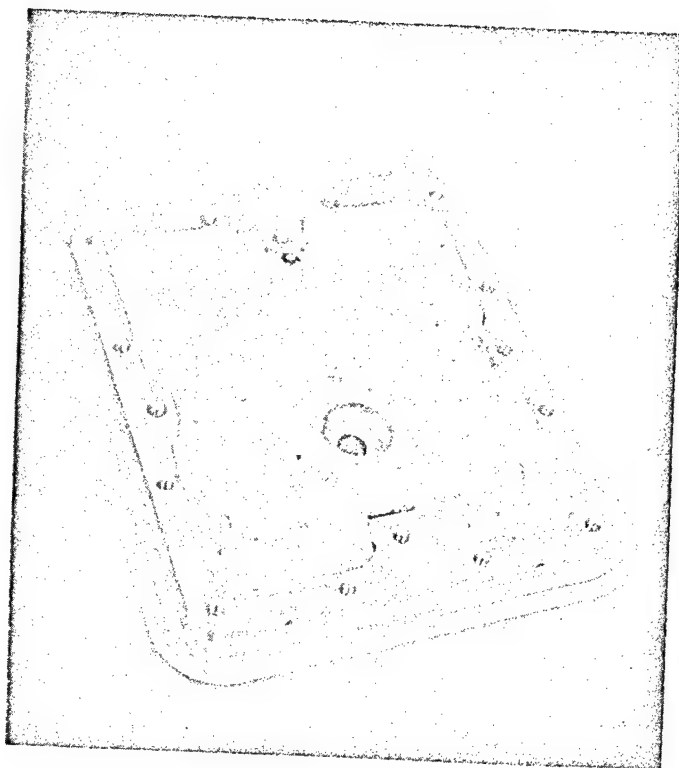


Figure 12.- Silicone sponge installed in the backplate.

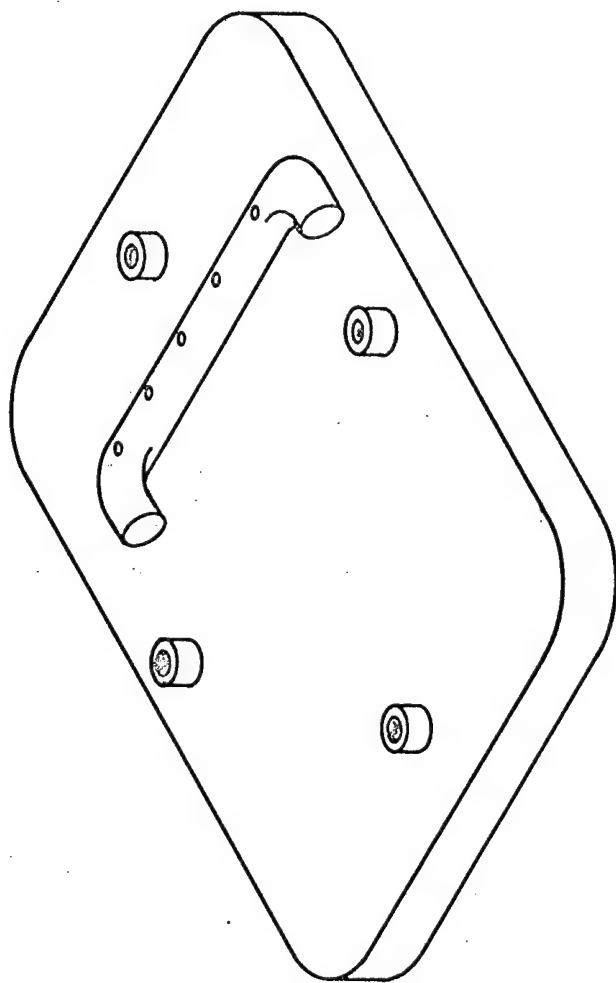
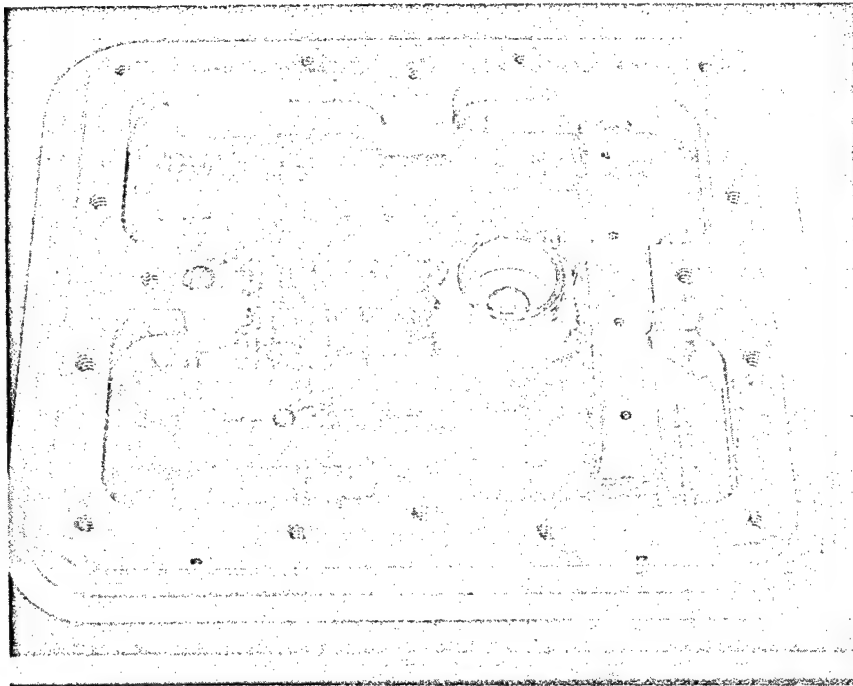
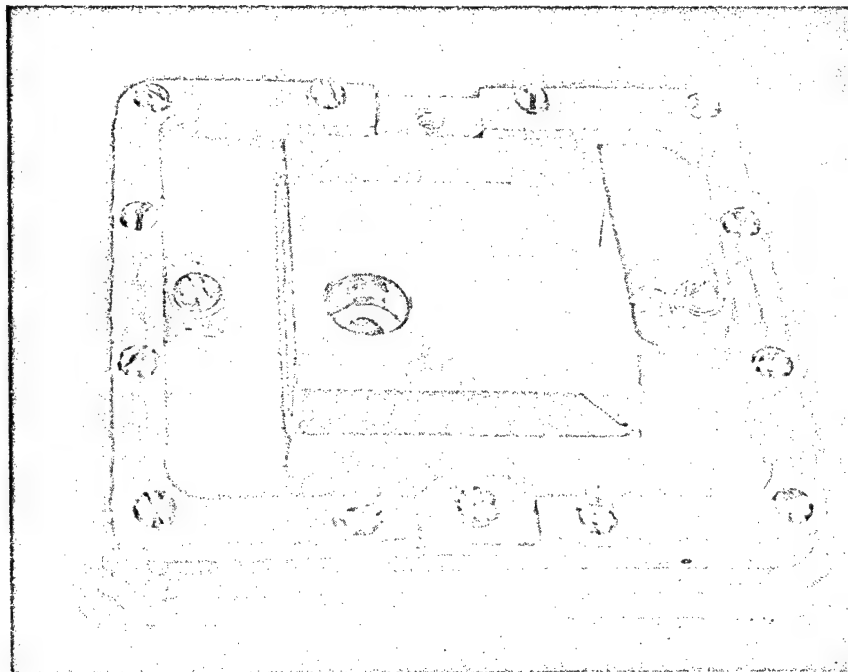


Figure 13. - Backplate for Inconel module 1.



a) Backplate



b) Backplate with silicone sponge, sailcloth pressure barrier, and coolant guide installed

Figure 14. - Backplate for Inconel module 2.

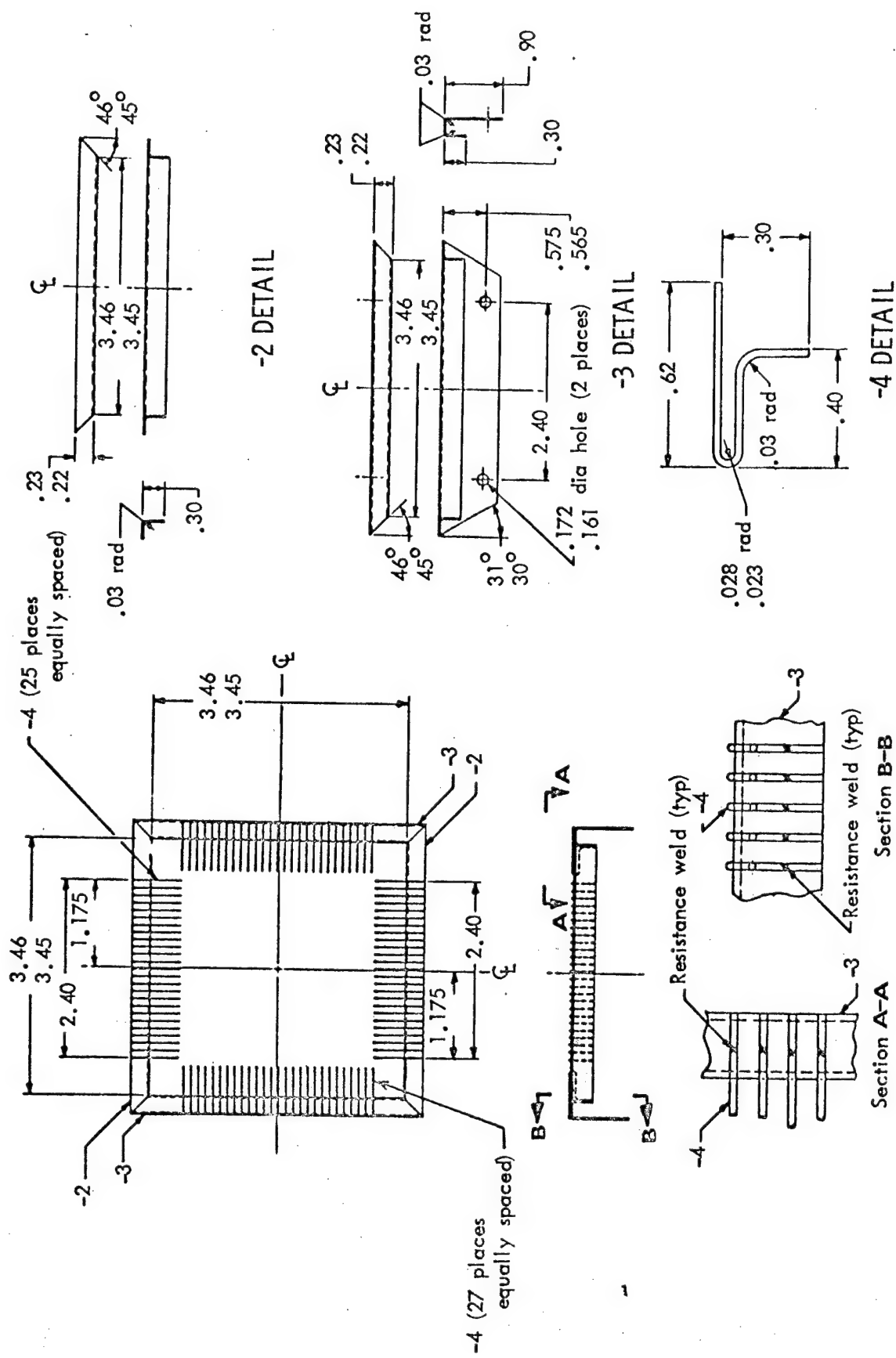
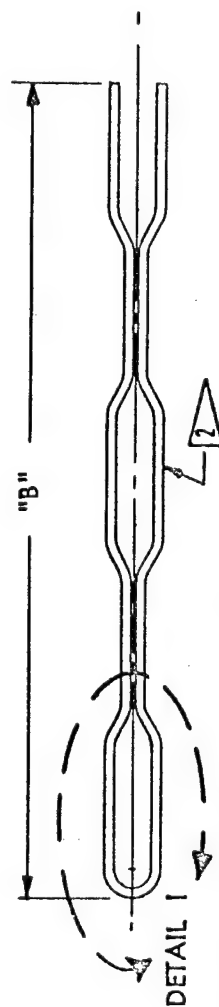
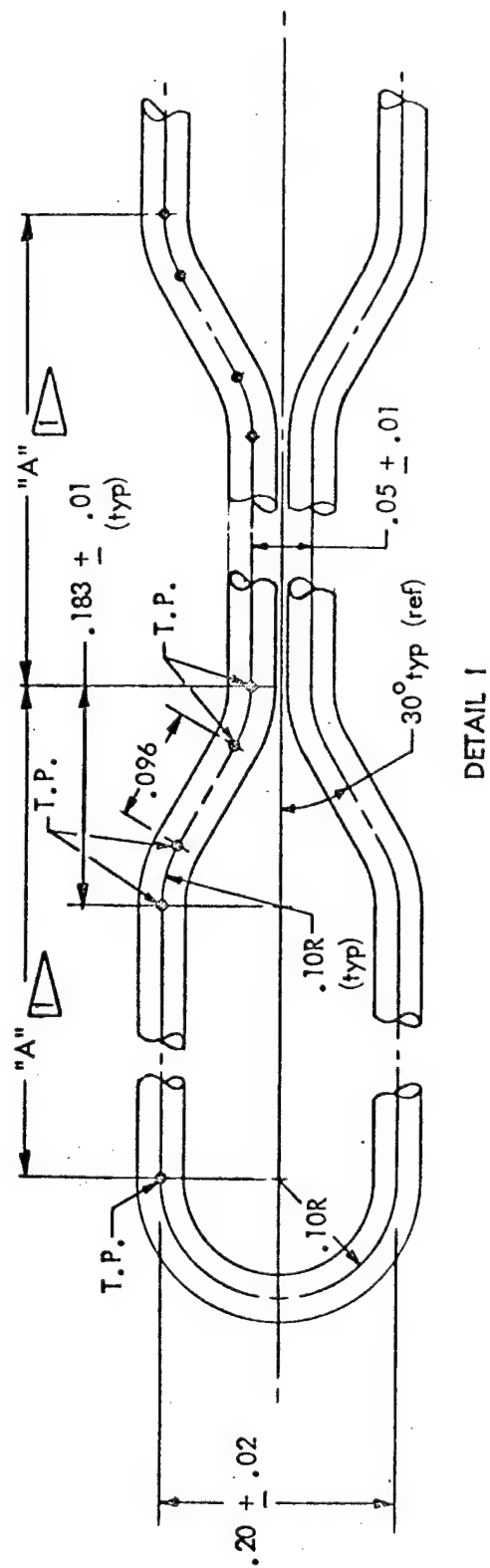


Figure 15.- Attachment frame for module during plasma tests.



Part No.	A	B
-1	.69	3.40
-2	.52	2.55

- 1 Dimension "A" is typ for first four sections of keeper final section (open end) used for tolerance control
- 2 After forming, coat with methyl cellulose .002 thick
Material: .040 dia. nichrome wire and
.030 dia. C-103 columbium wire

Figure 16.- Keeper pins.

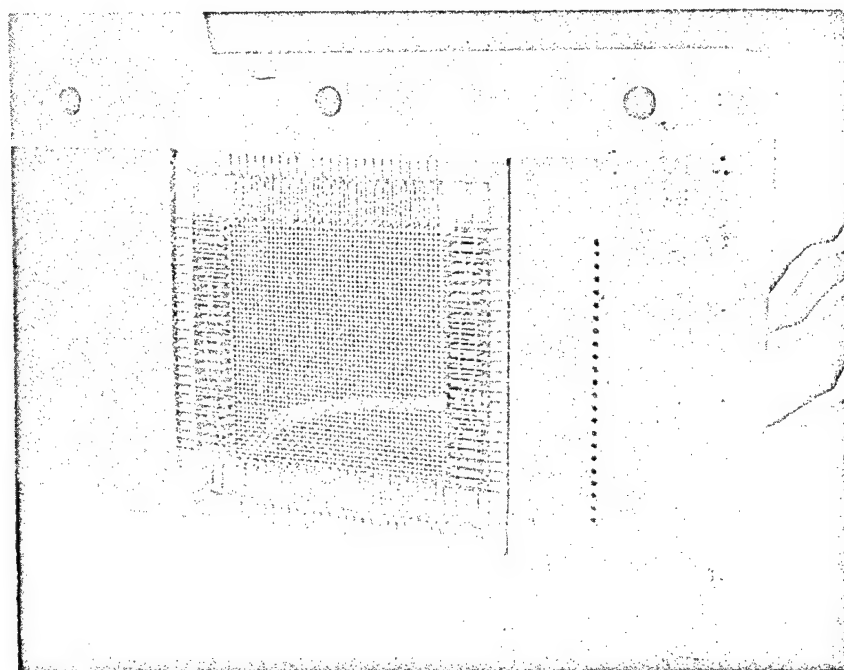
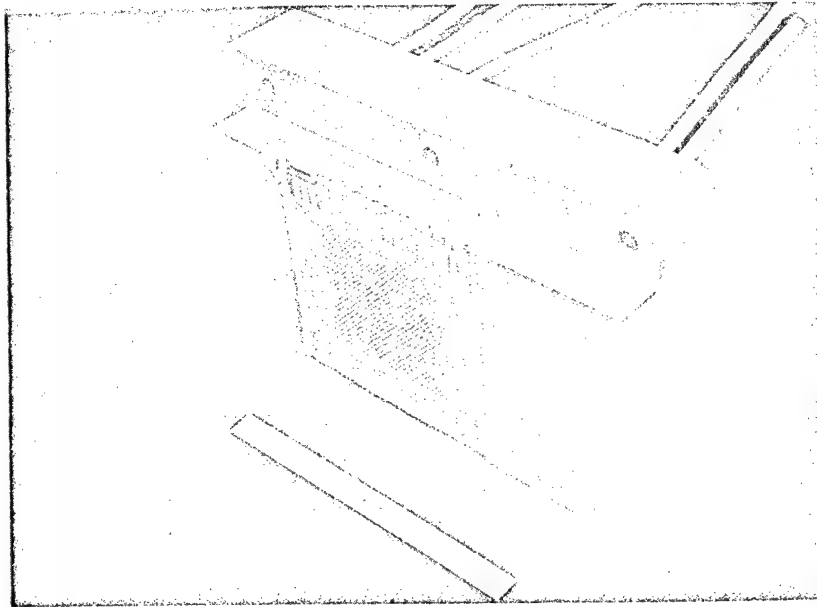
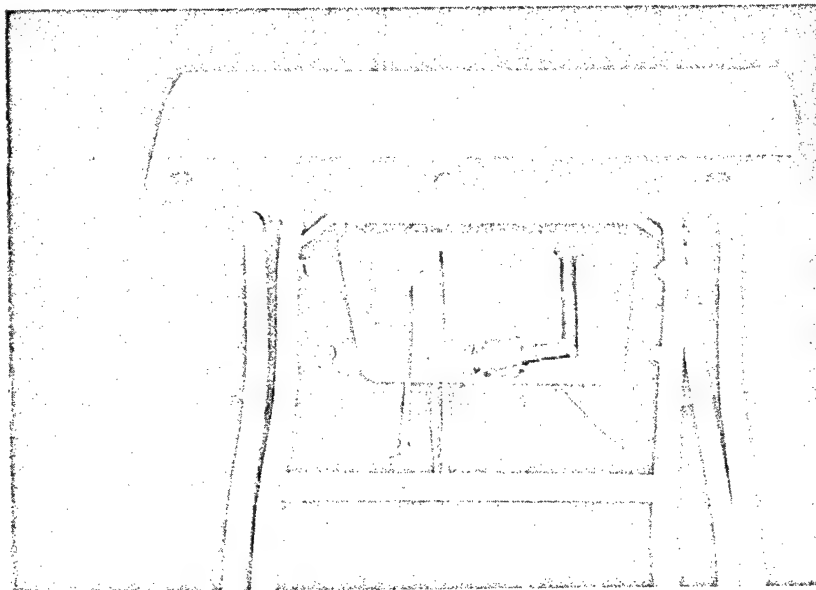


Figure 17.- Inconel screen and holder frame mounted in copper holder.



a) Front view



b) Back view

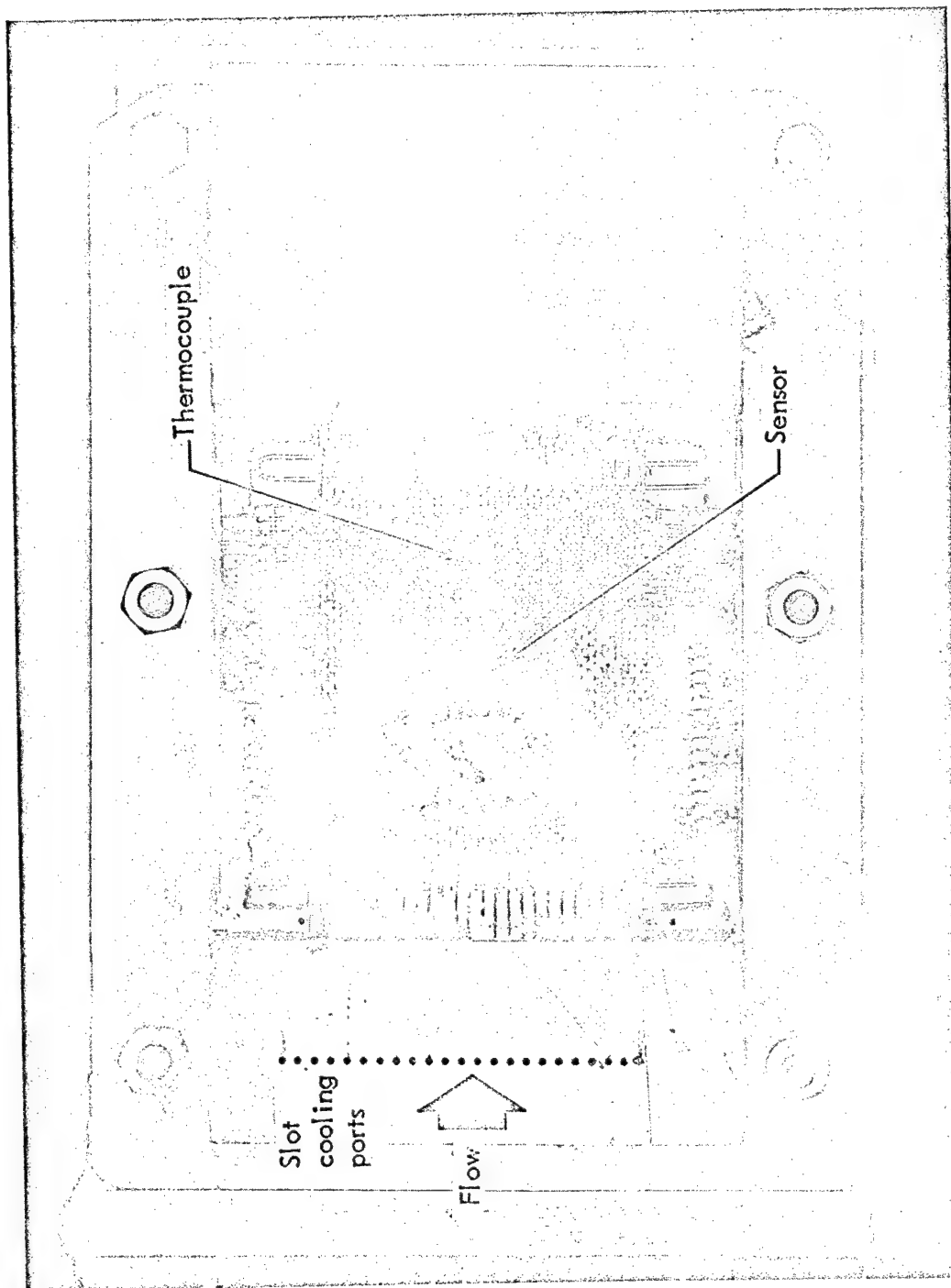


Figure 19. - Inconel module 1 in copper holder subsequent to testing in the Boeing arc plasma facility.

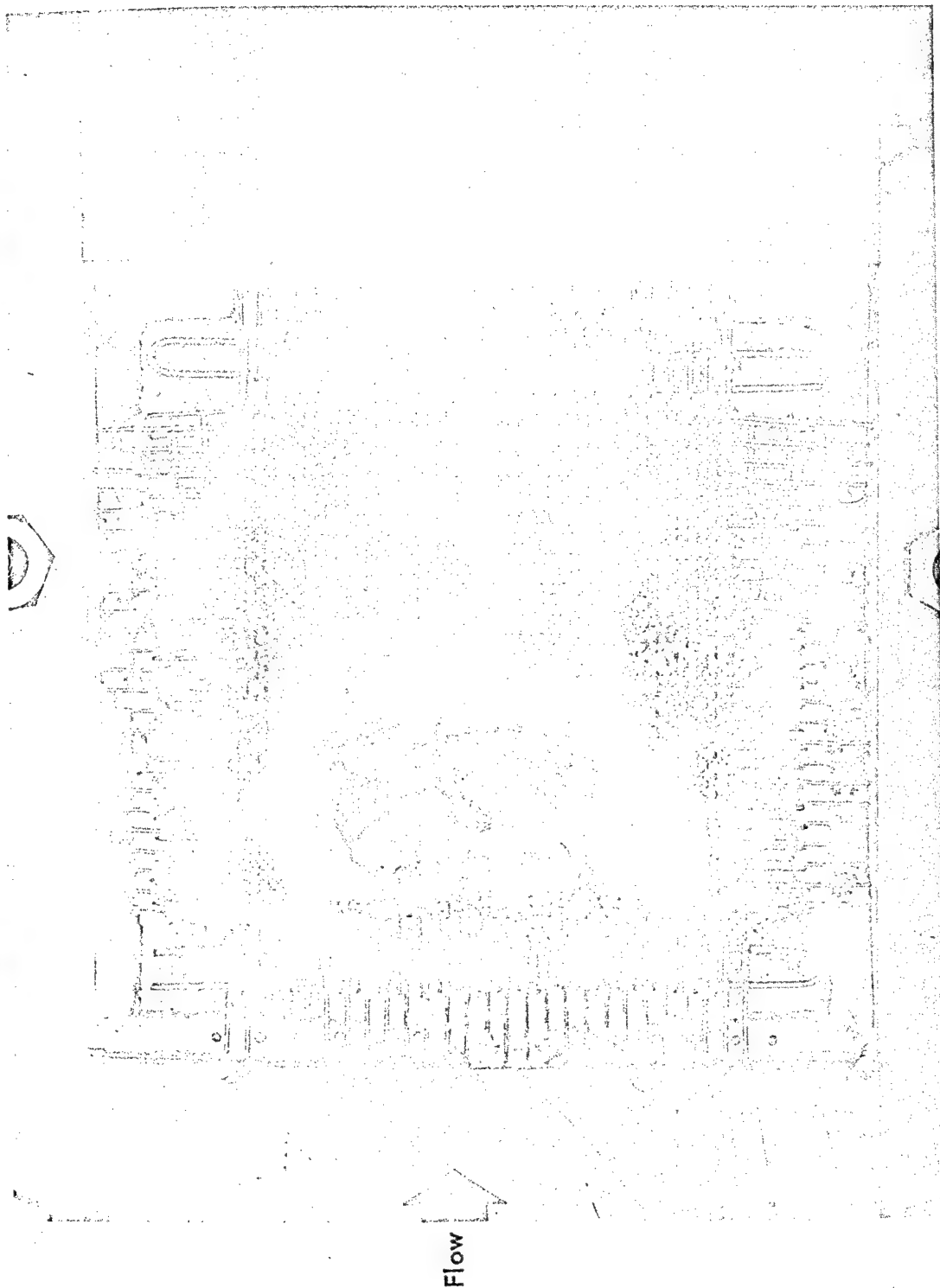


Figure 20. - Close-up of Inconel module 1 in copper holder.

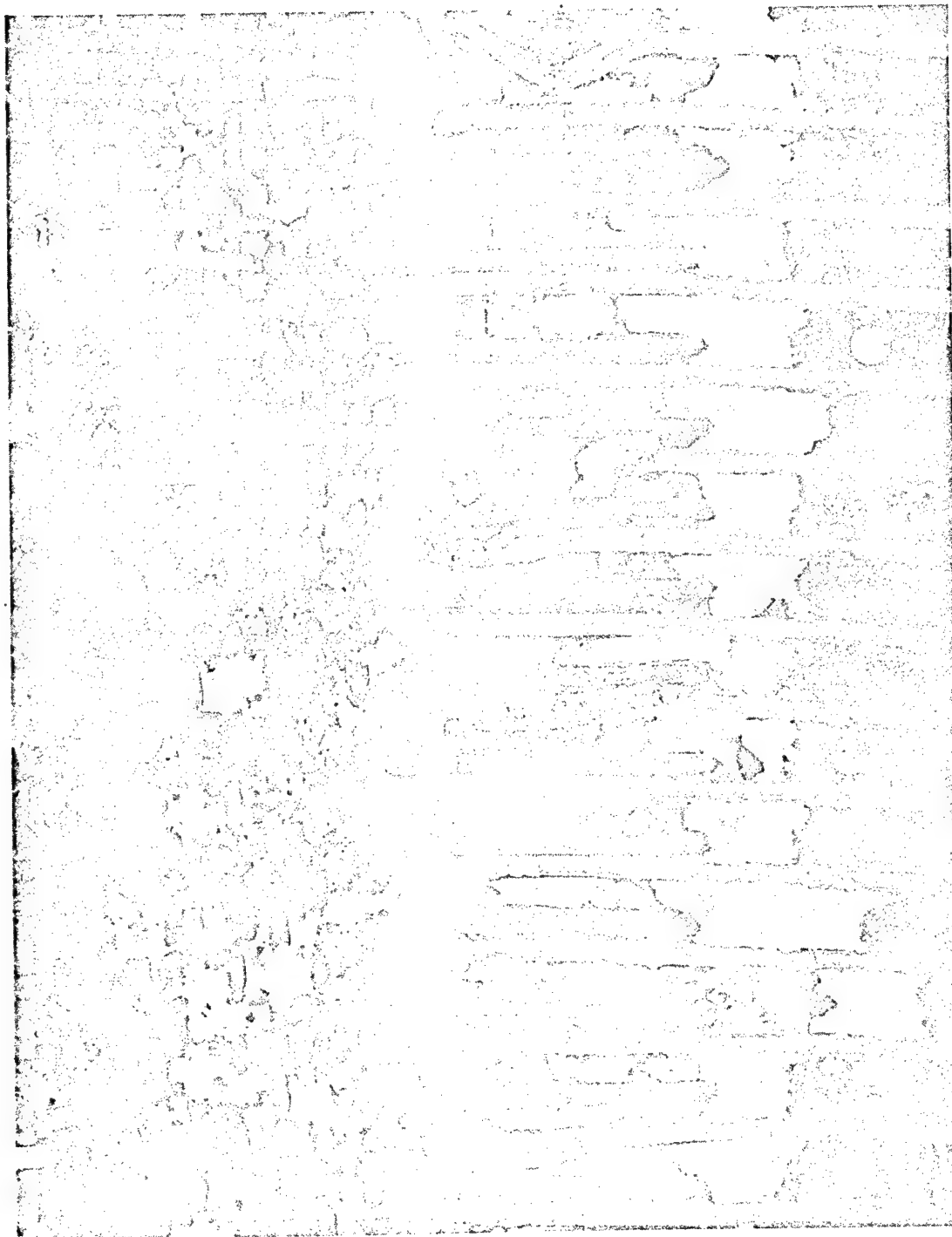


Figure 21. - Close-up of Inconel module 1 and frame showing gaps in insulation and damage to wire loops.

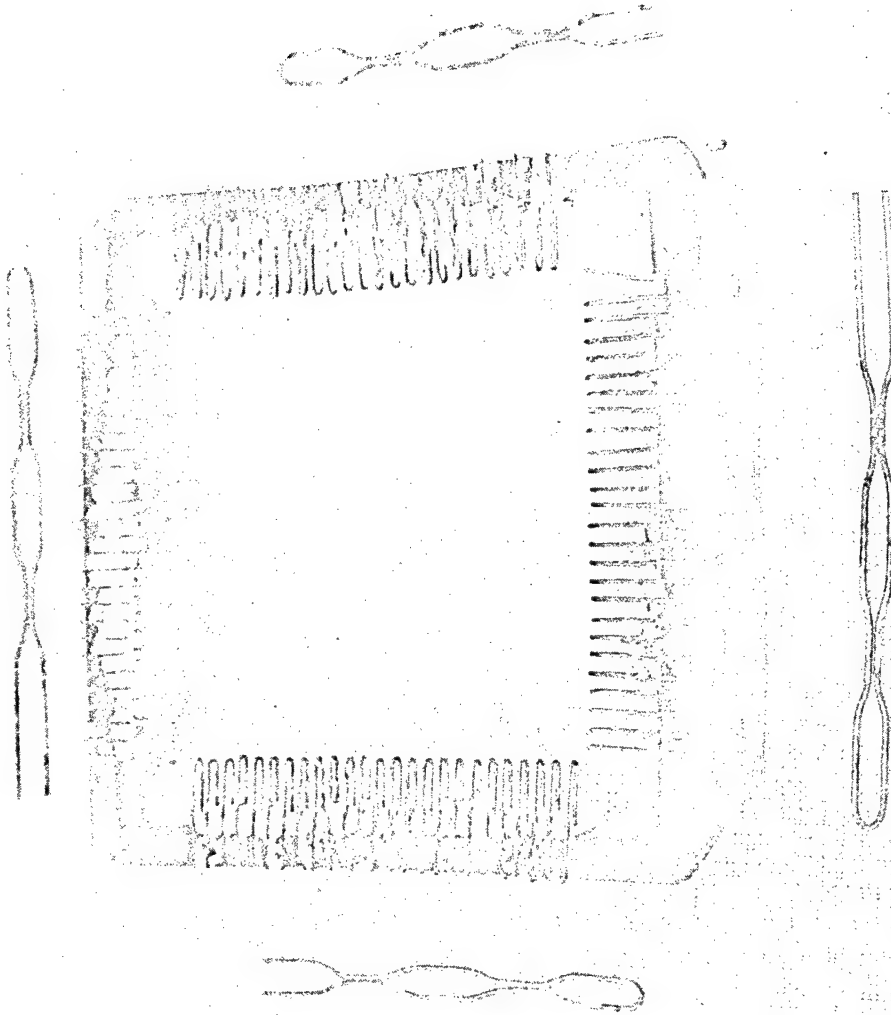




Figure 22. - Frame and keeper pins.

-  Unstabilized Q-felt
-  Heat stabilized Q-felt

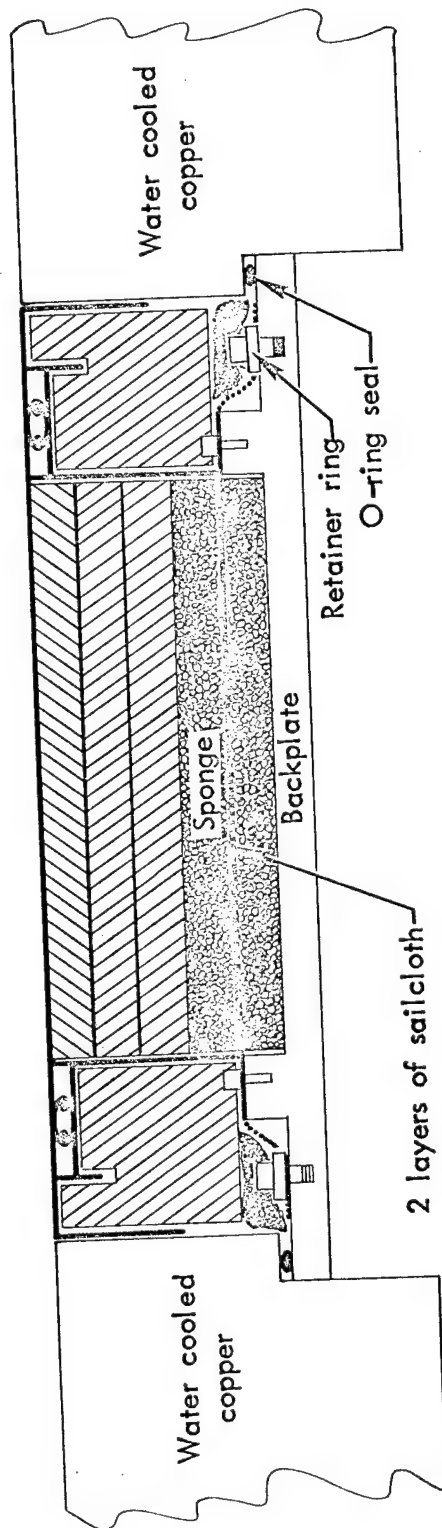


Figure 23.- Layout of Inconel module 1.

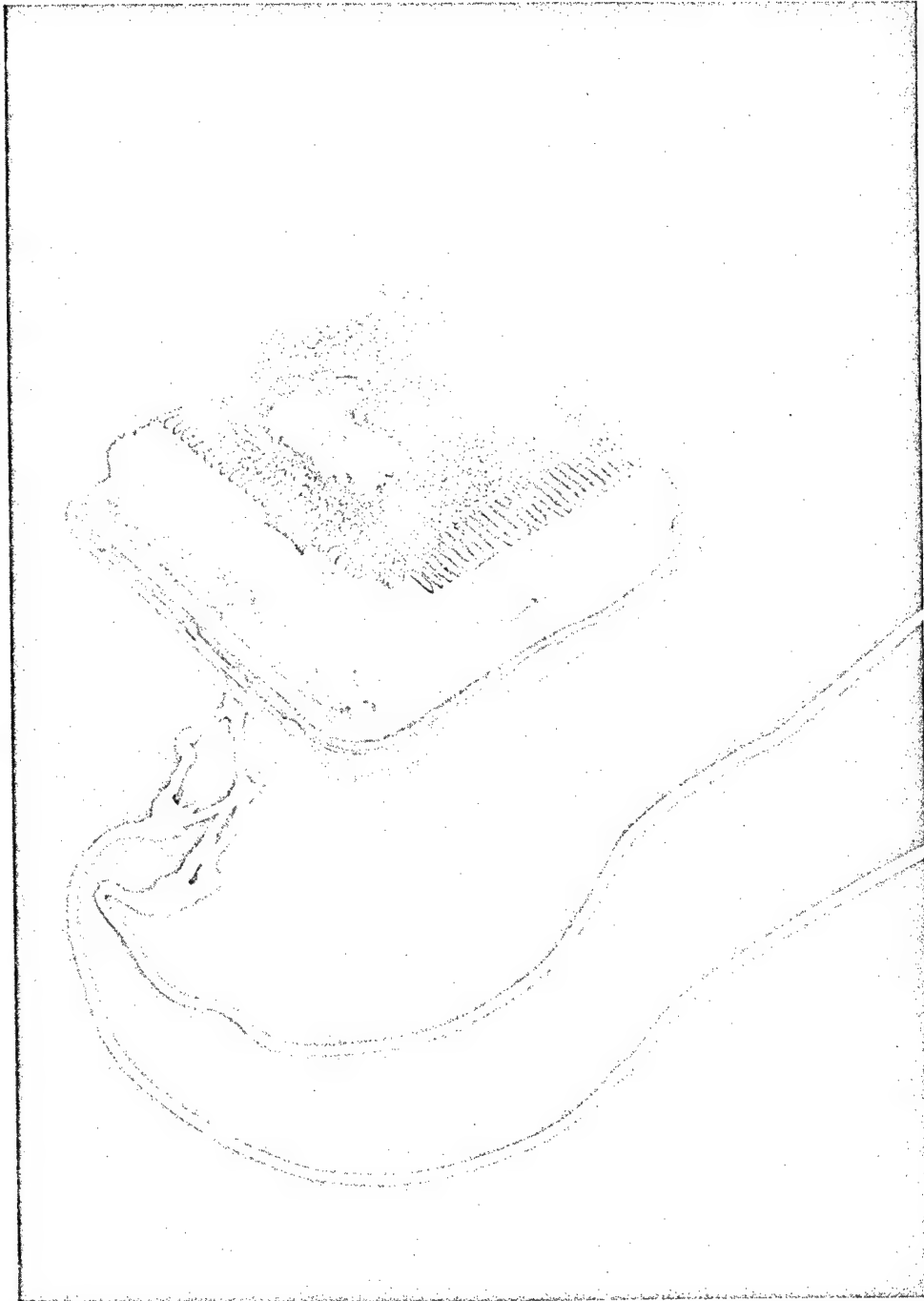
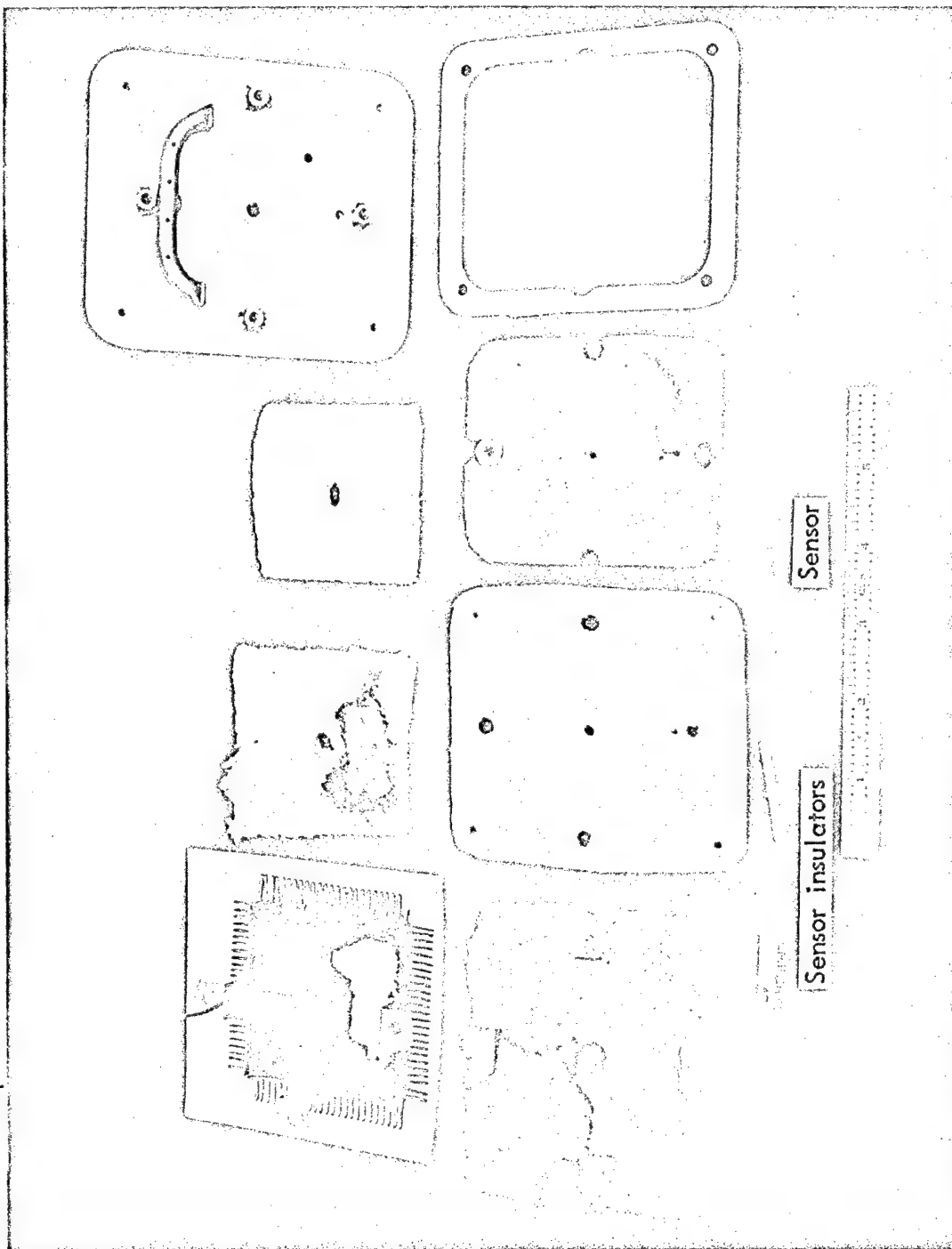


Figure 24. - Inconel module 1.

Inconel screen
component



Q-felt

Backplate



Upper sponge Sailcloth Lower sponge Retainer ring

Figure 25. - Post-test examination of Inconel module 1 components.

-  Heat stabilized Q-felt
-  Unstabilized Q-felt

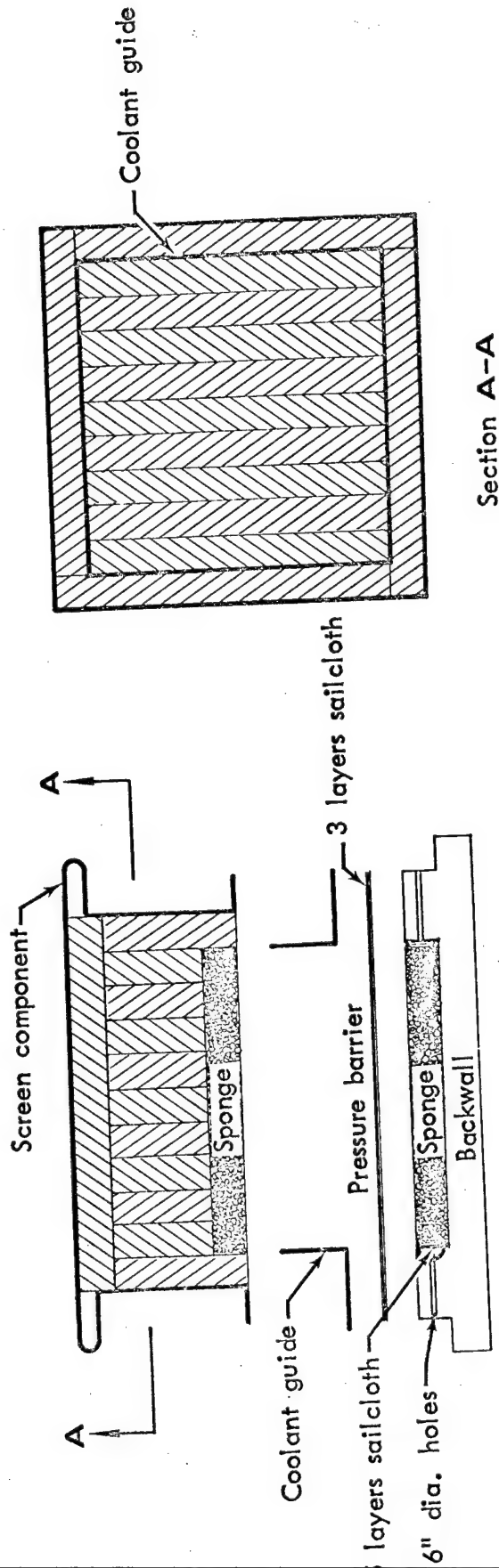
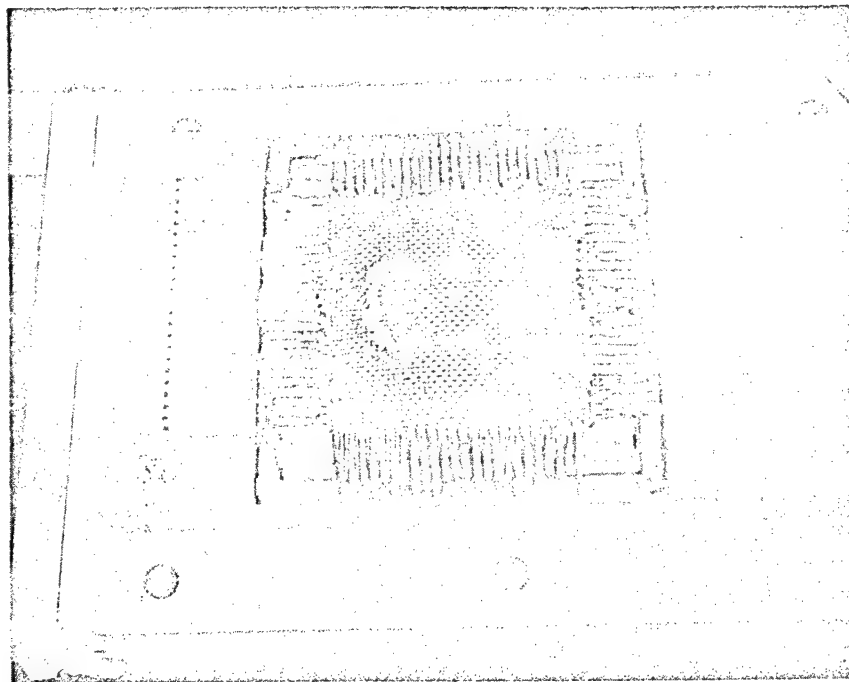
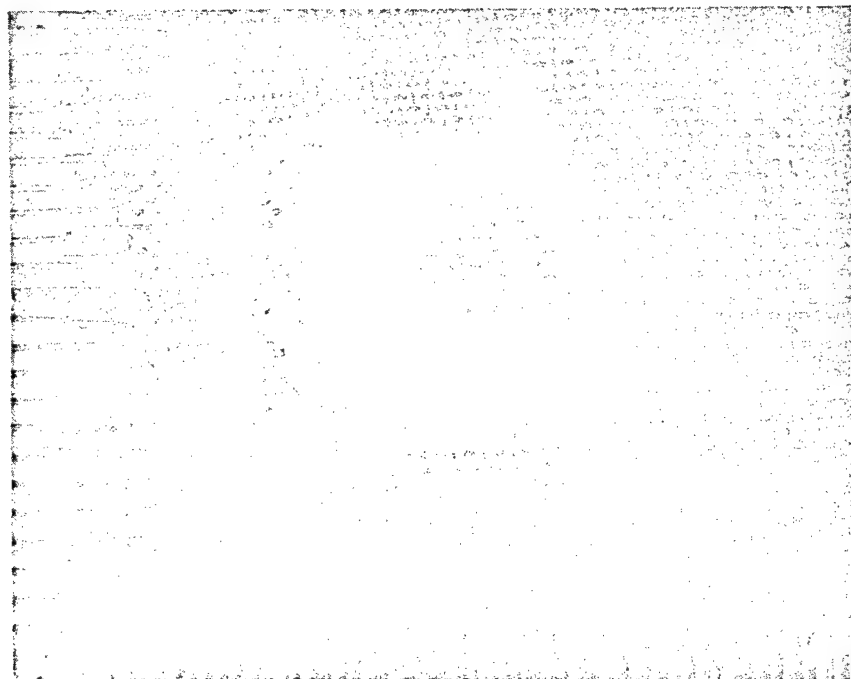


Figure 26. - Design changes to correct for coolant channeling.

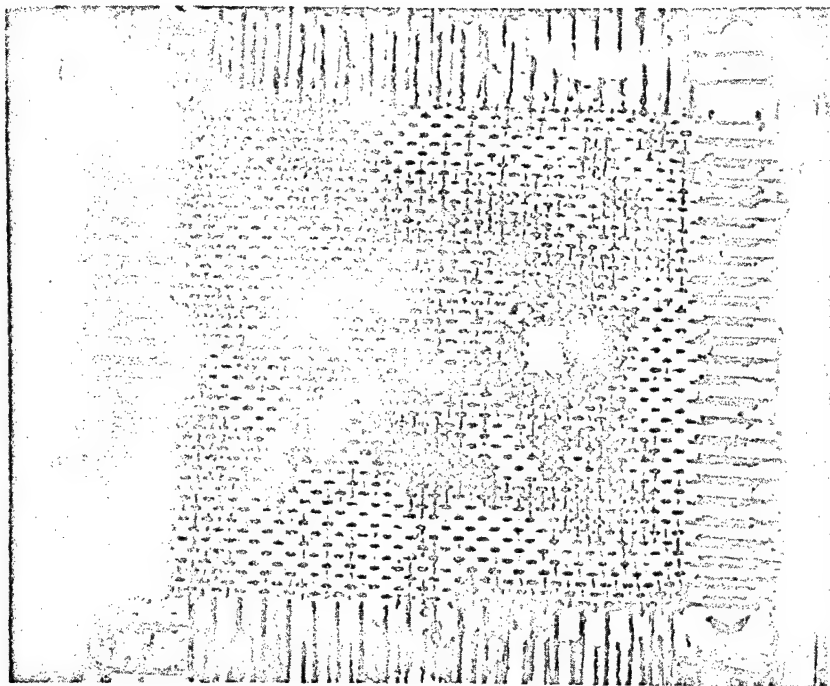


a) Front view

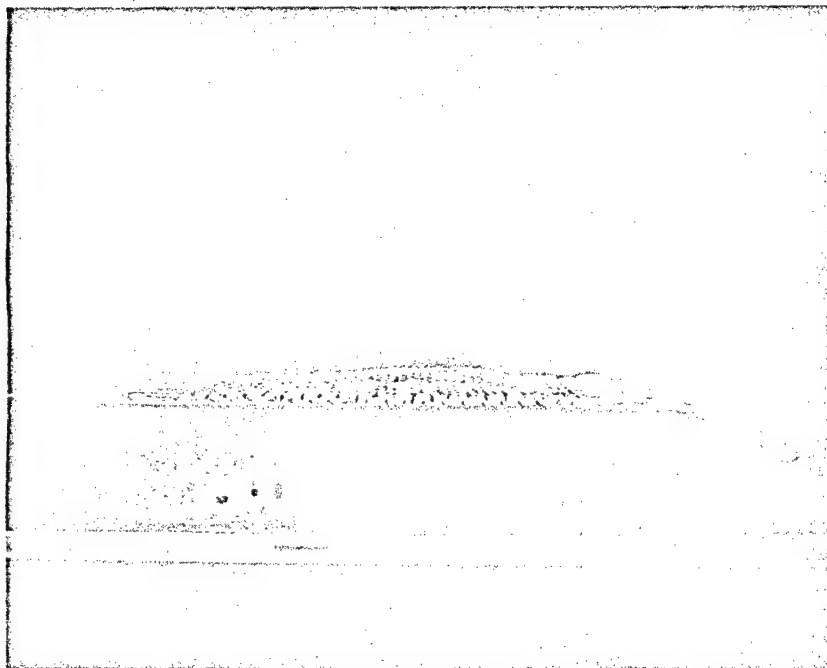


b) Closeup of module

Figure 27.- Inconel module 2 subsequent to testing in the Boeing arc plasma facility.

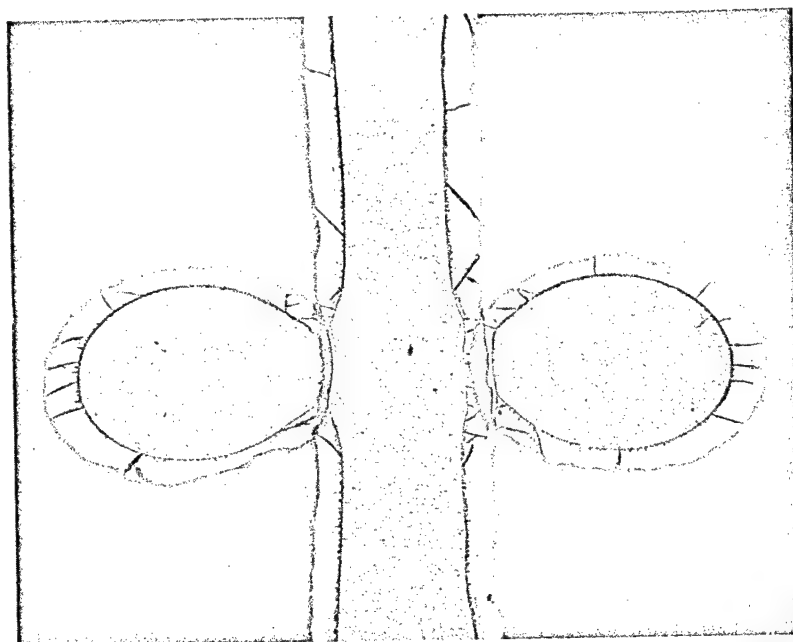


a) Front view



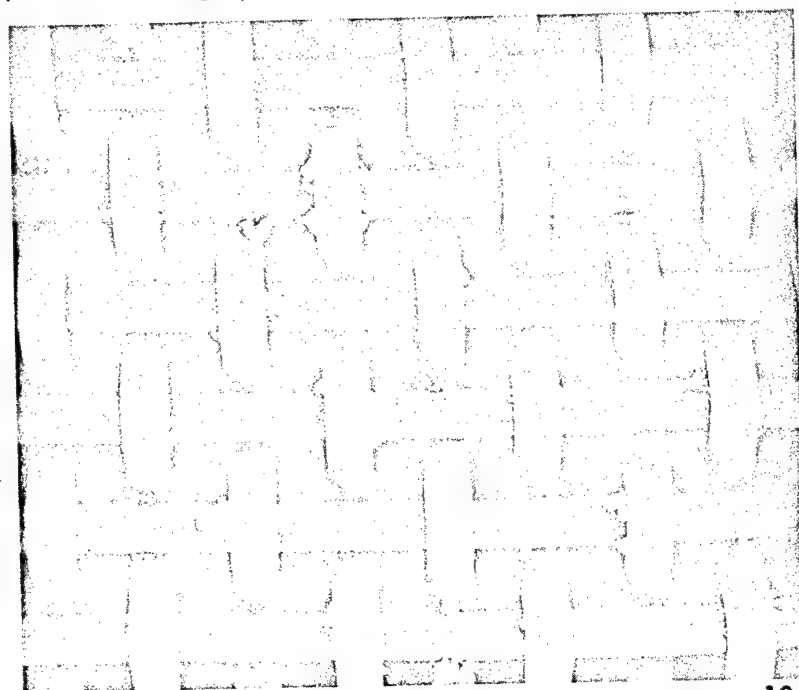
b) Side view showing surface distortion

Figure 28.- Columbia module 1 subsequent to testing in the Boeing arc plasma facility.



50x

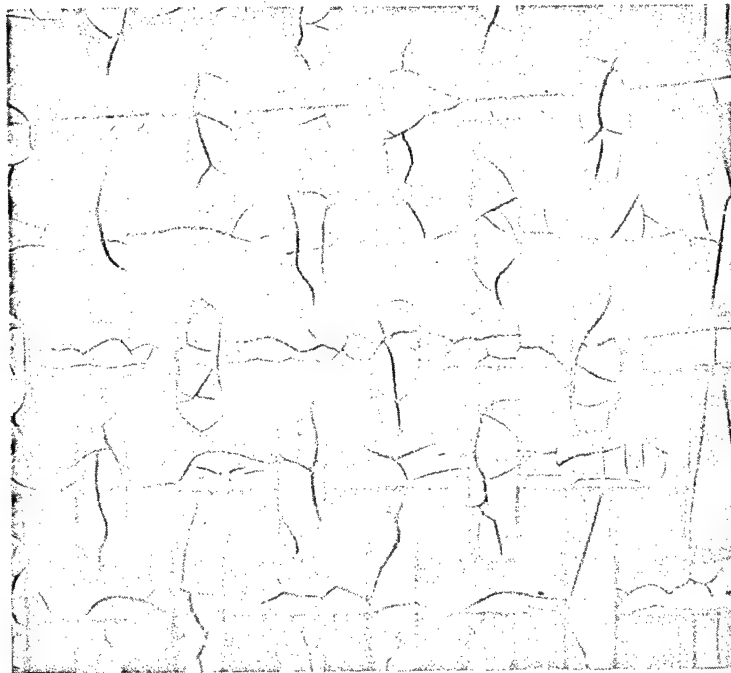
a) Photomicrograph of cross section of columbium screen



10x

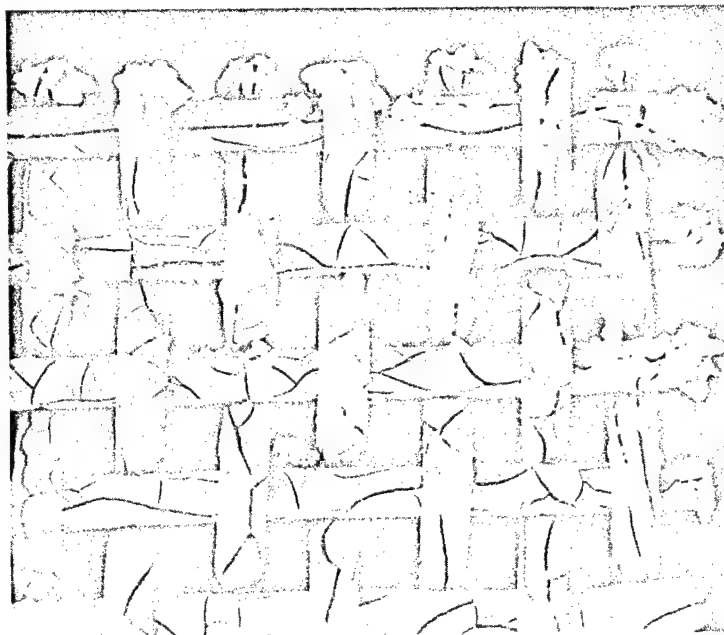
b) Columbium screen subsequent to oxidation testing at 2500 °F. Oxidation failure indicated by columbium oxide growing from wire intersections

Figure 29. - C-103 columbium wire screen with a thin disilicide coating.



10x

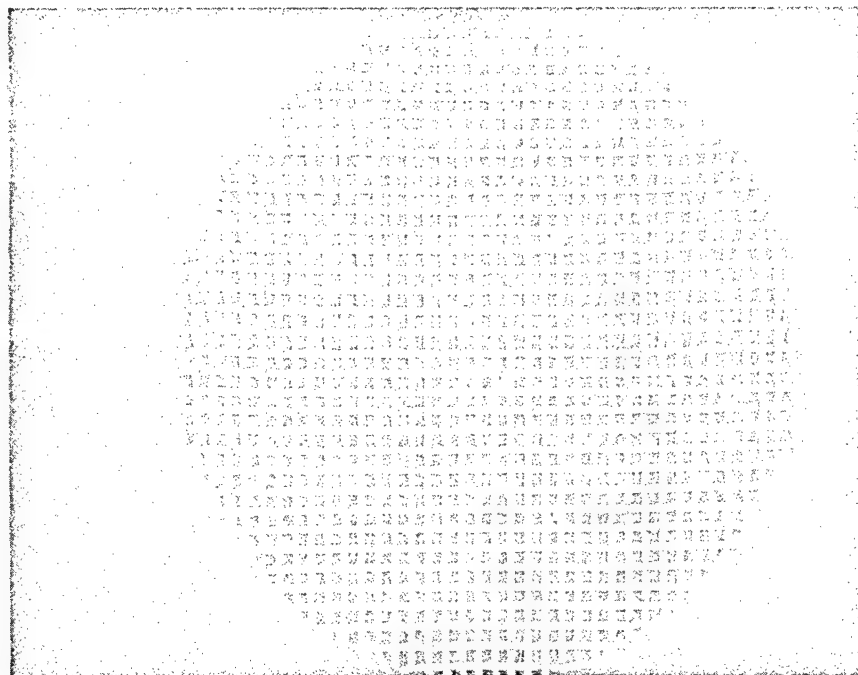
a) Thermal cracks in disilicide coating



10x

b) Columbium screen subsequent to oxidation testing for 1 hour at 2500 °F. Oxidation failure indicated by columbium oxide growing from wire intersections.

Figure 30. - C-103 columbium wire screen with a thick disilicide coating



2x

a) Columbium screen subsequent to oxidation testing at 2500 °F (10 cycles of 15 minutes each)

Failure



10x

b) Oxidation failure indicated by presence of columbium oxide

Figure 31. - C-103 columbium wire screen with an optimized disilicide coating.

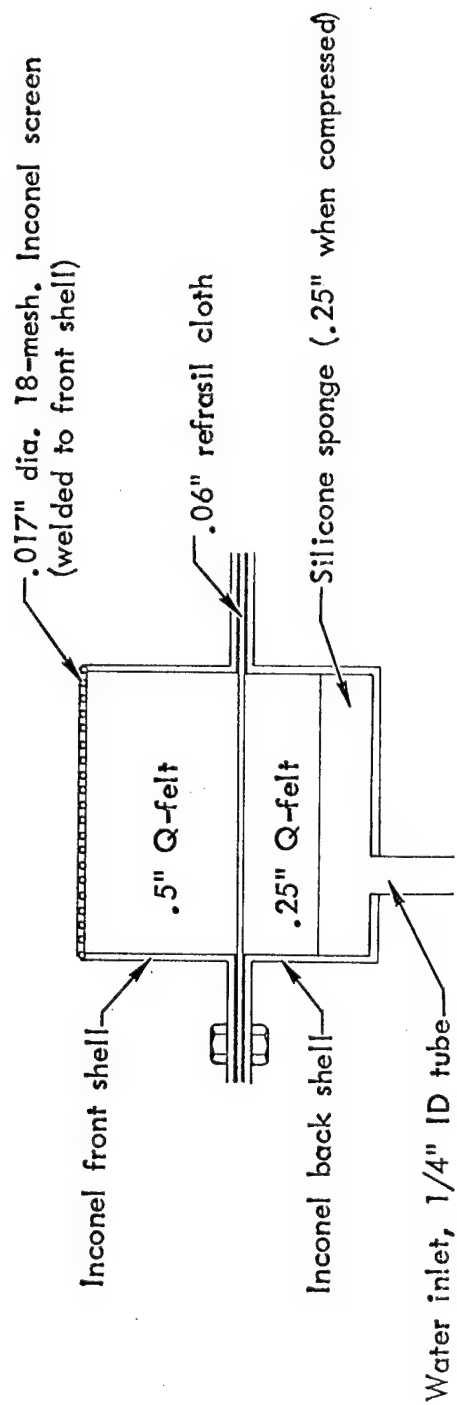


Figure 32. - Two-inch diameter flame test unit design I.

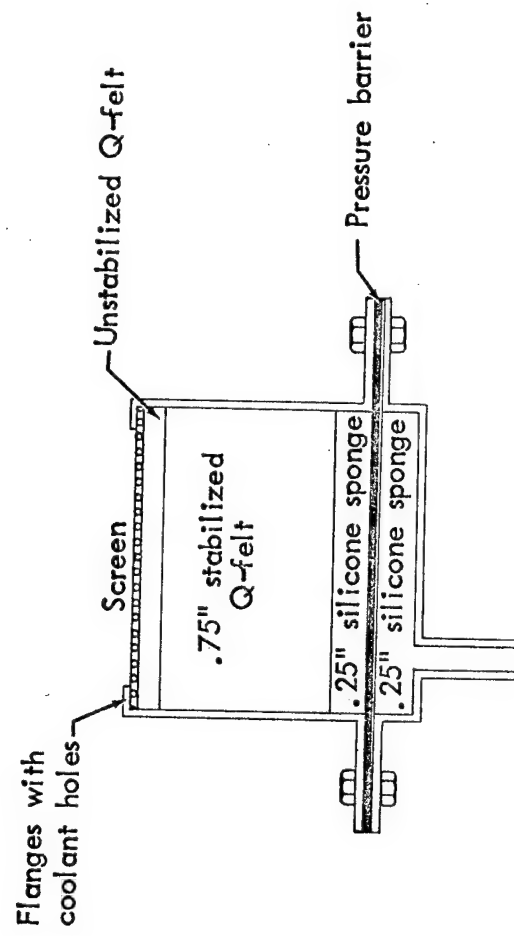


Figure 33.- Two-inch diameter flame test unit design II.

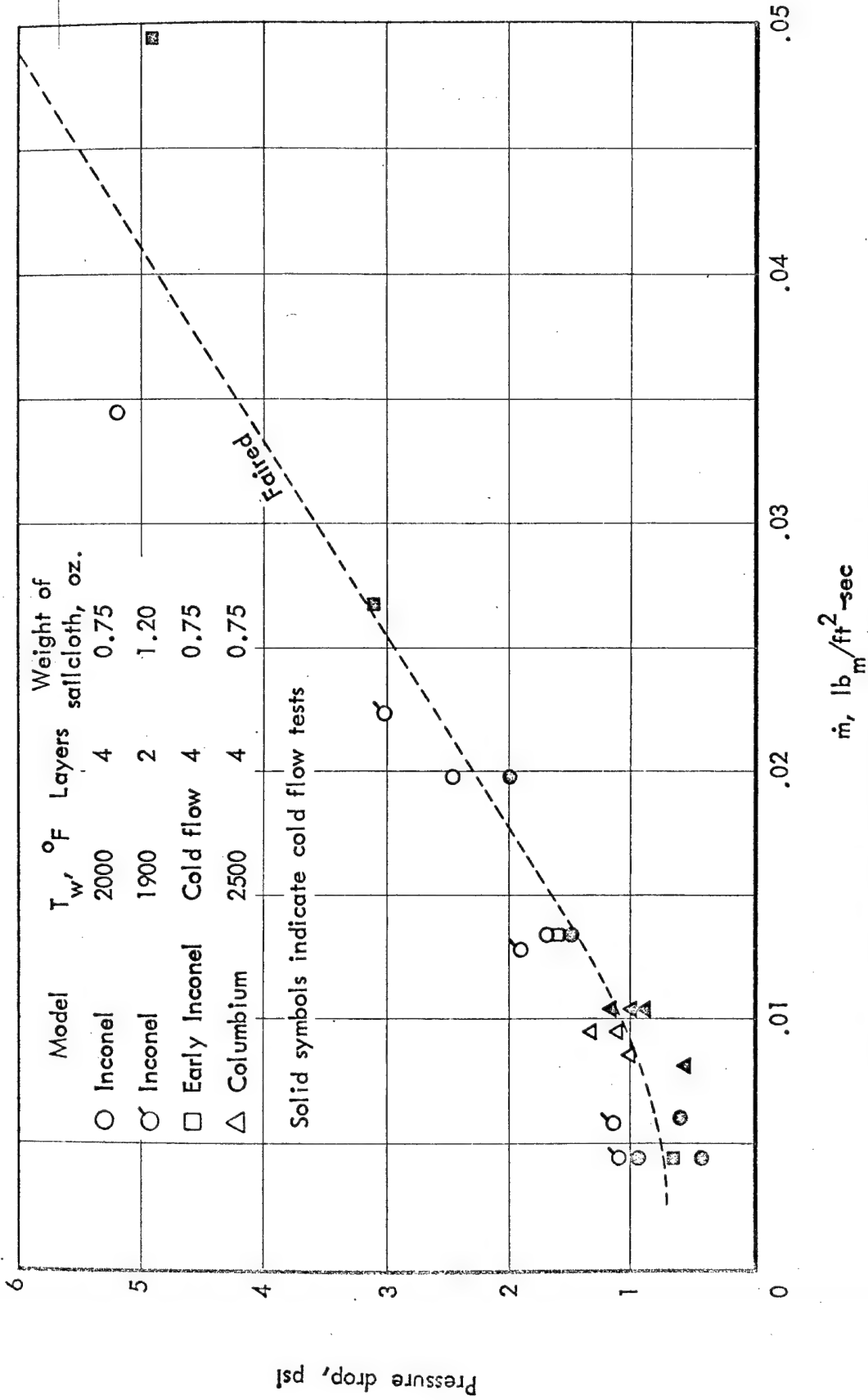


Figure 34. - Transpiration cooling module pressure drop without sensor or thermocouple.

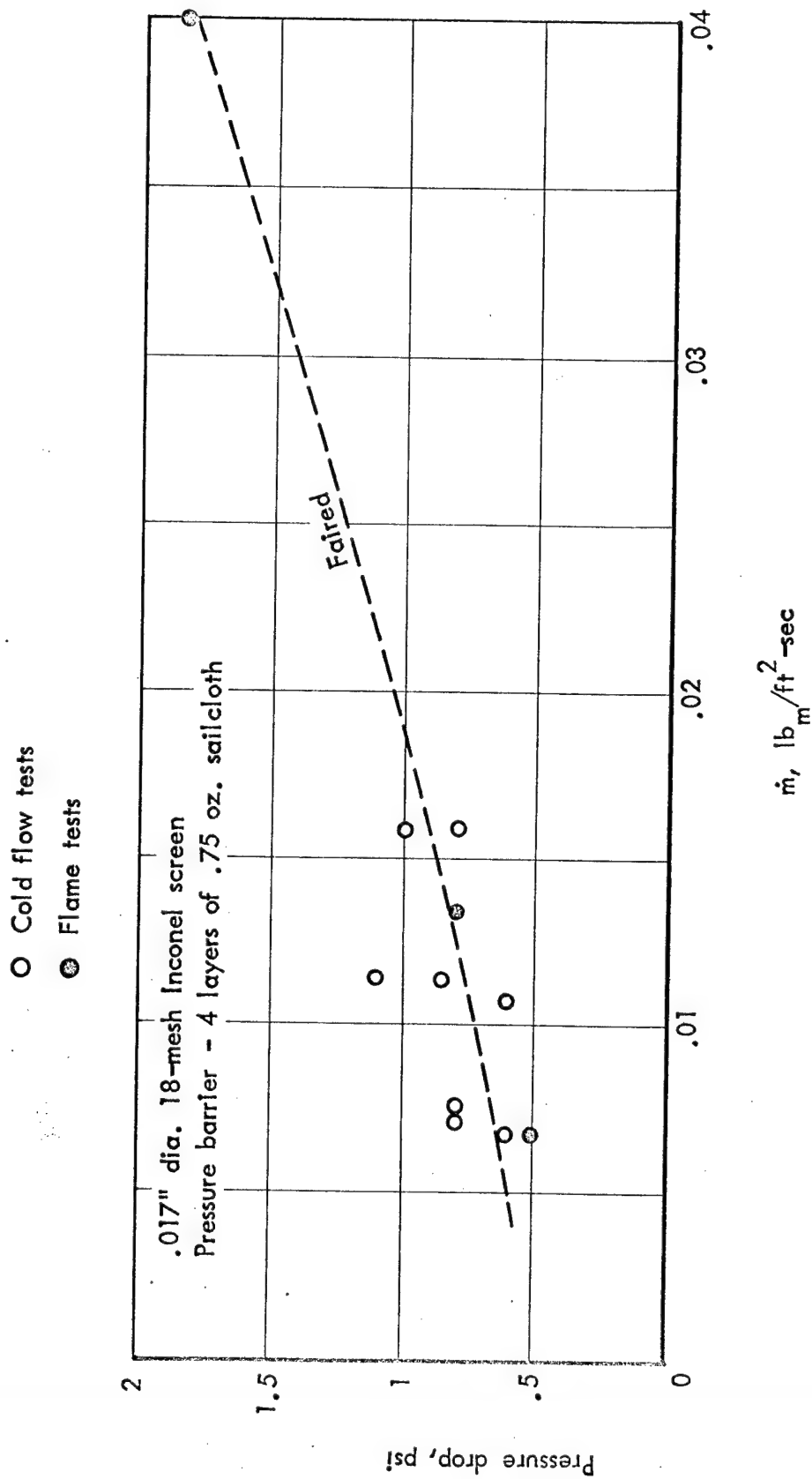


Figure 35.- Transpiration cooling module pressure drop with ceramic sensor tube and thermocouples.

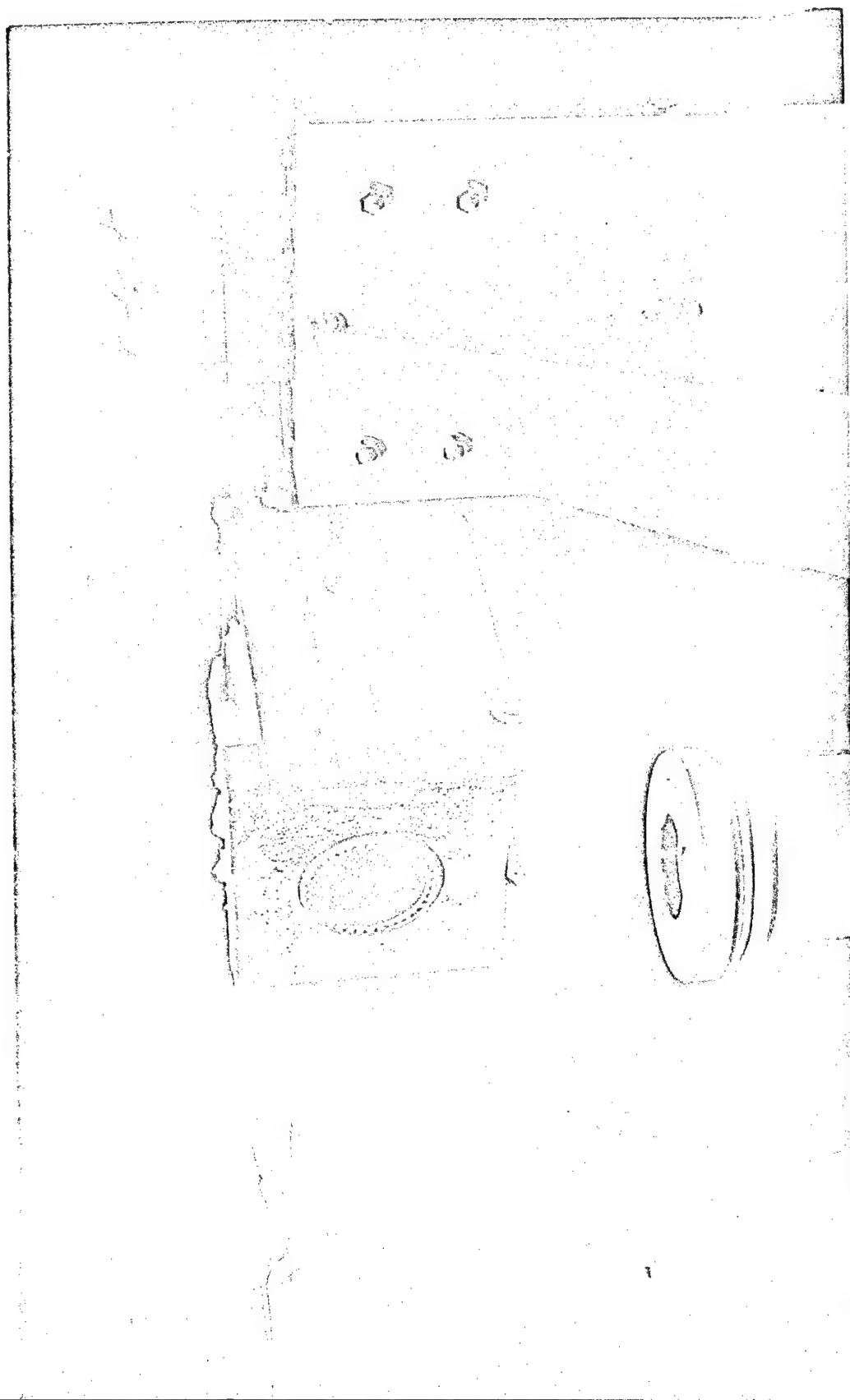


Figure 36. - Flame test unit with .025" dia. 20-mesh Inconel screen.

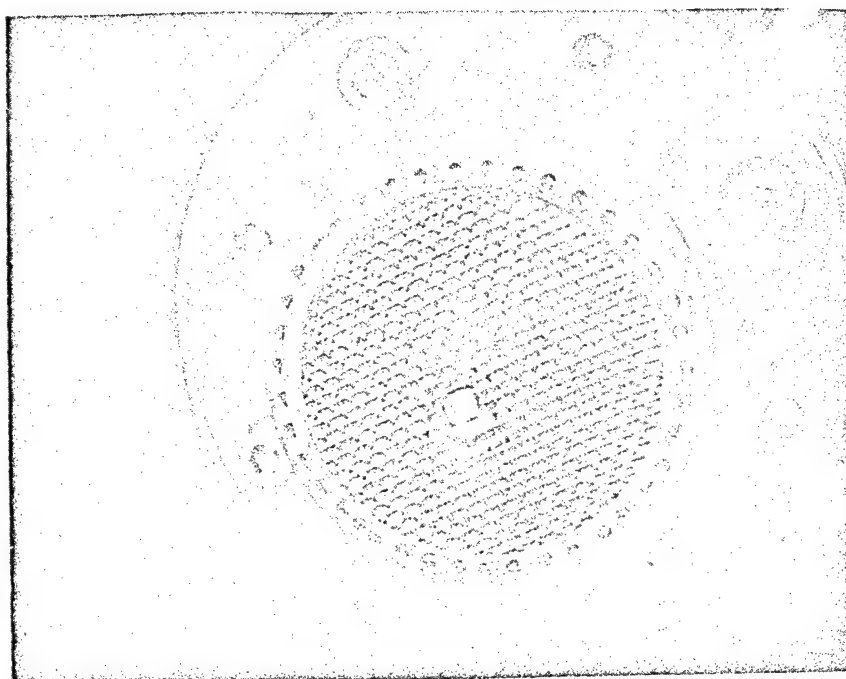


Figure 37.- Columbium flame test unit subsequent to 4 hours of flame testing for sensor and controller calibration.

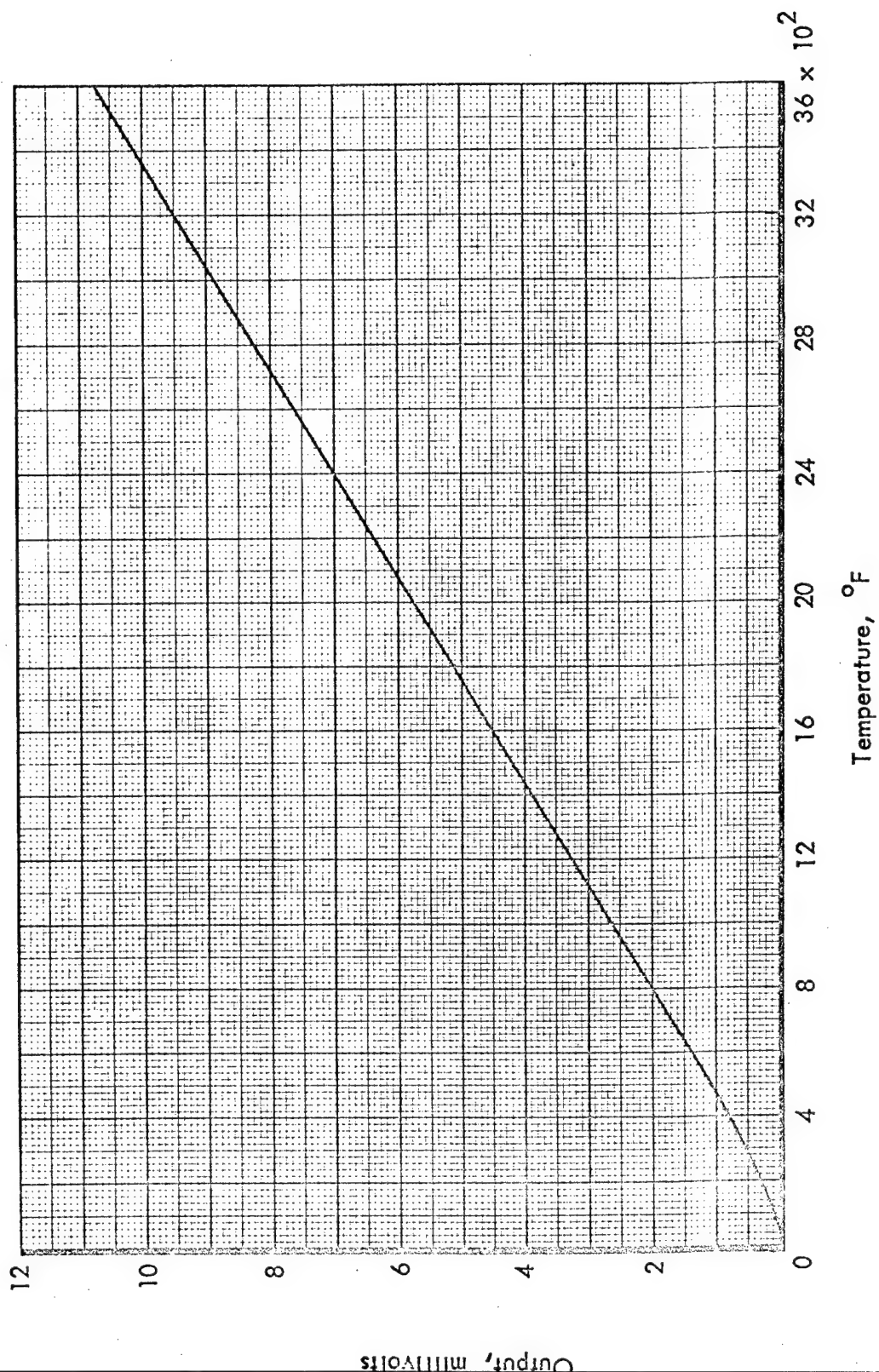


Figure 38. - Calibration curve for iridium - 40 rhodium/iridium thermocouple.

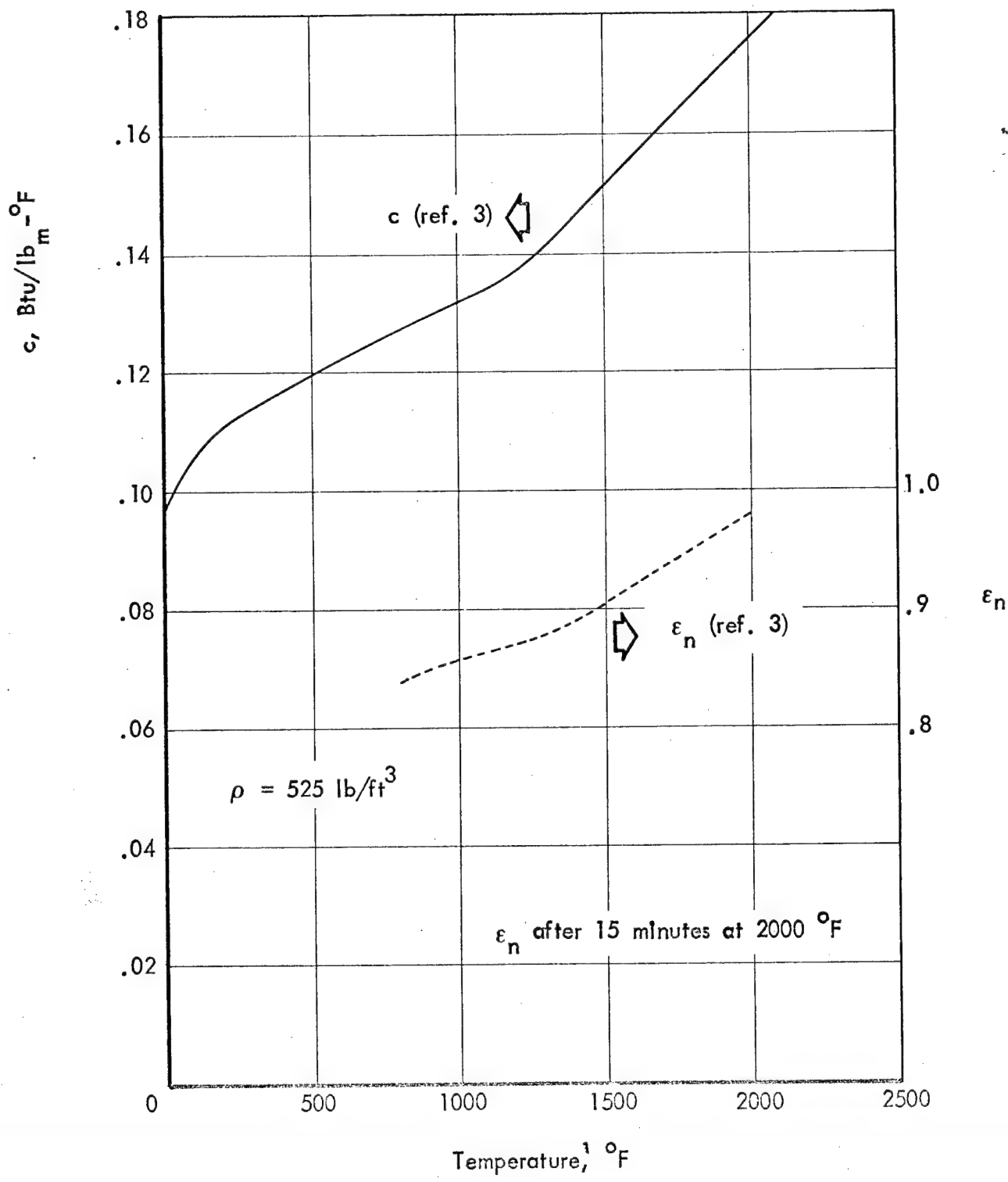


Figure 39. - Properties of Inconel.

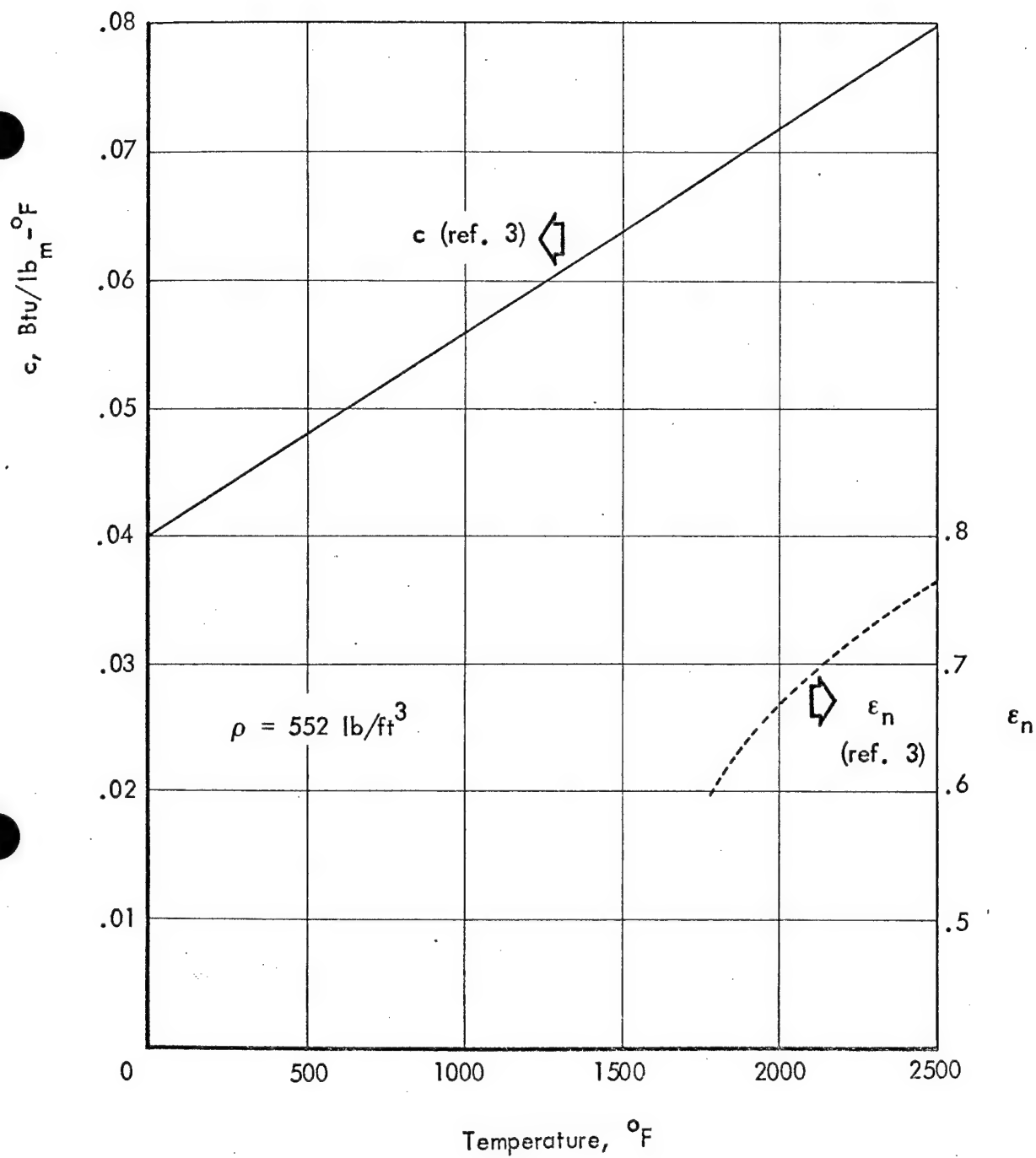


Figure 40. - Properties of columbium.

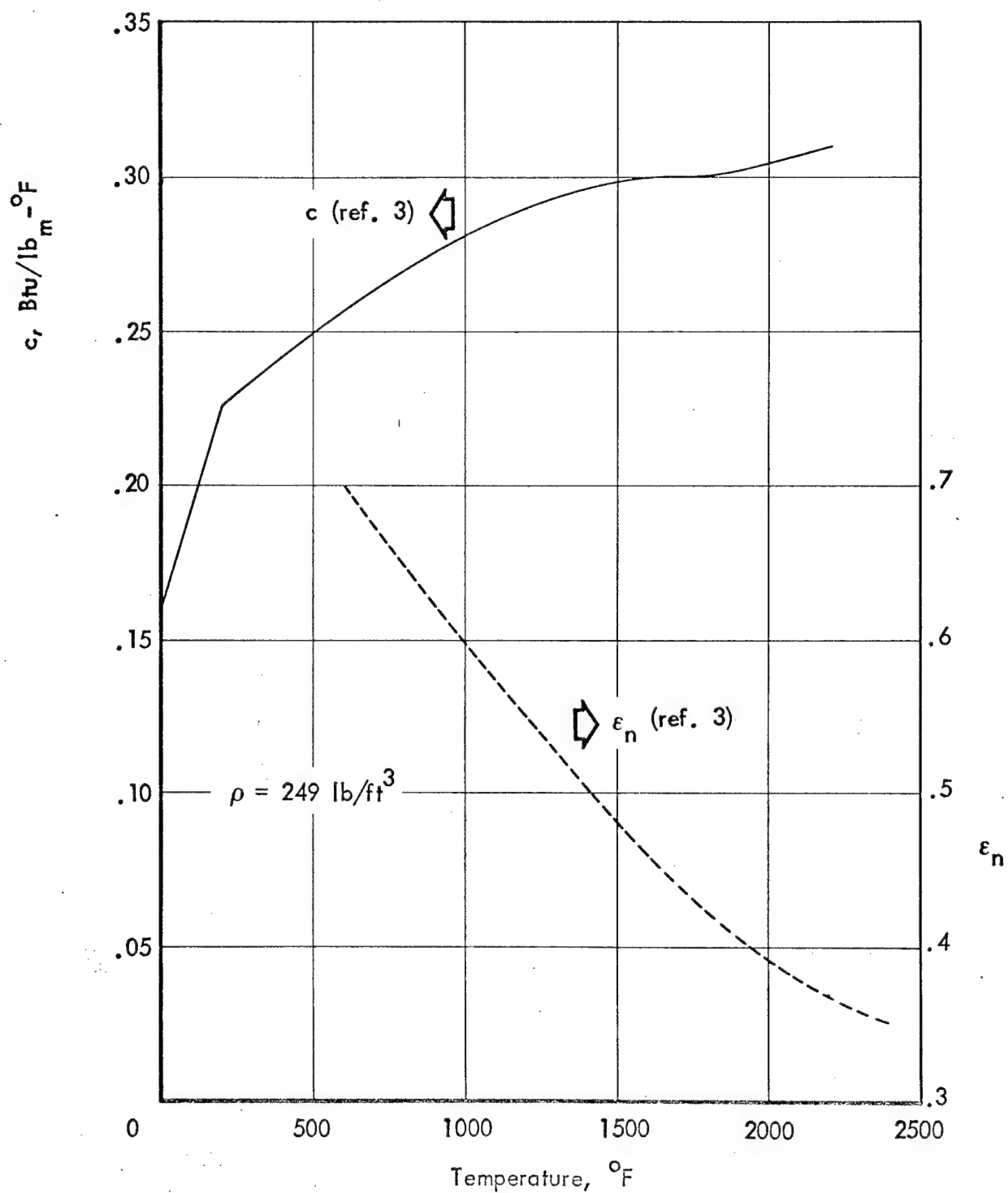


Figure 41. - Properties of aluminum oxide.

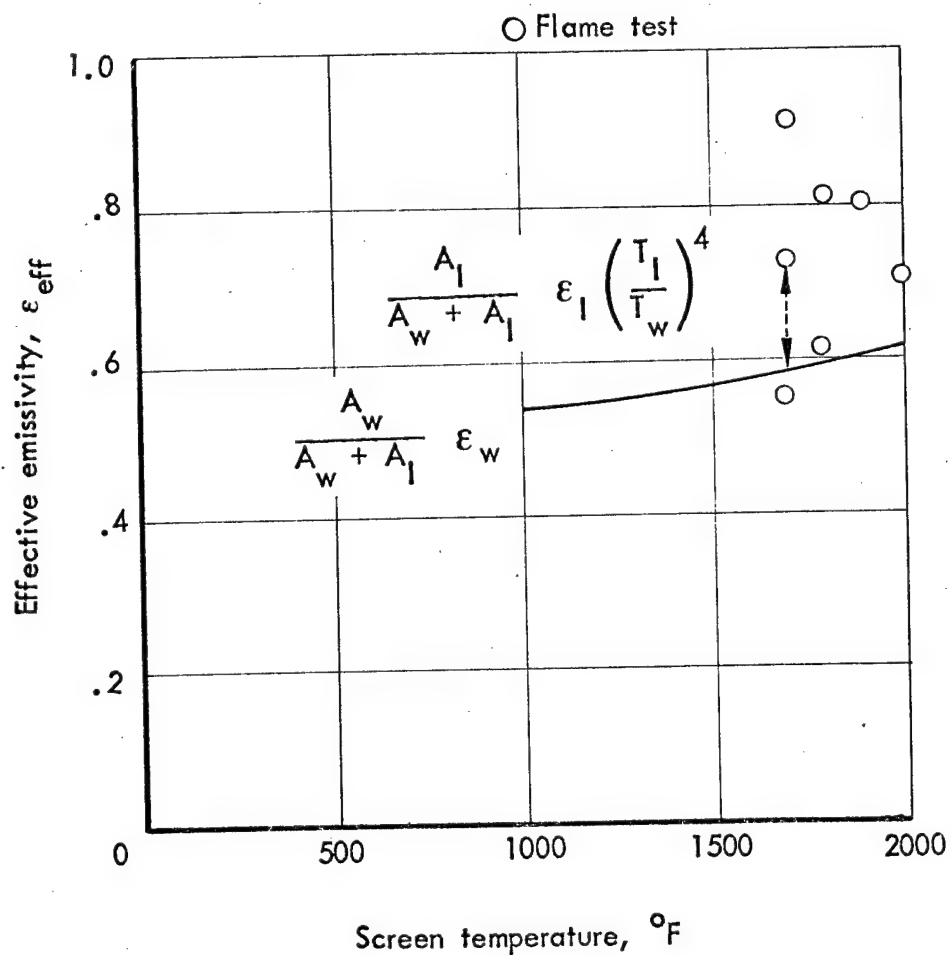


Figure 42.- Effective emissivity of .017" dia. 18-mesh Inconel screen.

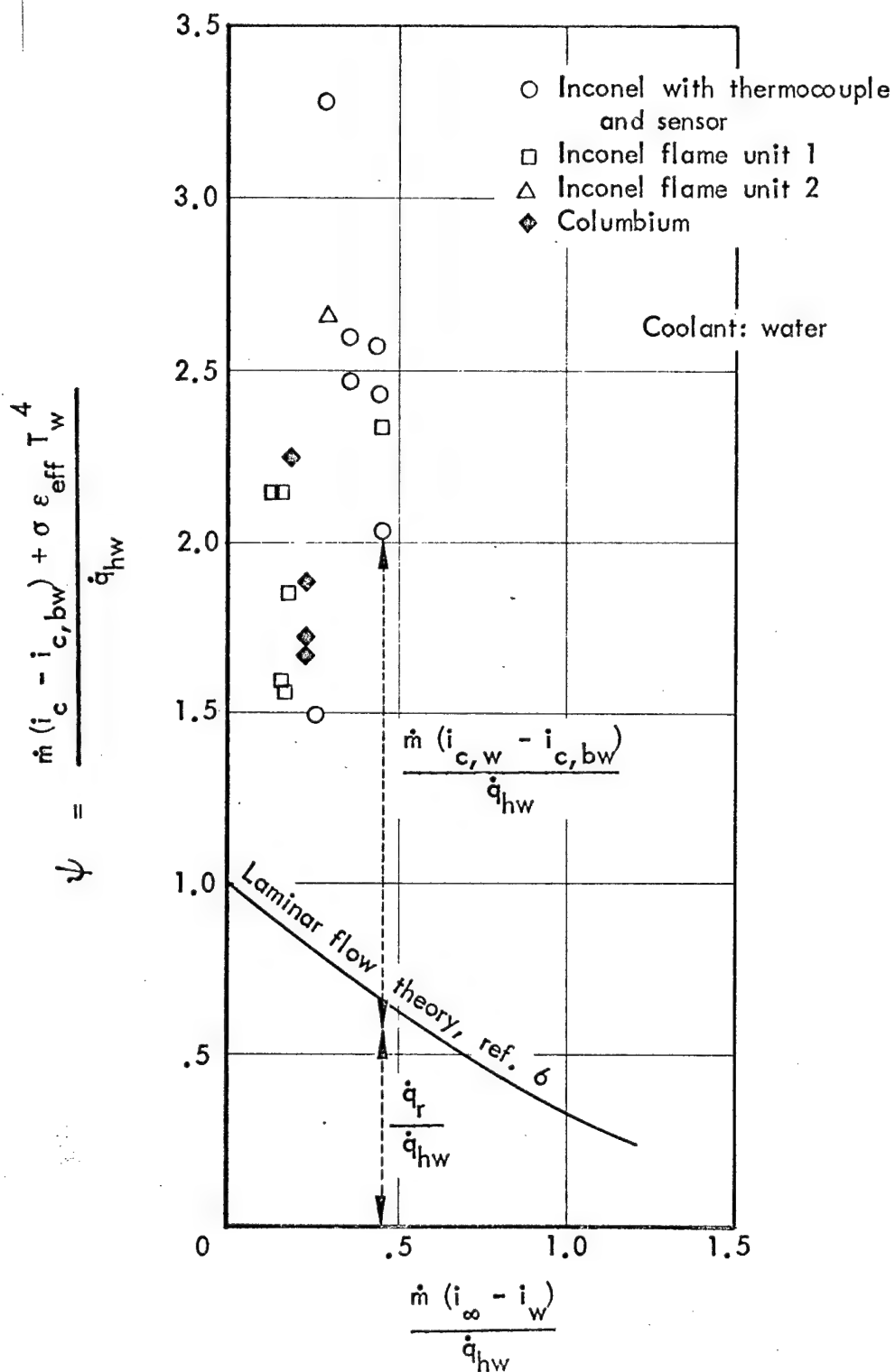


Figure 43.- Data-theory comparison of the laminar blocking function ψ for the 2" dia. flame specimens.

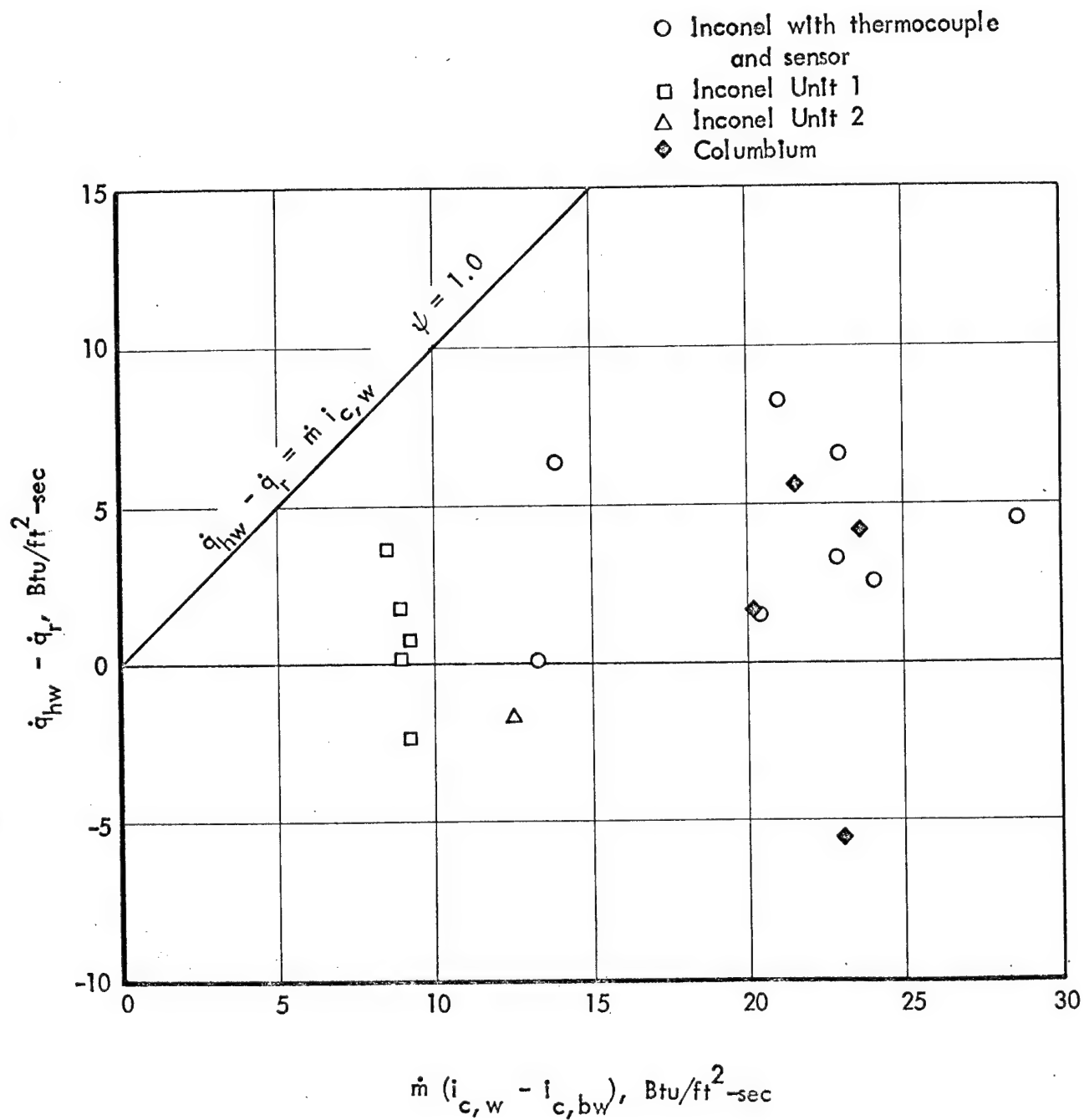
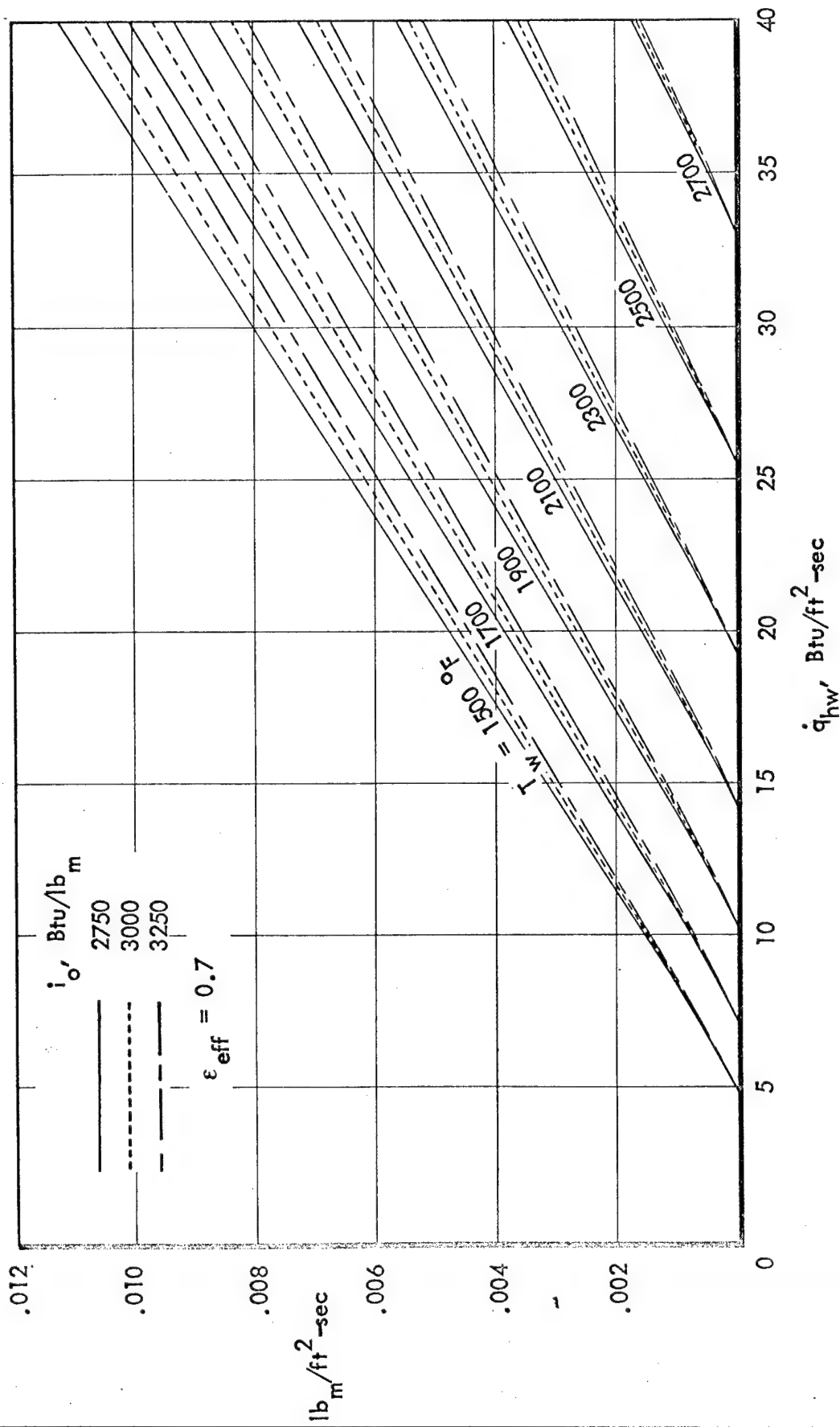
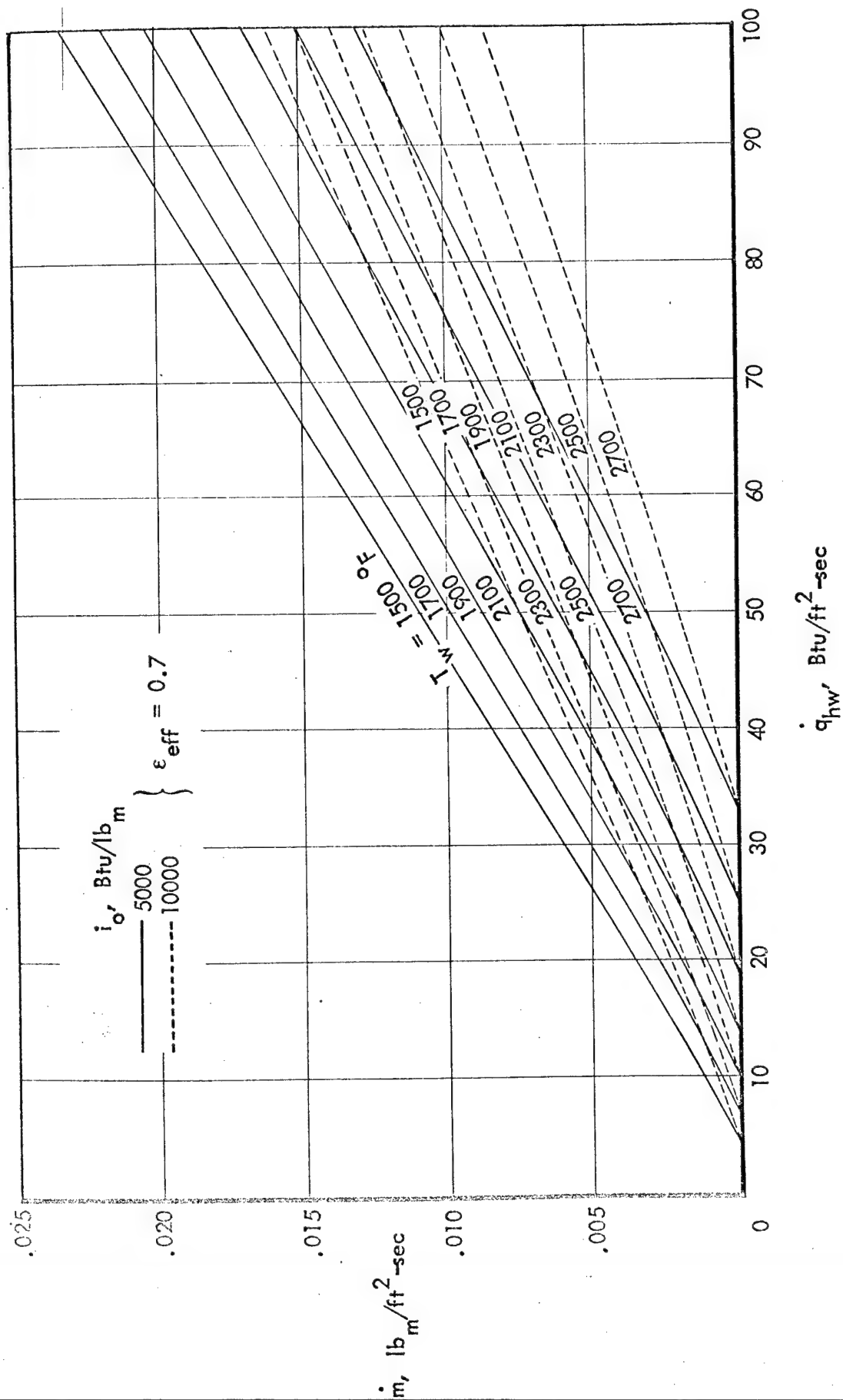


Figure 44.- Examination of discrepancies in flame test data for constant efficiency.



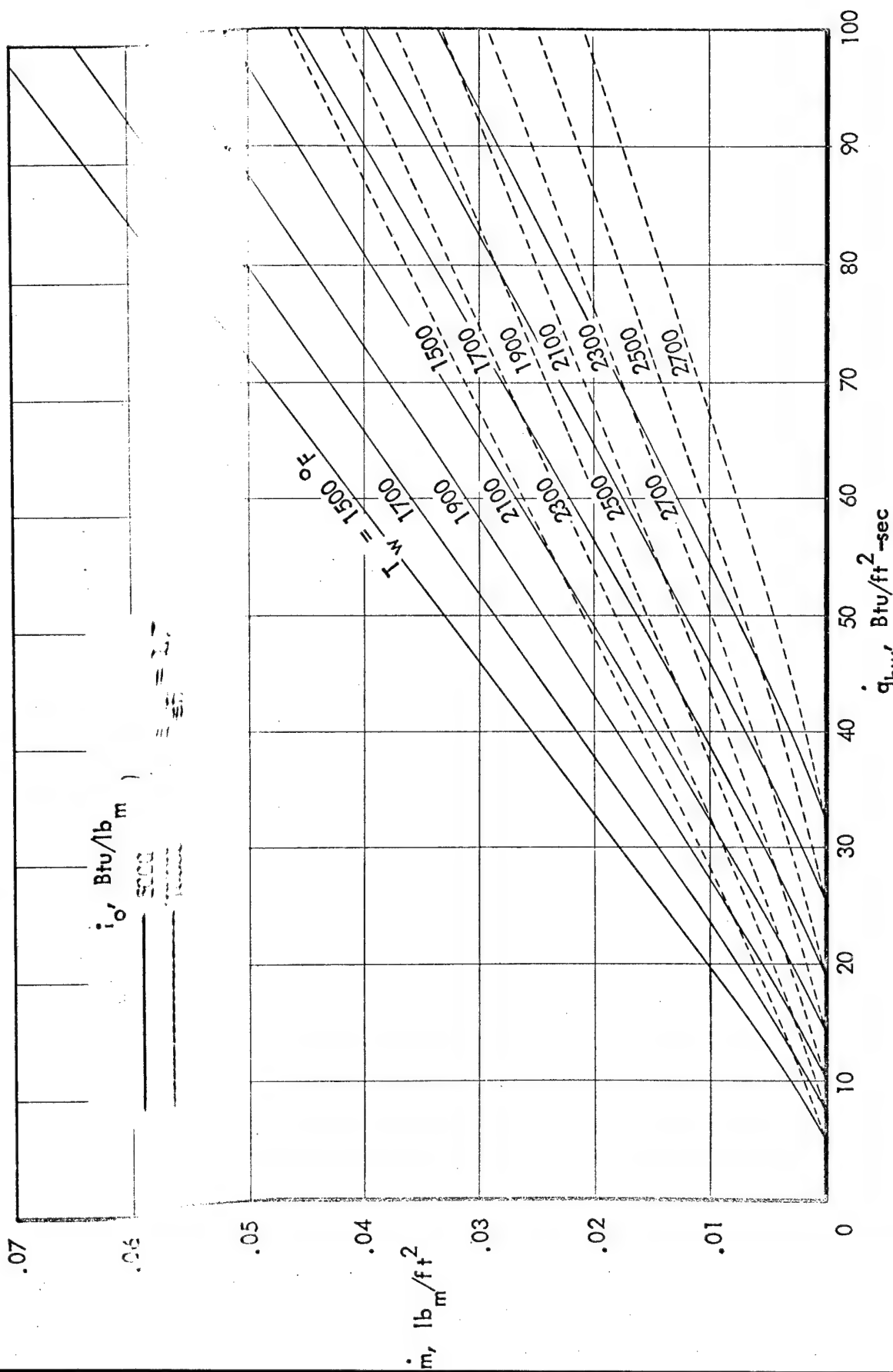
a) Coolant: water. Total enthalpy = 2750, 3000, and 3250 Btu/lb_m .

Figure 45. - Calculated coolant flow rates.



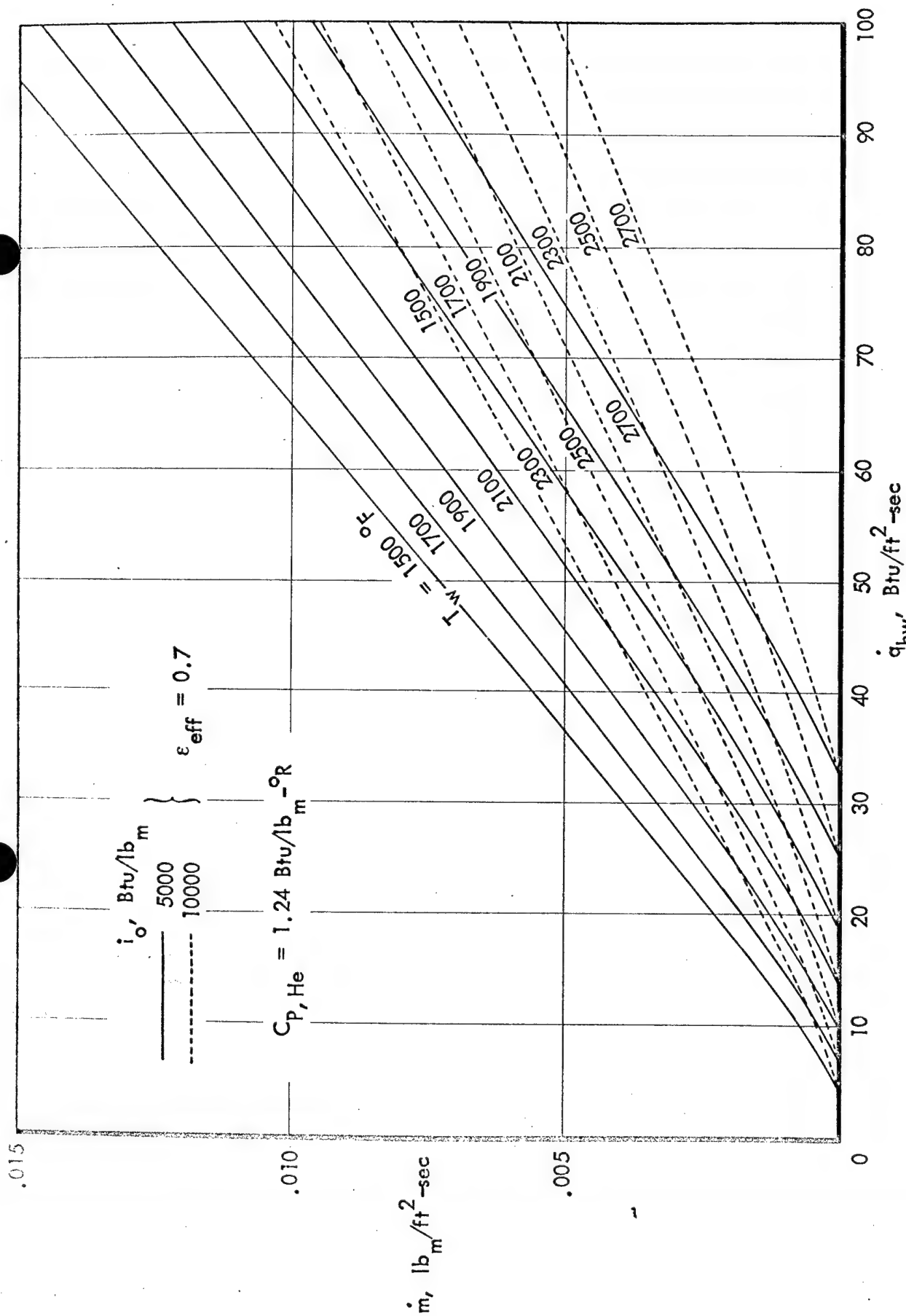
b) Coolant: water. Total enthalpy = 5000 and 10000 Btu/lb_m.

Figure 45.- Continued.



c) Coolant: nitrogen. Total enthalpy = 5000 and 10000 Btu/lb_m .

Figure 45.- Continued.



d) Coolant: helium. Total enthalpy = 5000 and 10000 Btu/lb_m.

Figure 45. - Concluded.

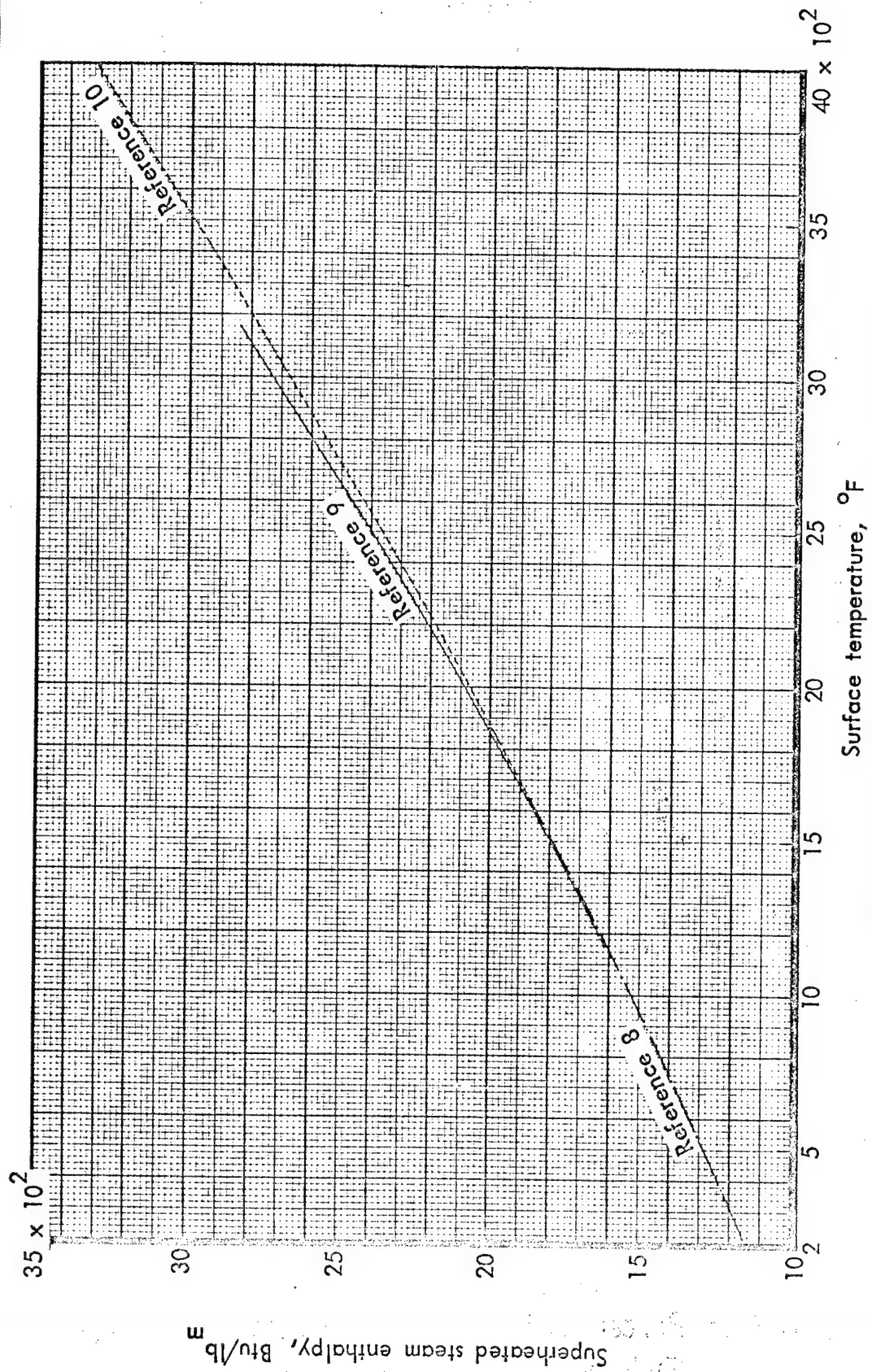


Figure 46.- Enthalpy of superheated steam.

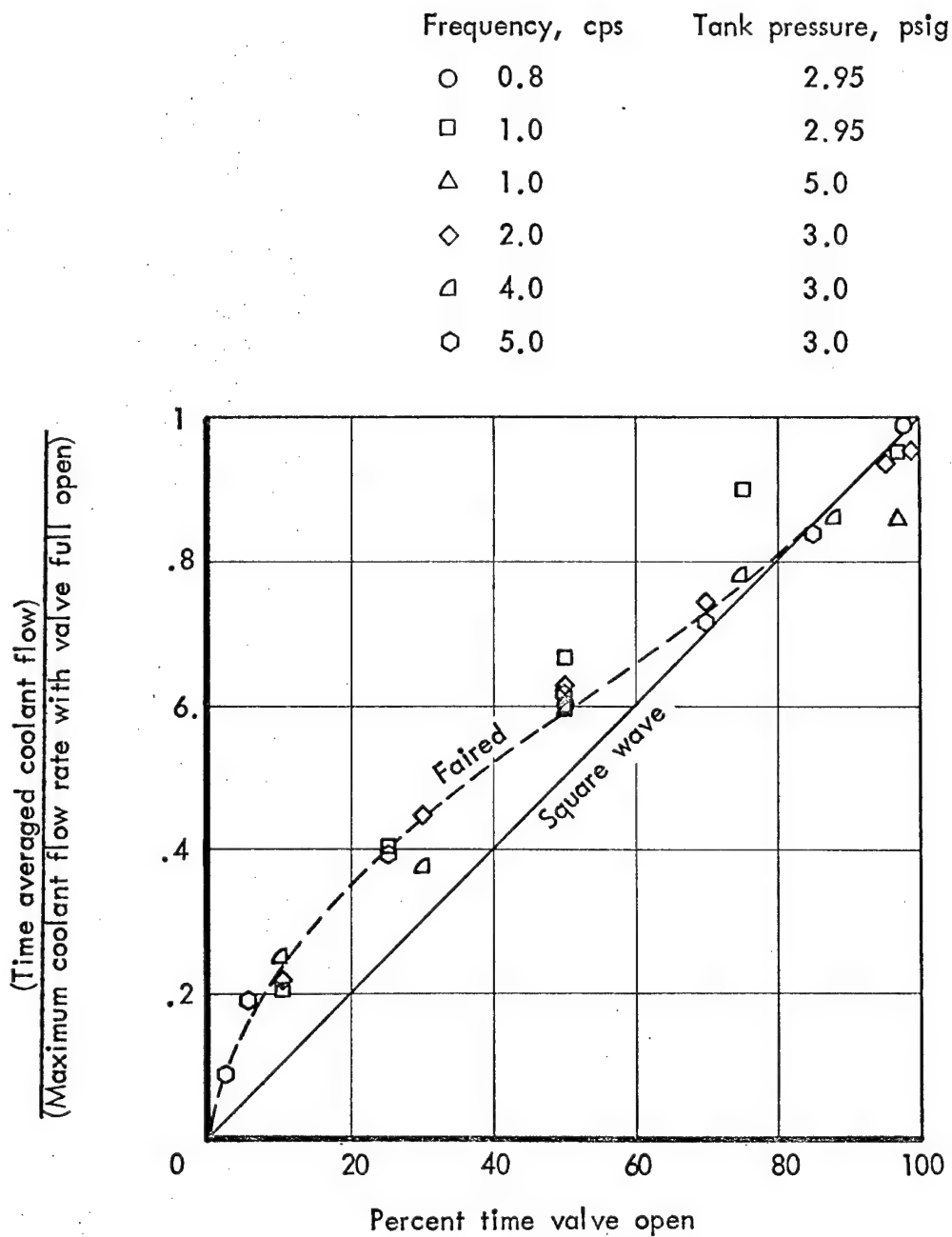


Figure 47.- Percent reduction in flow rate by pulse width modulation of the solenoid valve.

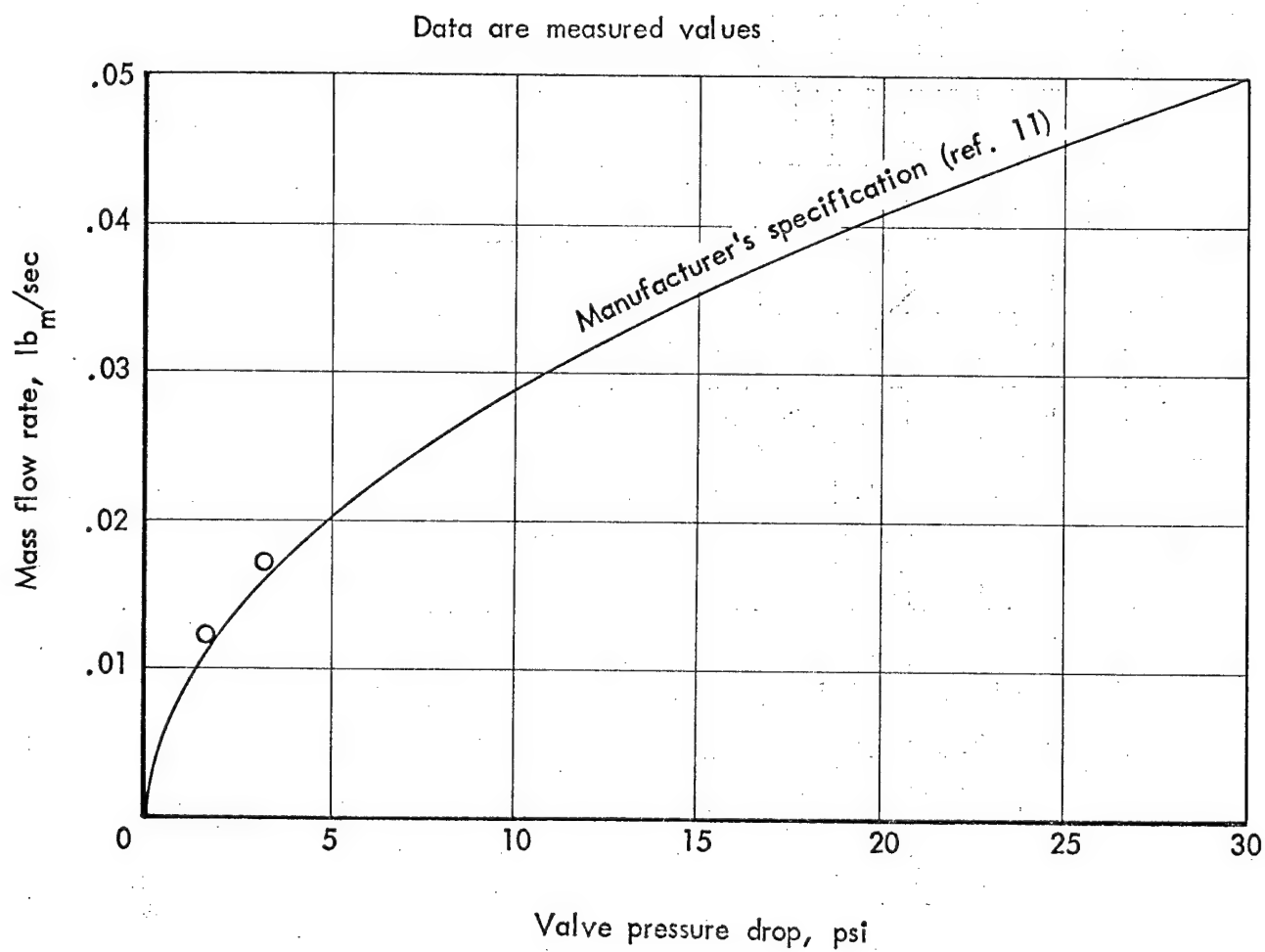


Figure 48. - Valve characteristics - Skinner two-way B2 series.

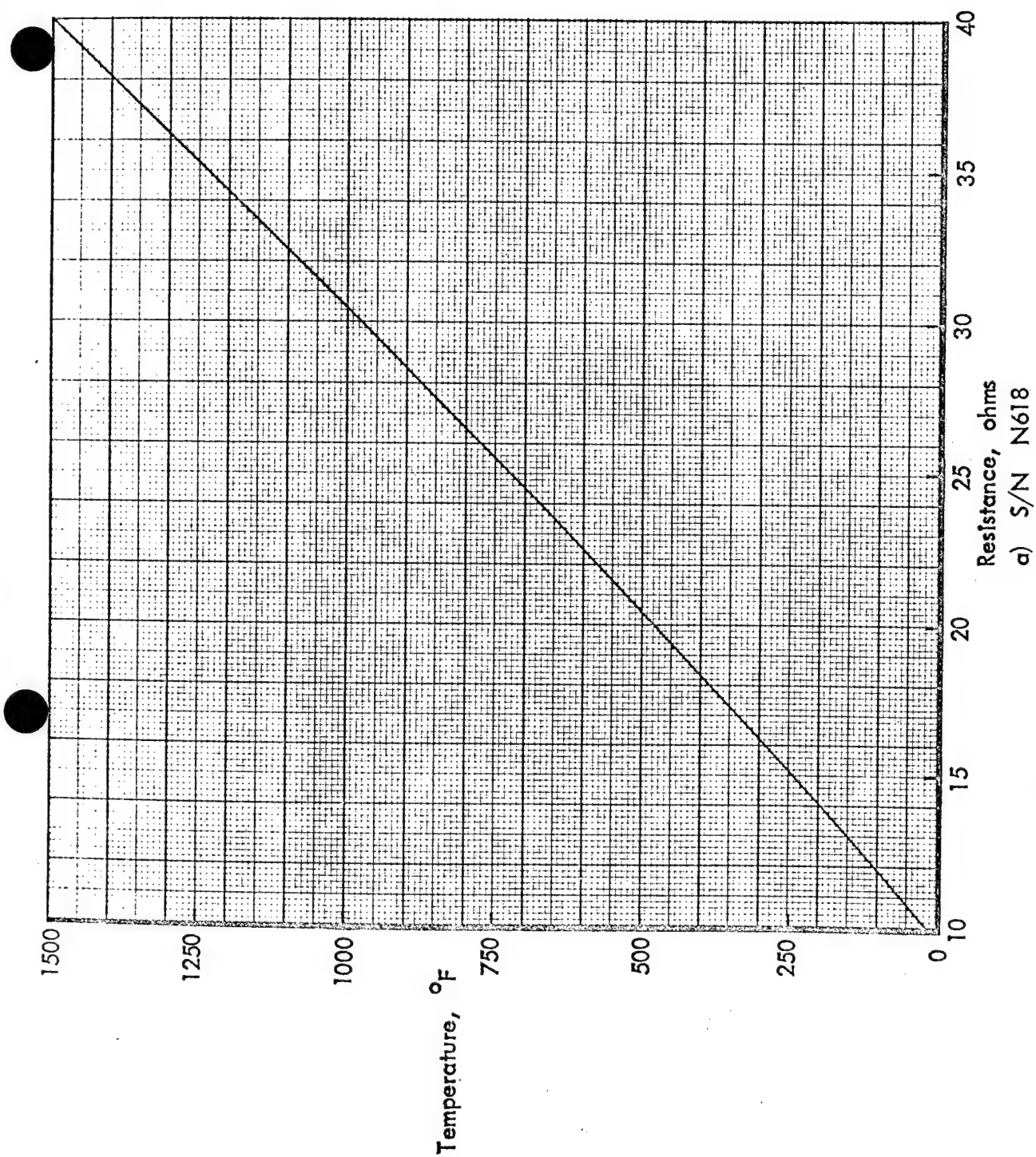
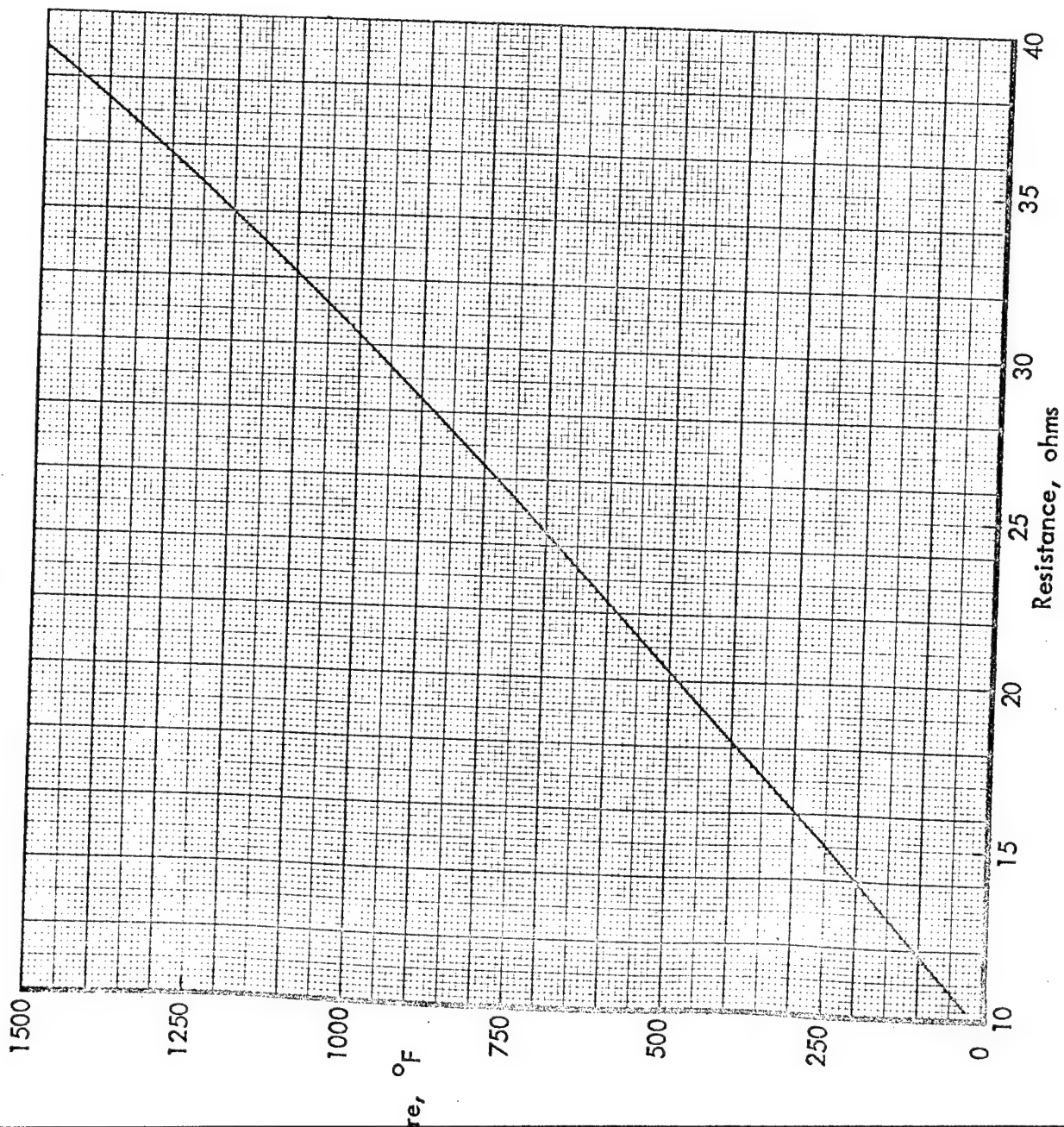


Figure 49. - Platinum resistance thermometer calibration curve.



b) S/N N623

Figure 49. - Continued.

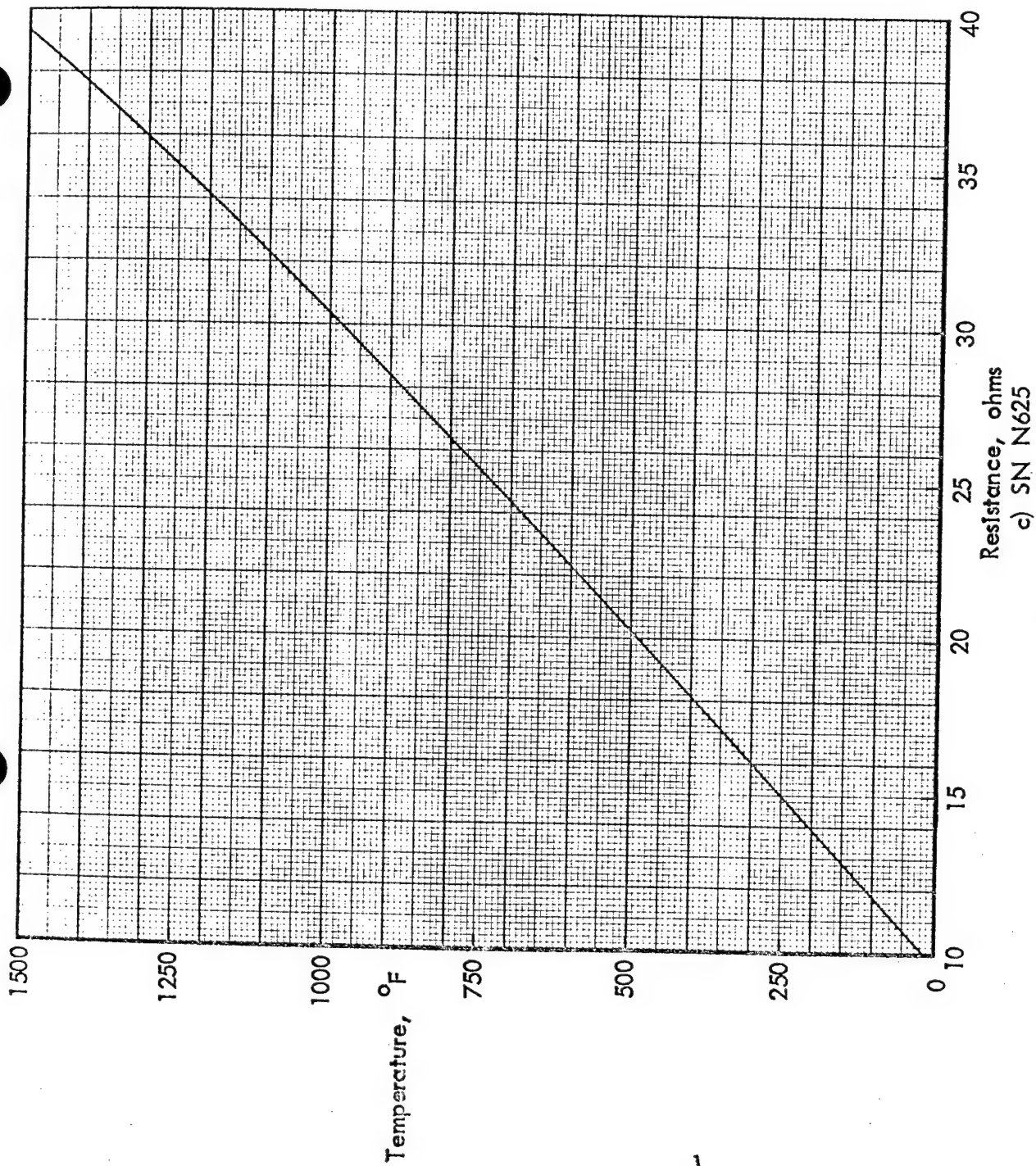


Figure 49.- Continued.

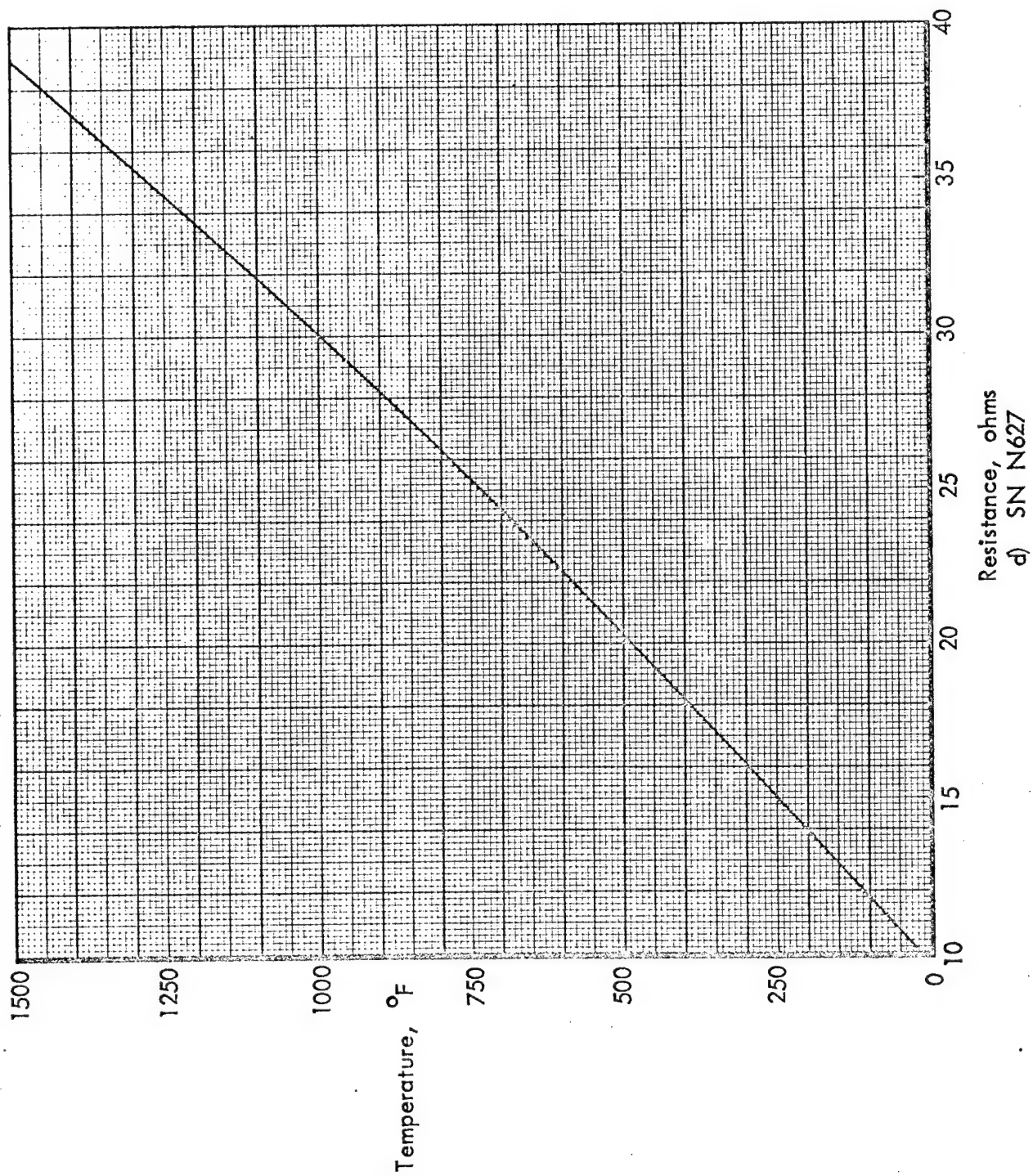


Figure 49.- Concluded.

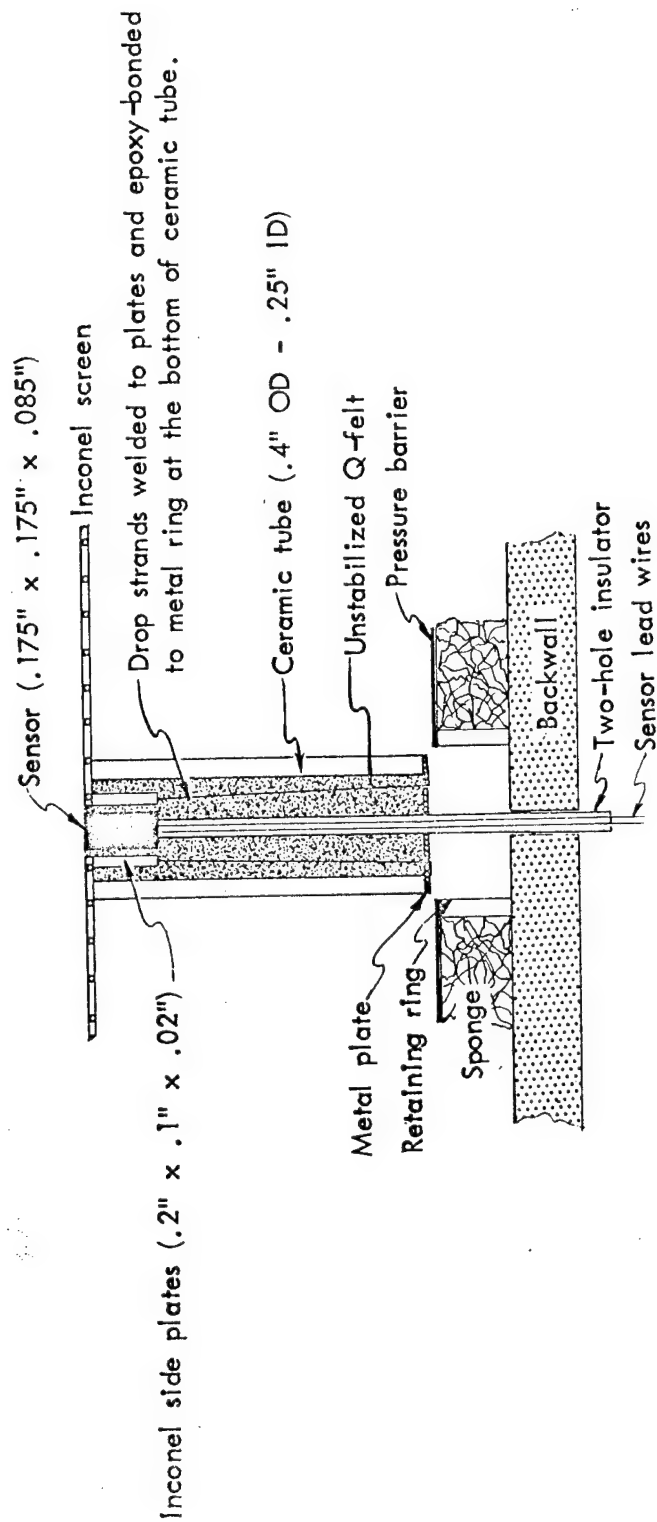
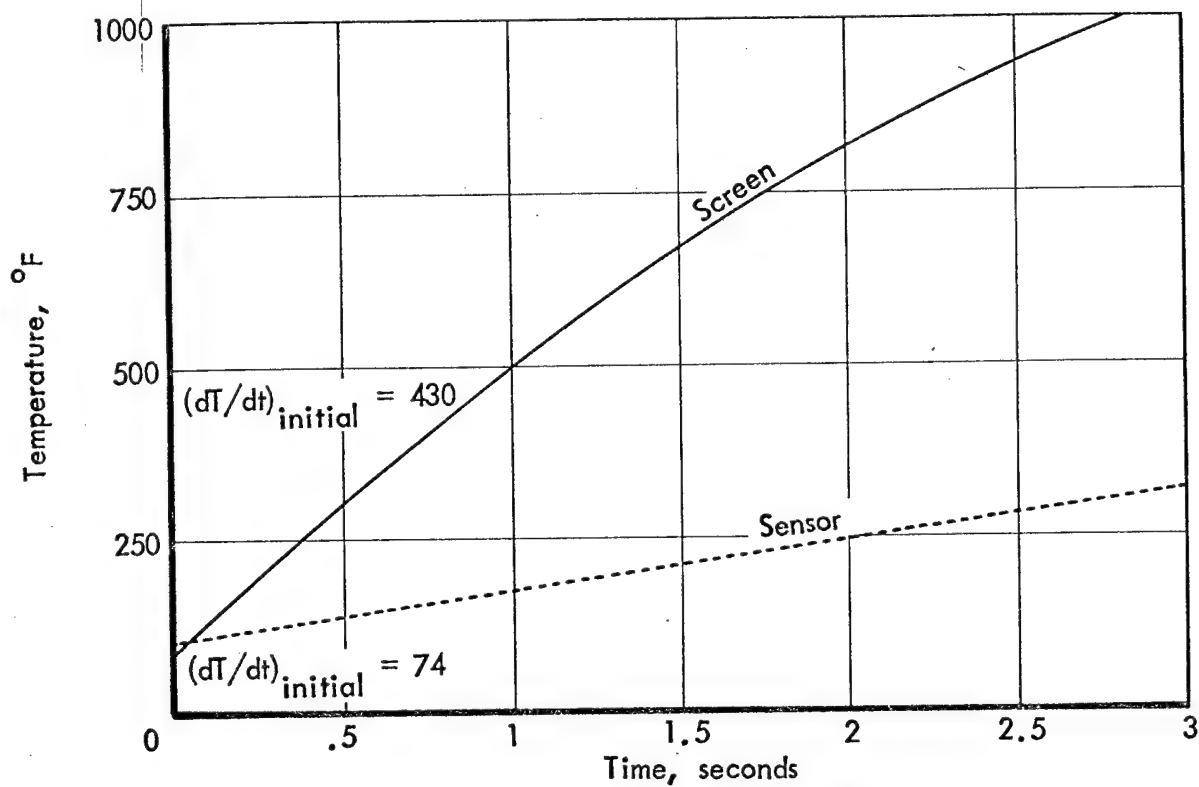


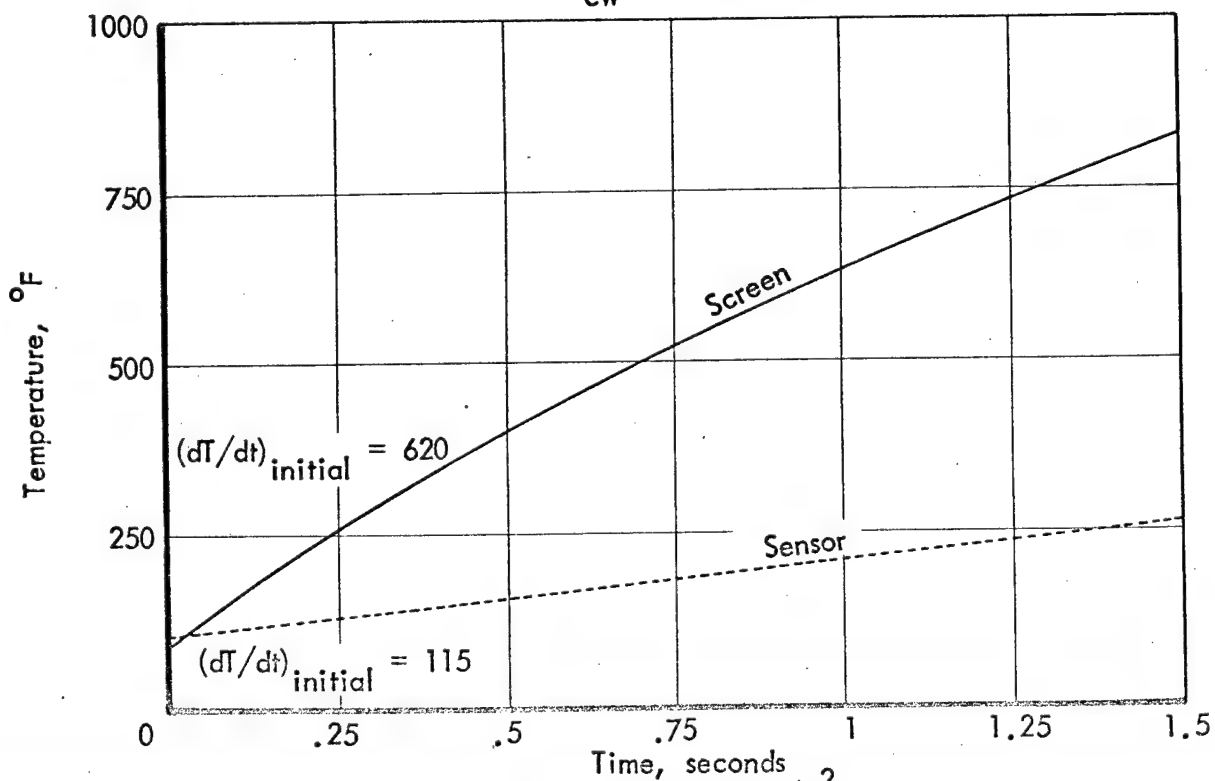
Figure 50. - Sensor installation I.



Figure 51. - Inconel flame test unit with sensor installation 1
subsequent to 9 hours of flame testing.



a) $\dot{q}_{\text{cw}} = 34.5 \text{ Btu/ft}^2\text{-sec}$



b) $\dot{q}_{\text{cw}} = 48.8 \text{ Btu/ft}^2\text{-sec}$

Figure 52. - Temperature history of the .017" dia. 18-mesh Inconel screen and sensor with zero coolant flow.

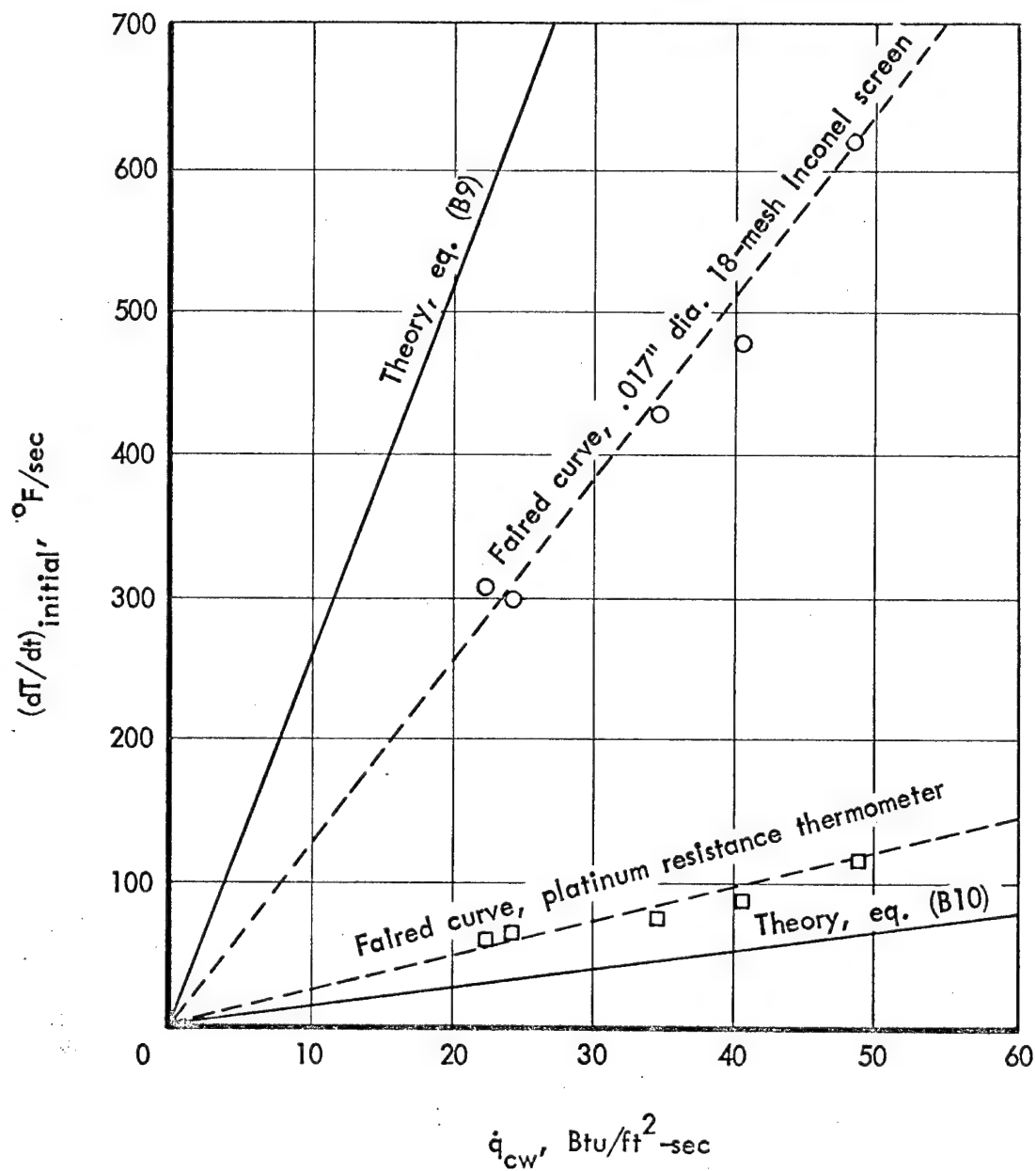


Figure 53.- Data-theory comparison of the temperature response of the wire and sensor near time zero and with zero coolant flow.

Eq. (B11)		\dot{q}_{cw} , Btu/ft ² -sec	T_{∞} , °R
—————	○	22.4	3120
- - - - -	□	34.5	3260
- · - · -	△	48.8	3660

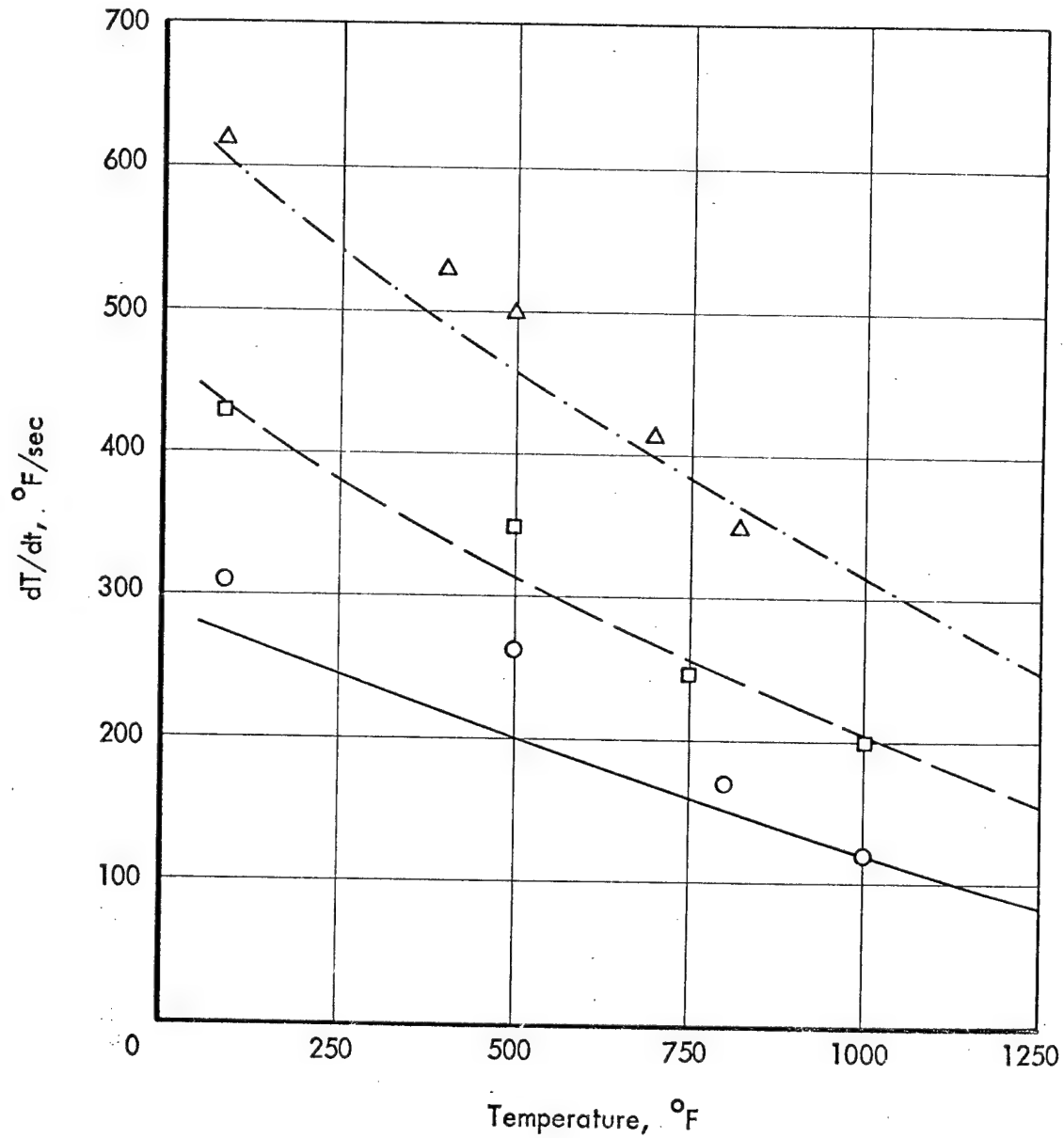
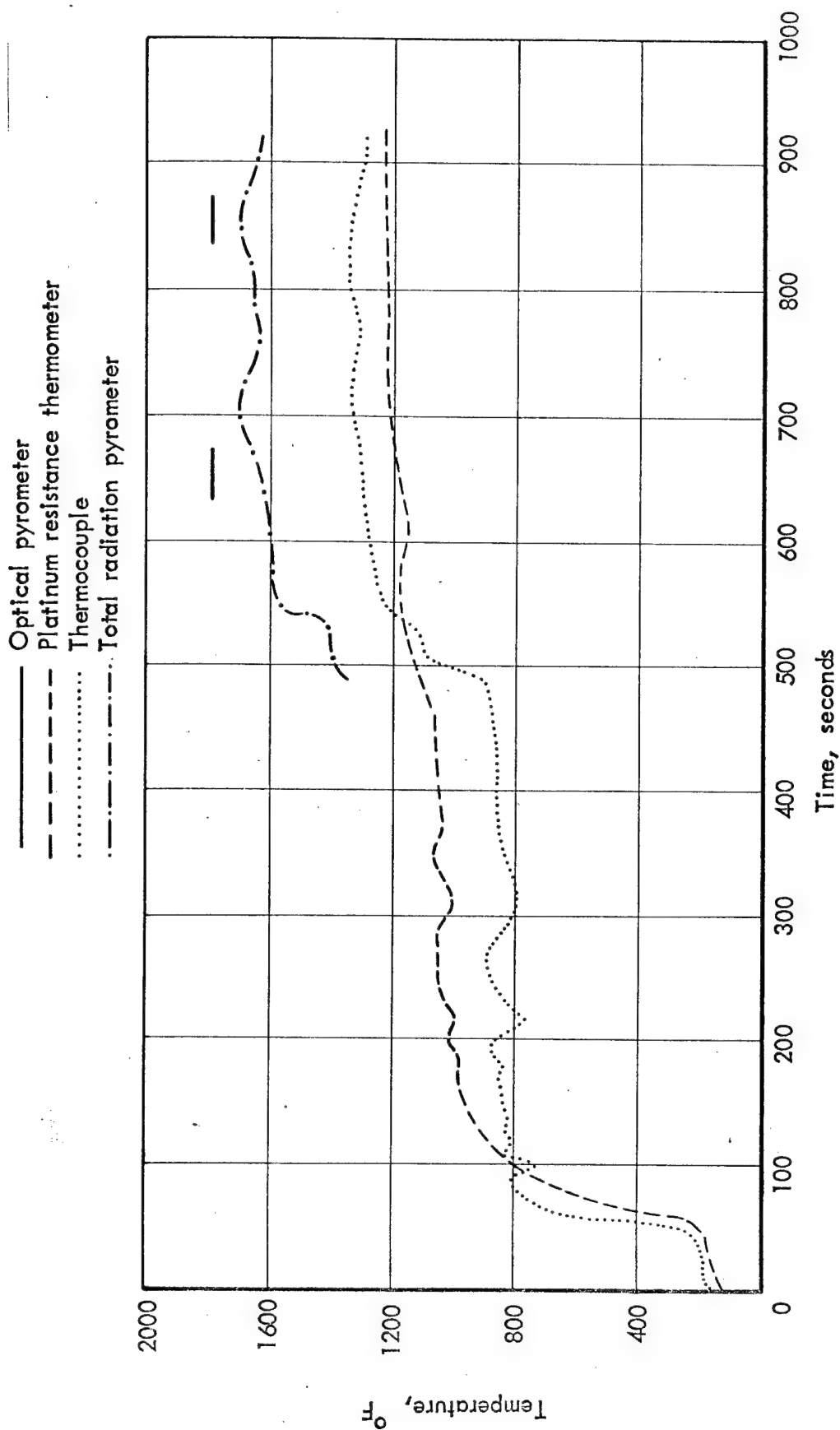
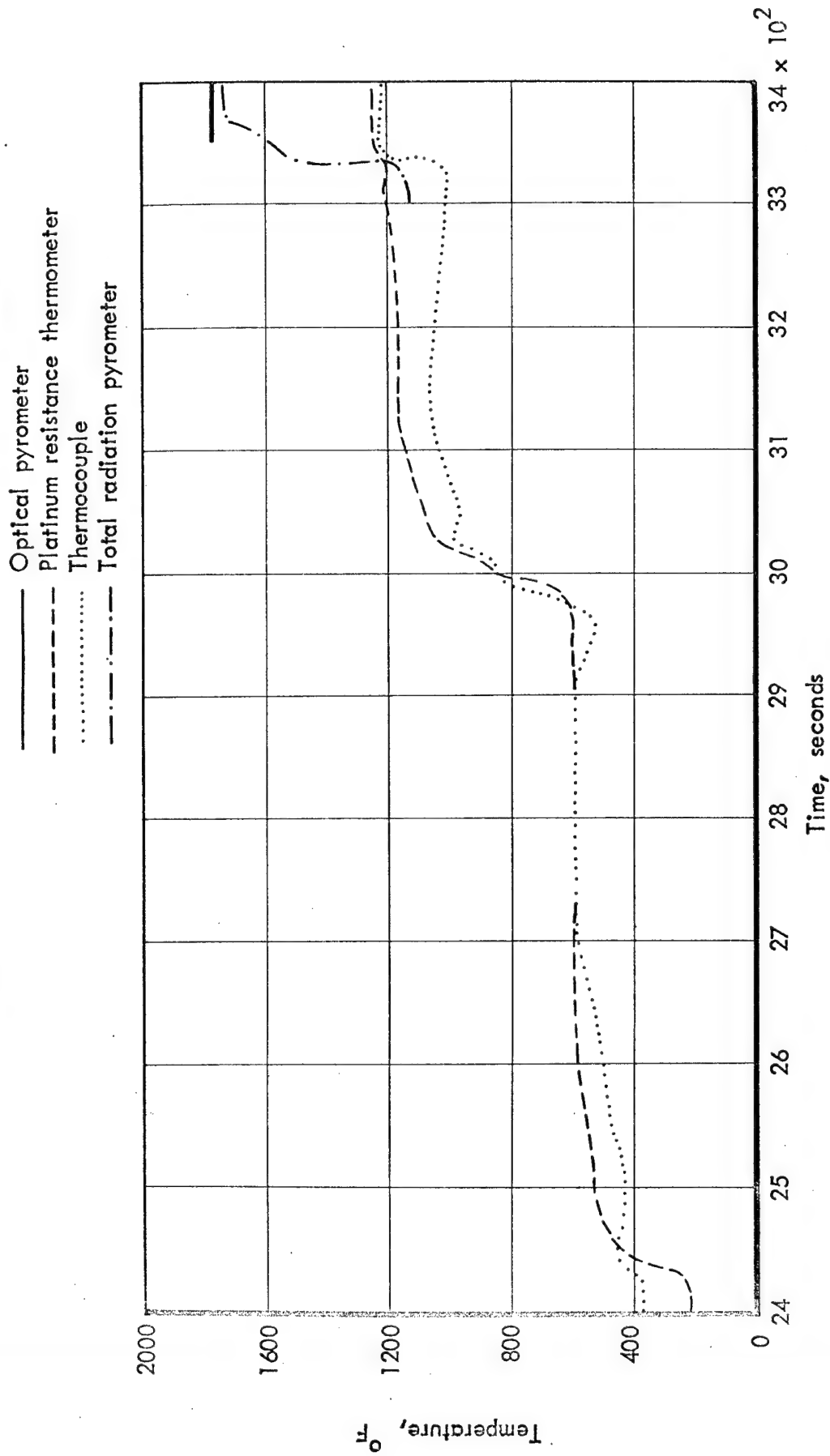


Figure 54. - Data-theory comparisons for the temperature-time derivative of .017" dia. 18-mesh Inconel screen.



a) $\dot{q}_{cw} = 22.2 \text{ Btu/ft}^2\text{-sec}$; $\dot{m} = .0063 \text{ lb}_m/\text{ft}^2\text{-sec}$; and $T_\infty \approx 3250^\circ\text{R}$

Figure 55. - Temperature history of .017" dia. 18-mesh Inconel screen and sensor with coolant flow.



b) $\dot{q}_{cw} = 22.2 \rightarrow 36.4 \text{ Btu/ft}^2\text{-sec}$; $\dot{m} = .007 \text{ lb}_m/\text{ft}^2\text{-sec}$; and $T_\infty = 3250 \rightarrow 3450 \text{ }^\circ\text{R}$.

Figure 55.- Concluded.

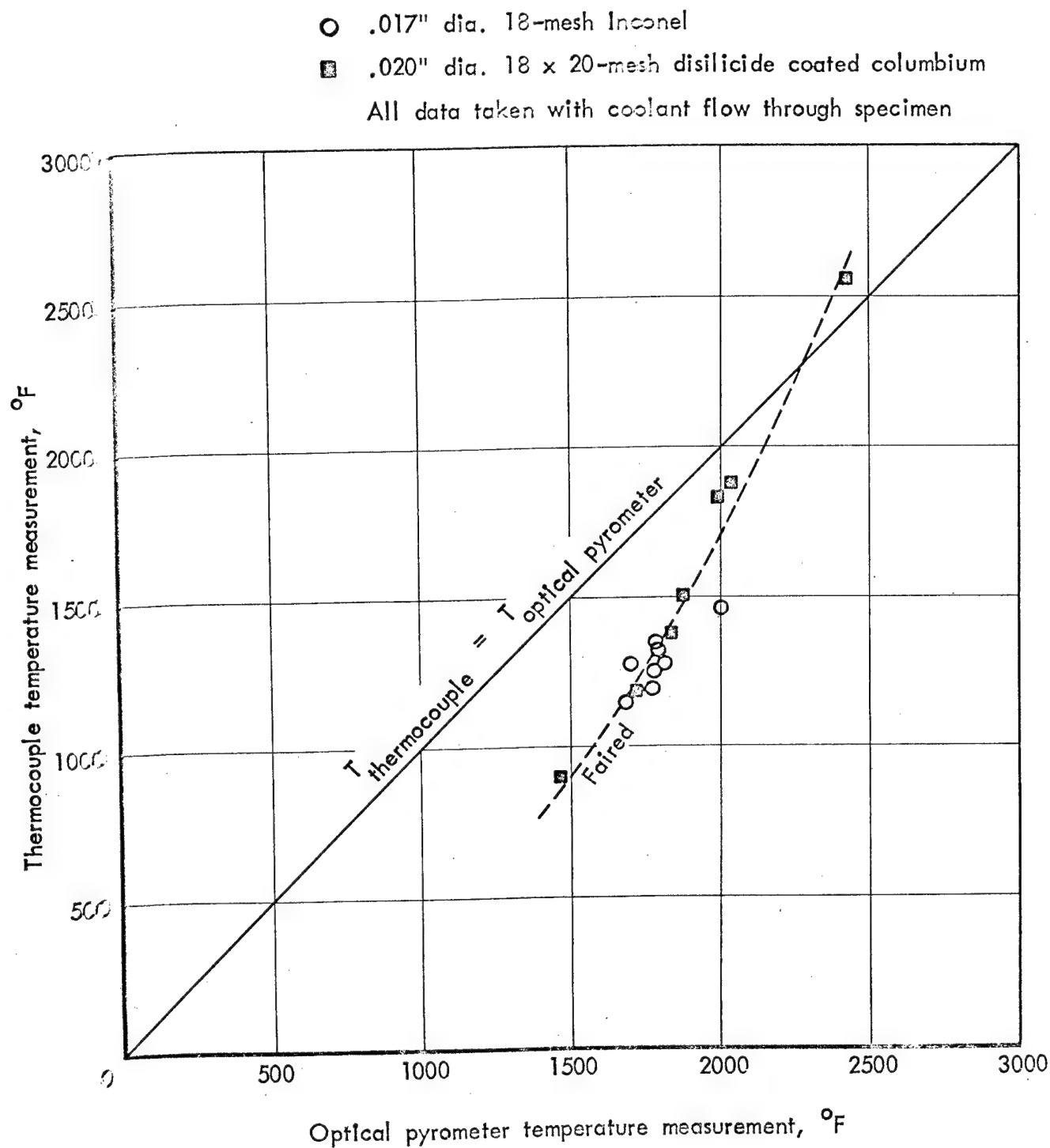


Figure 56. - Comparison of surface screen temperature measurements from a thermocouple and an optical pyrometer.

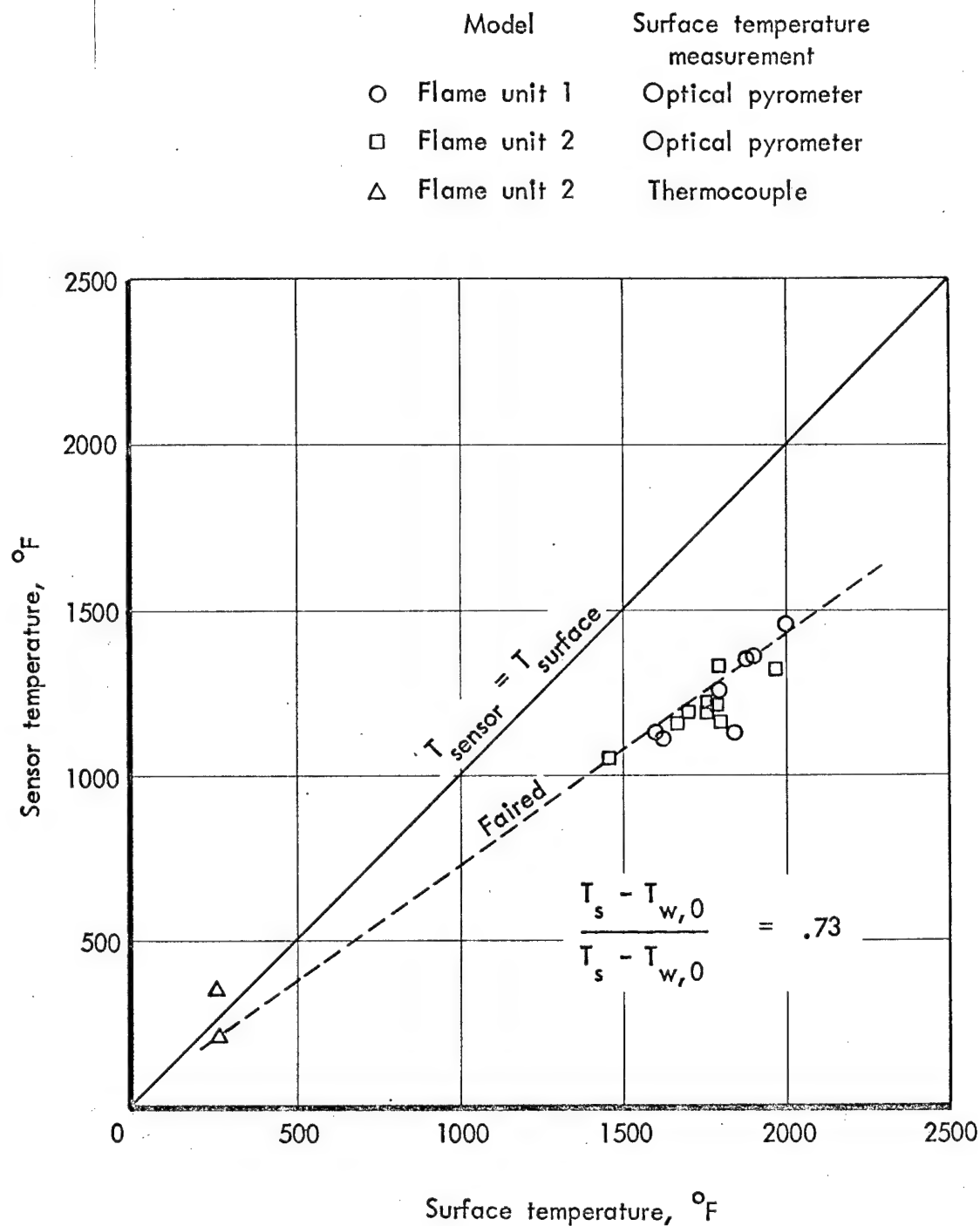
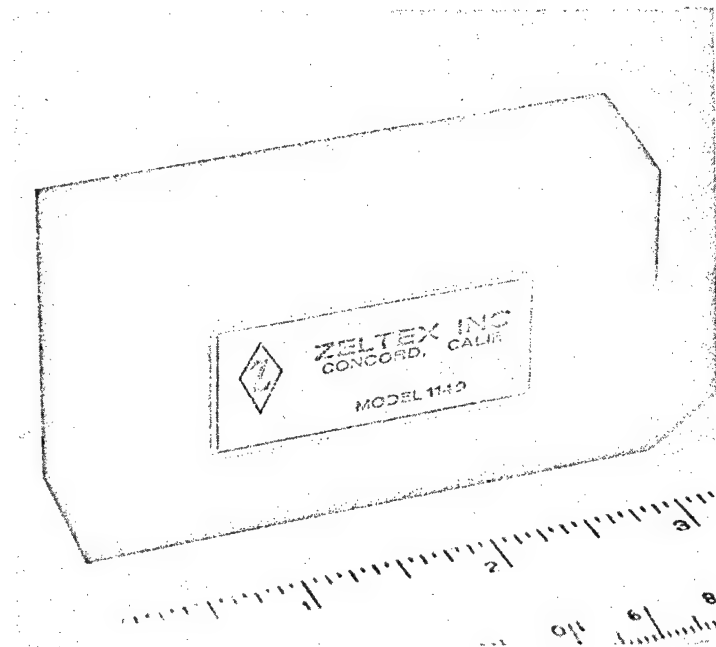
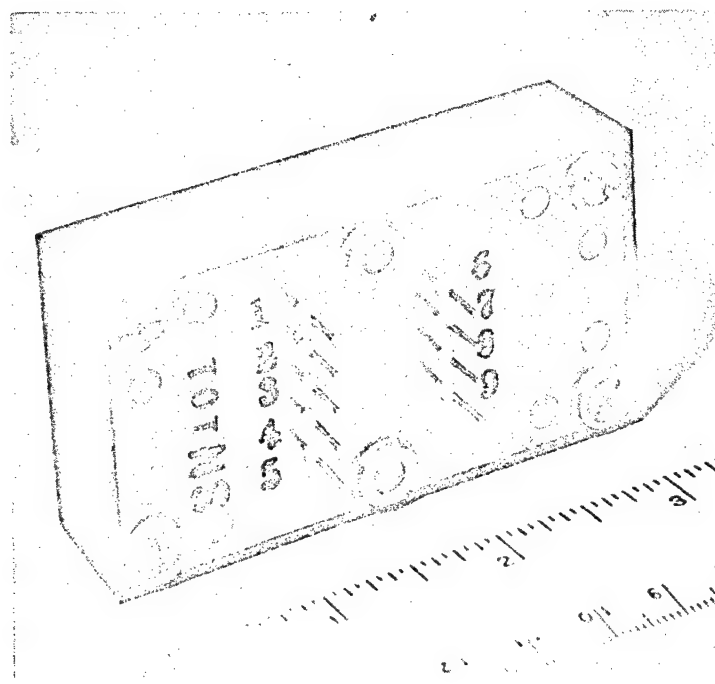


Figure 57.- Calibration of sensor installation I in a flame test unit with .017" dia. 18-mesh Inconel screen.

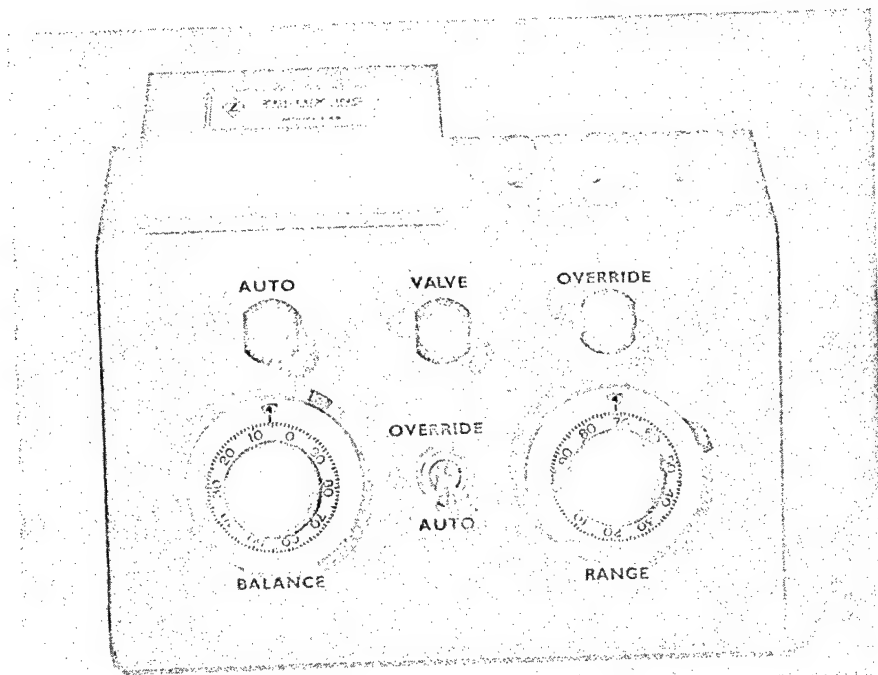


a) Front view

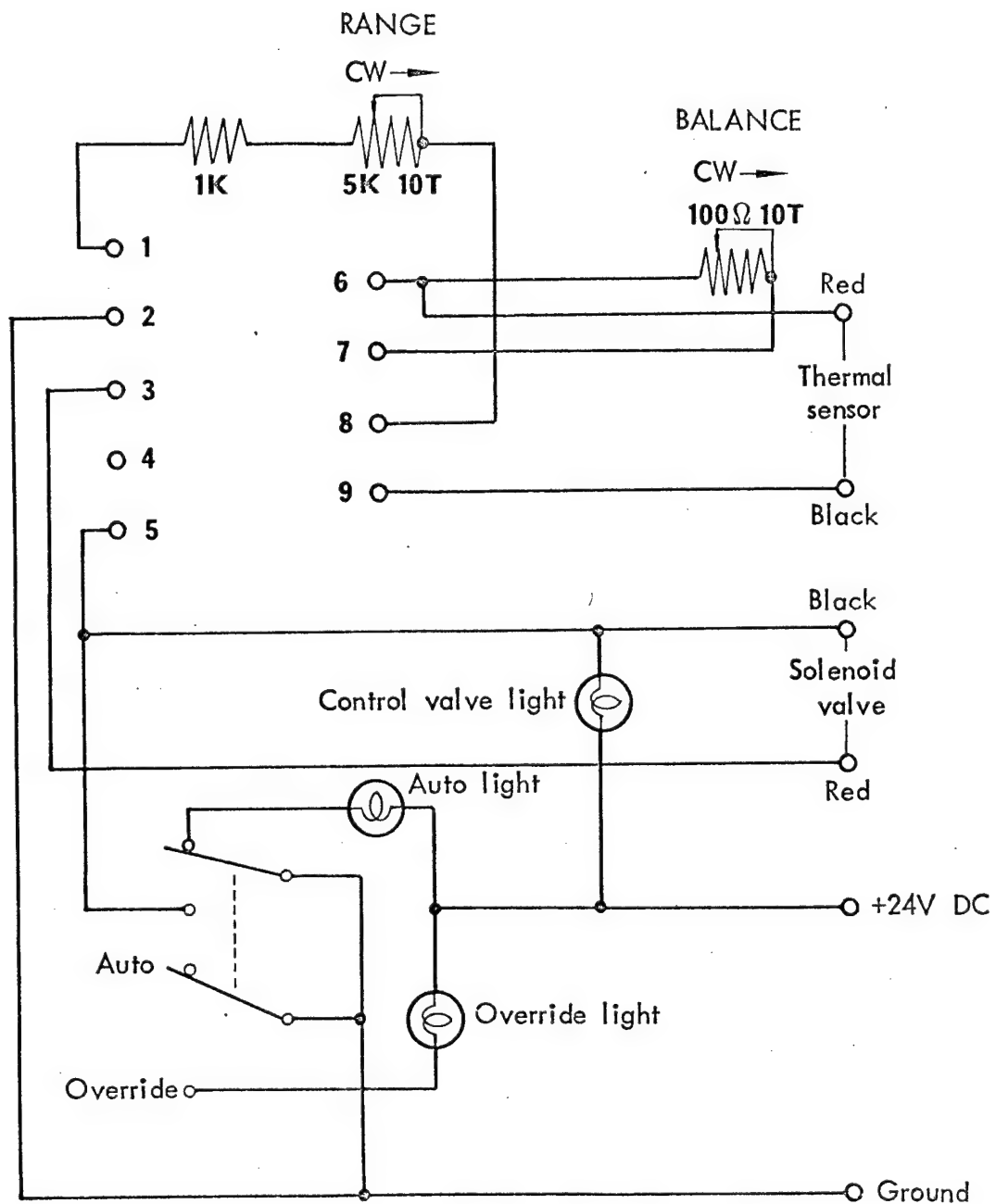


b) Back view

Figure 58.- Controller.



a) External features



b) Circuit diagram

$$\dot{q}_{cw} \approx 65 \text{ Btu/ft}^2\text{-sec and } T \approx 4200 \text{ }^\circ\text{R.}$$

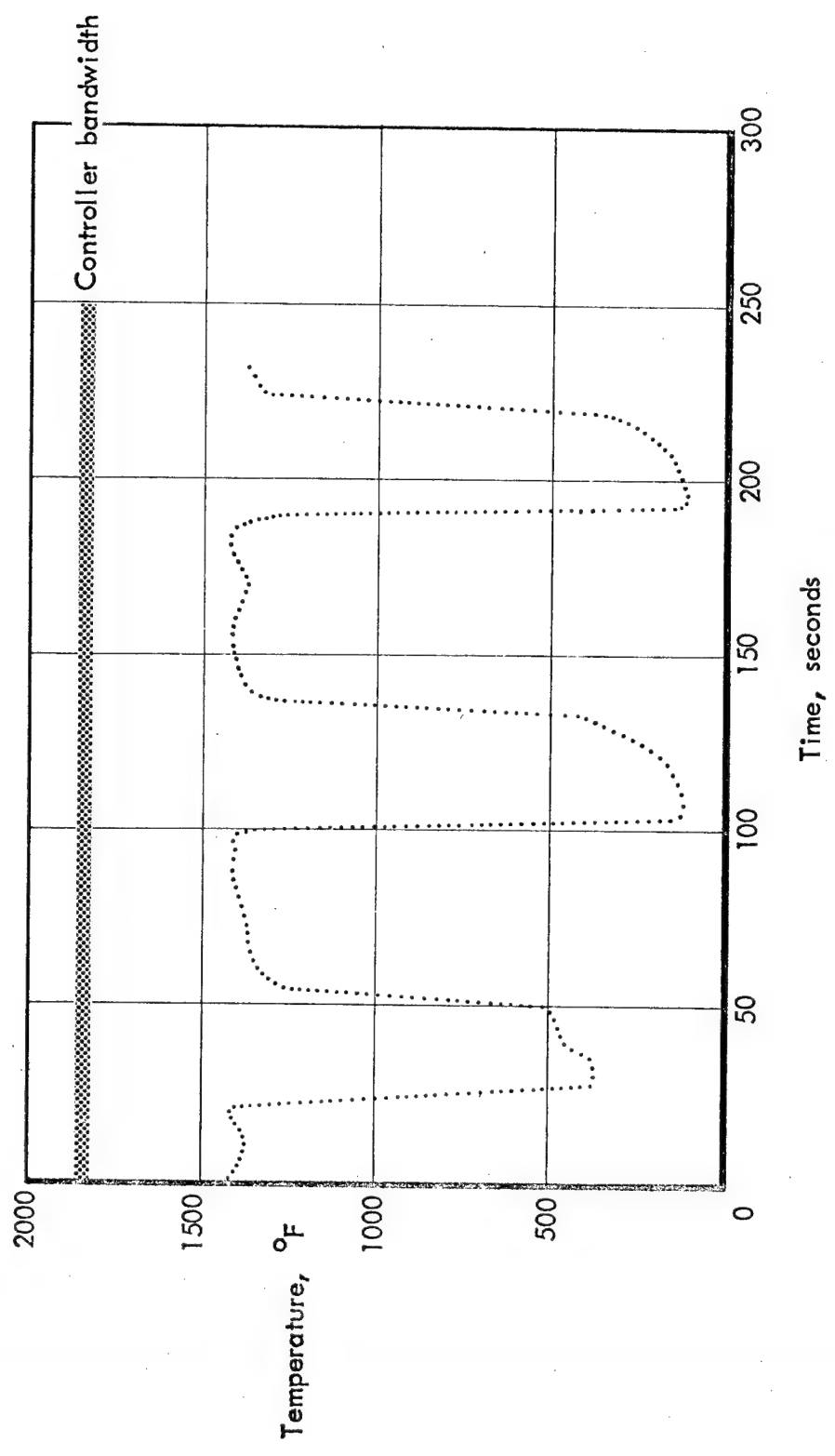
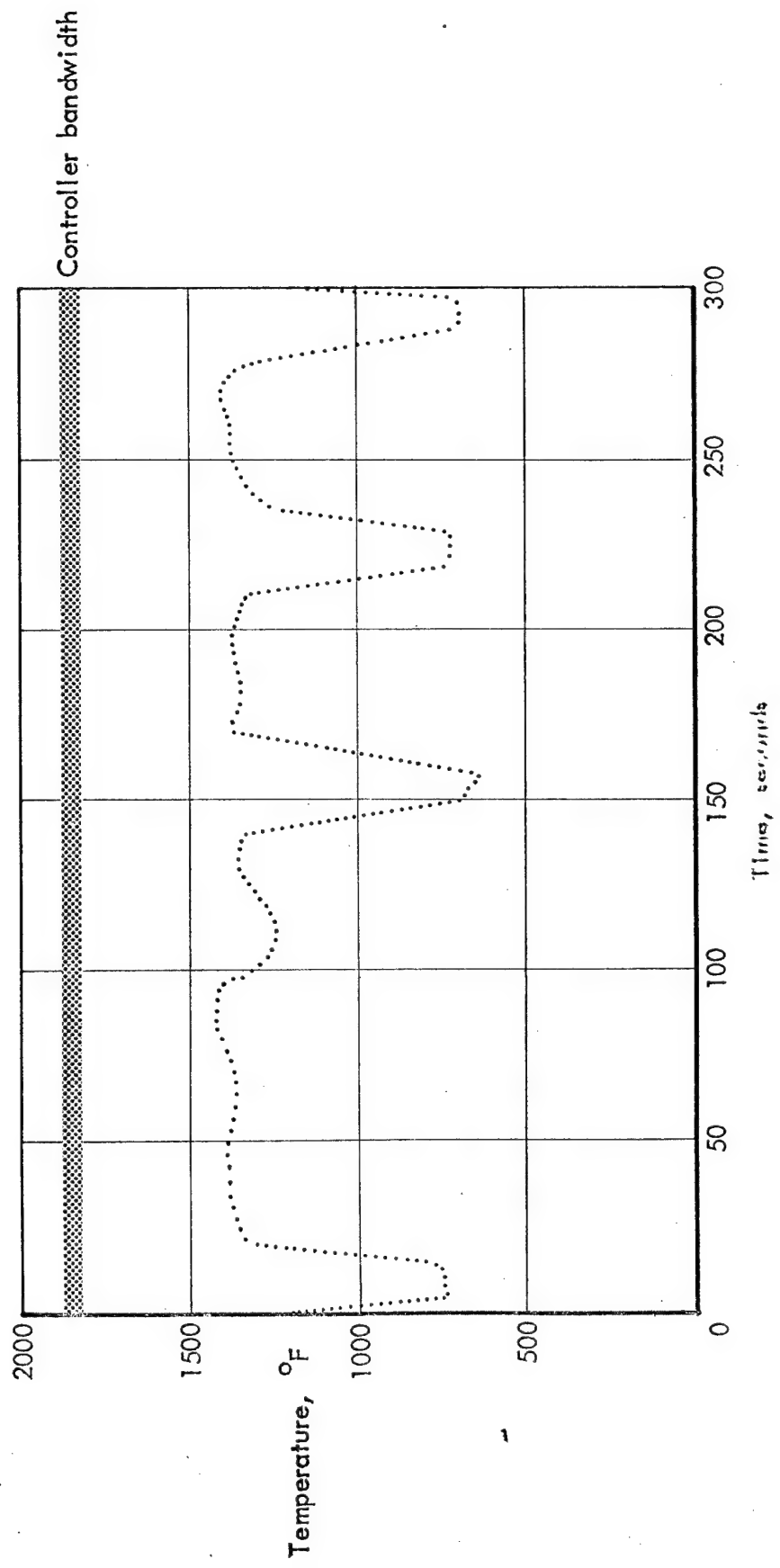
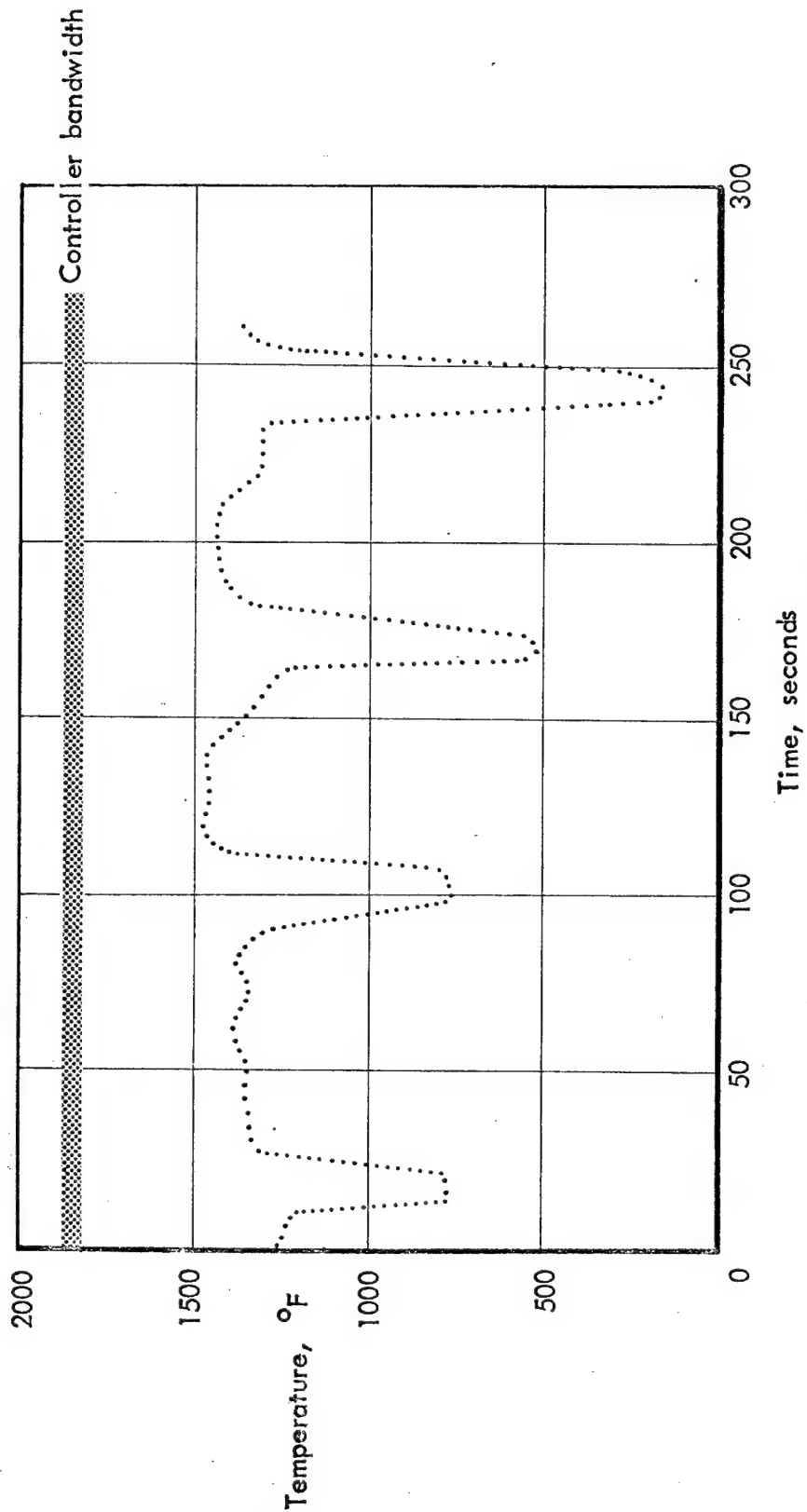


Figure 60. - Temperature history of .017" dia. 18-mesh Inconel screen as maintained by the automatic control system.



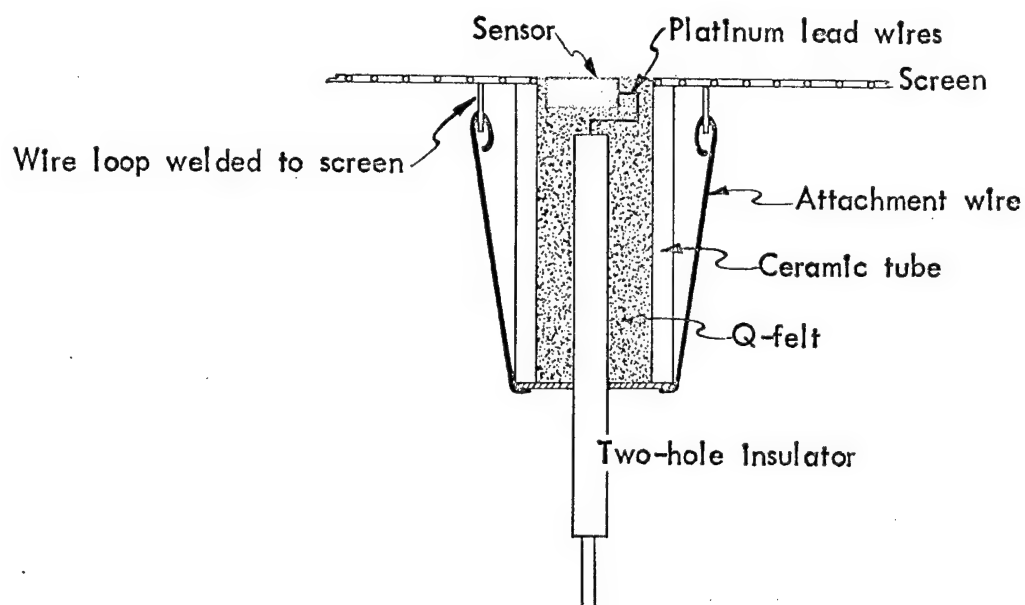
b) Supply pressure = 7.5 psig

Figure 60.- Continued.

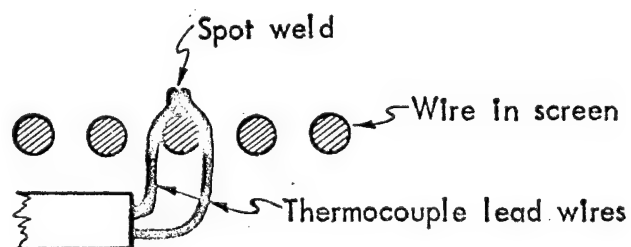


c) Supply pressure = 3.6 psig

Figure 60. - Concluded.

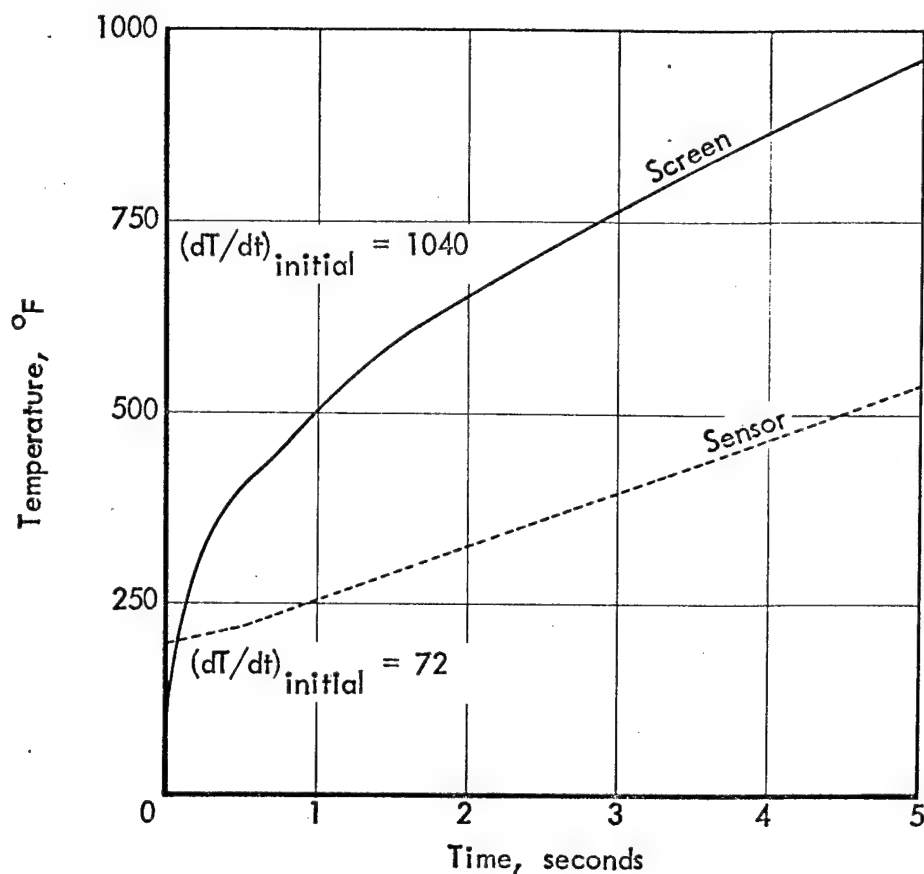


a) Sensor Installation II

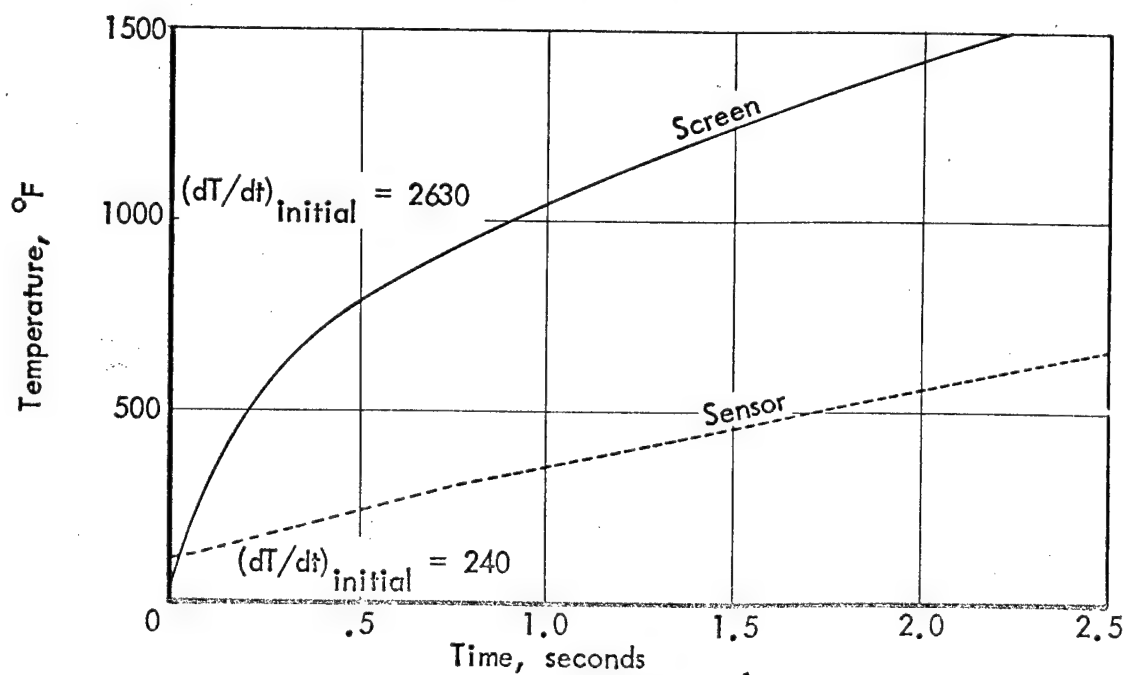


b) Thermocouple attachment technique

Figure 61.- Sensor and thermocouple installation.



a) $\dot{q}_{cw} = 20 \text{ Btu/ft}^2\text{-sec}$



b) $\dot{q}_{cw} = 60 \text{ Btu/ft}^2\text{-sec}$

Figure 62.- Temperature history of the .020" dia. 18 x 20-mesh disilicide coated columbium screen and sensor with

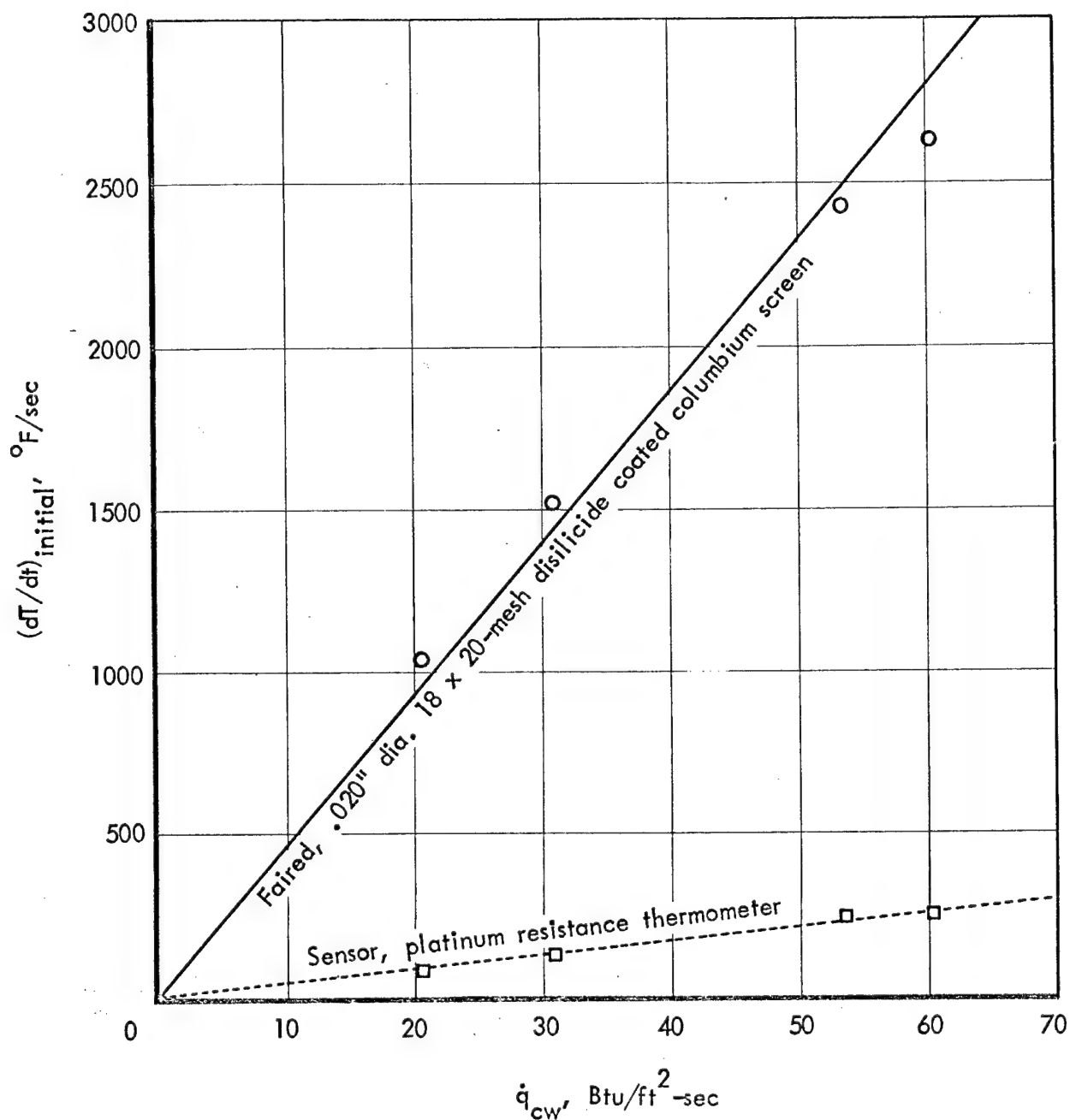


Figure 63.- Comparison of the temperature response of the wire and sensor near time zero and with zero coolant flow.

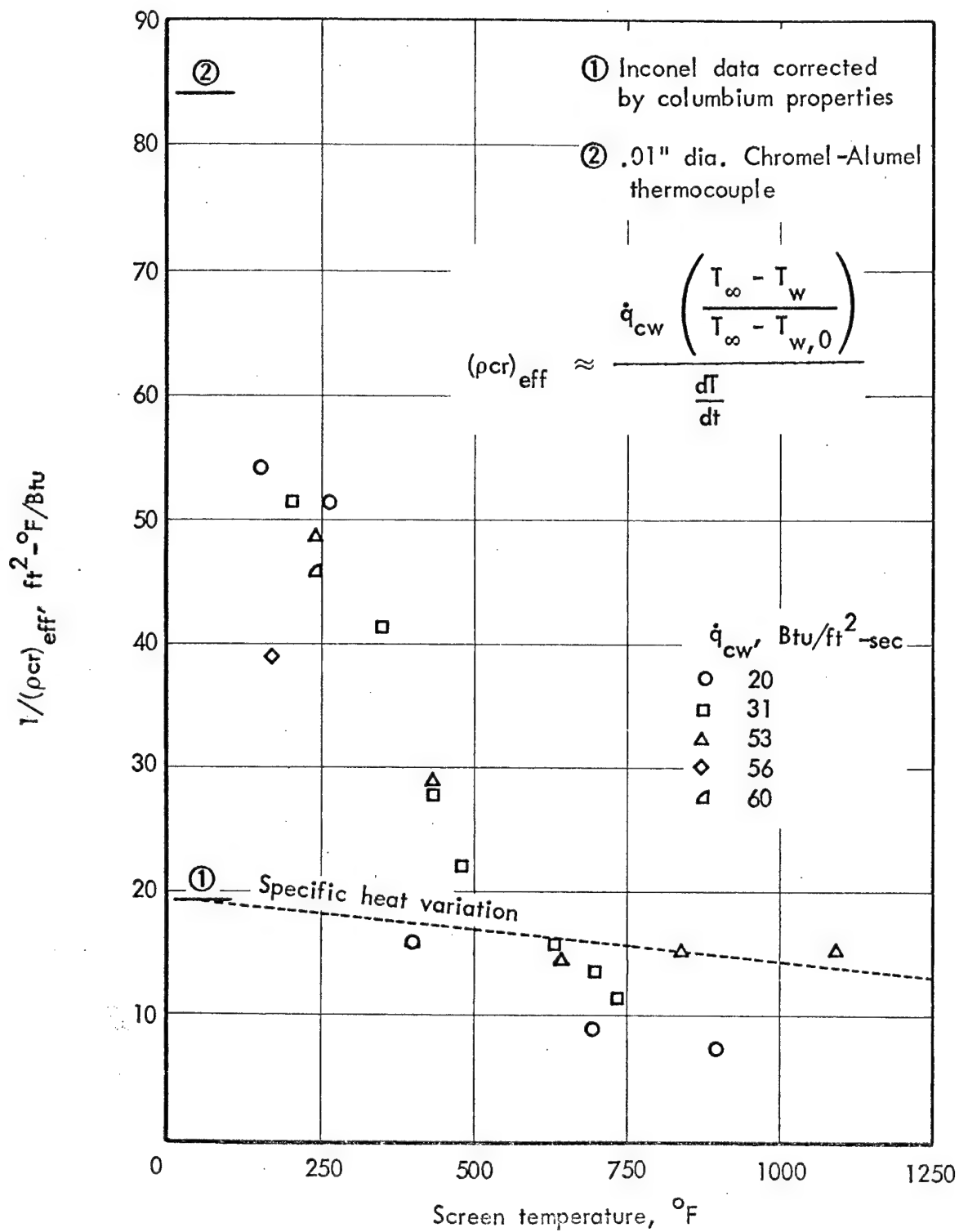


Figure 64.- The effective ρcr for disilicide coated columbium screen.

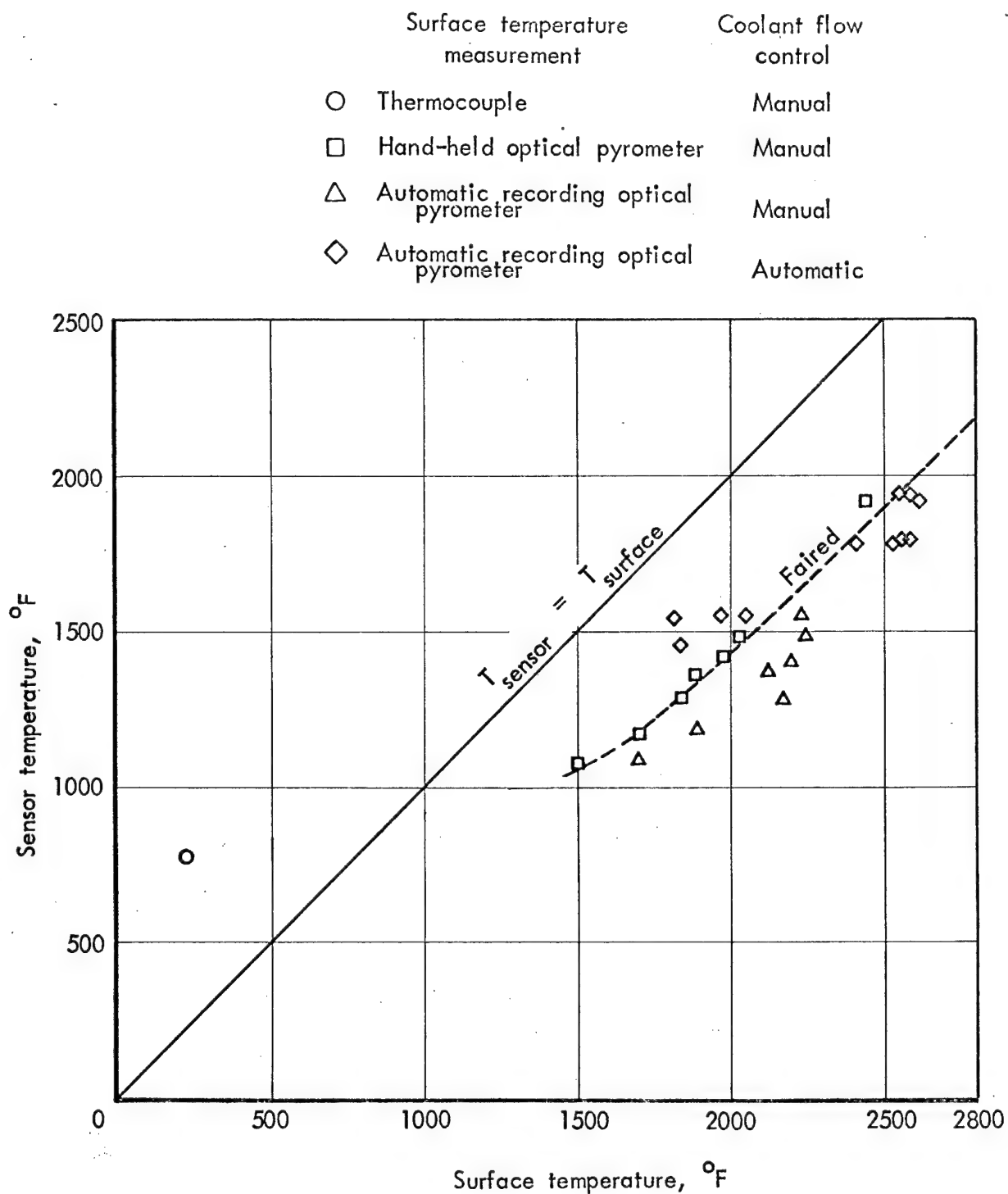


Figure 65.- Calibration of sensor installation II installed in a flame test unit with .020" dia. 18 x 20-mesh disilicide coated columbium screen.

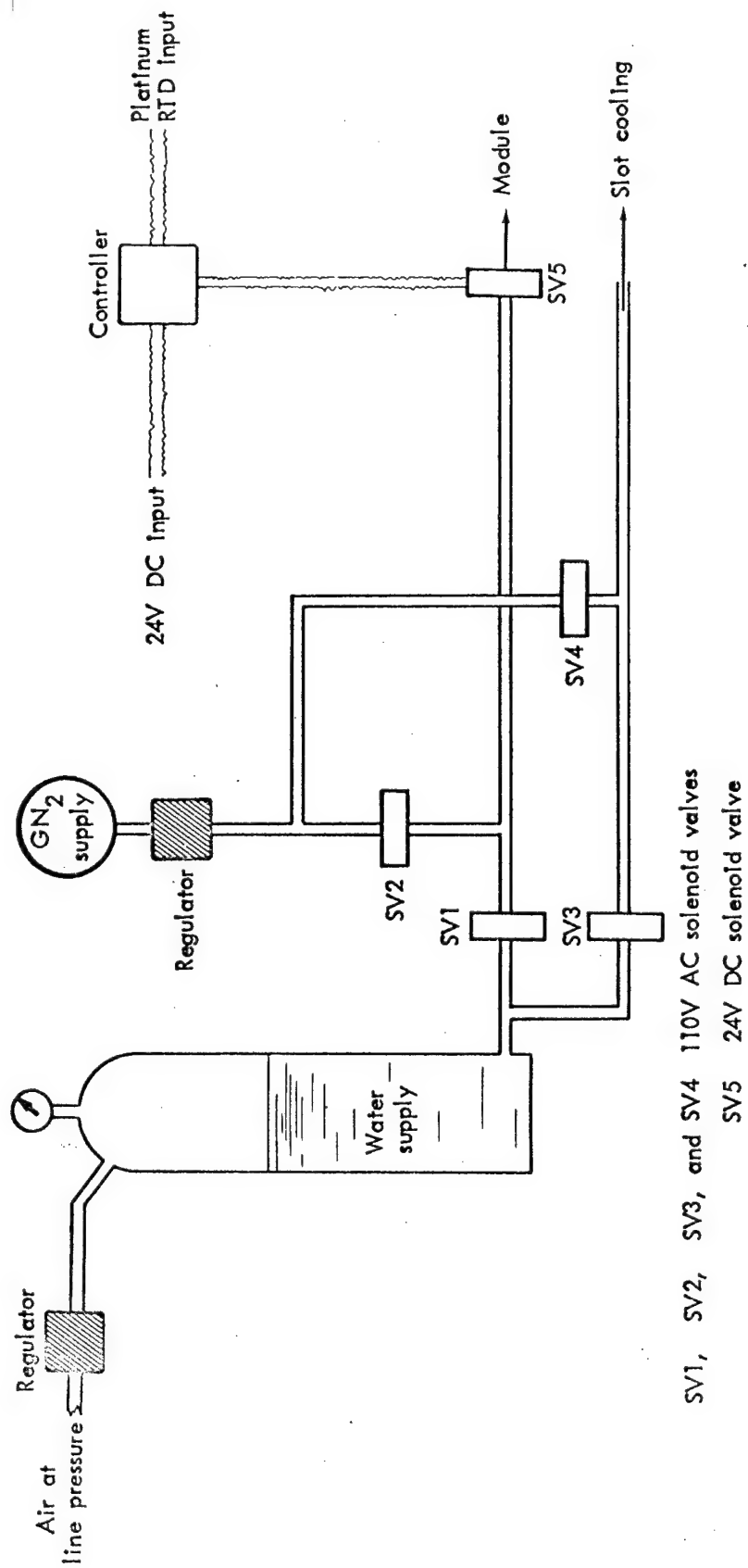


Figure 66. - GN₂ purge system.

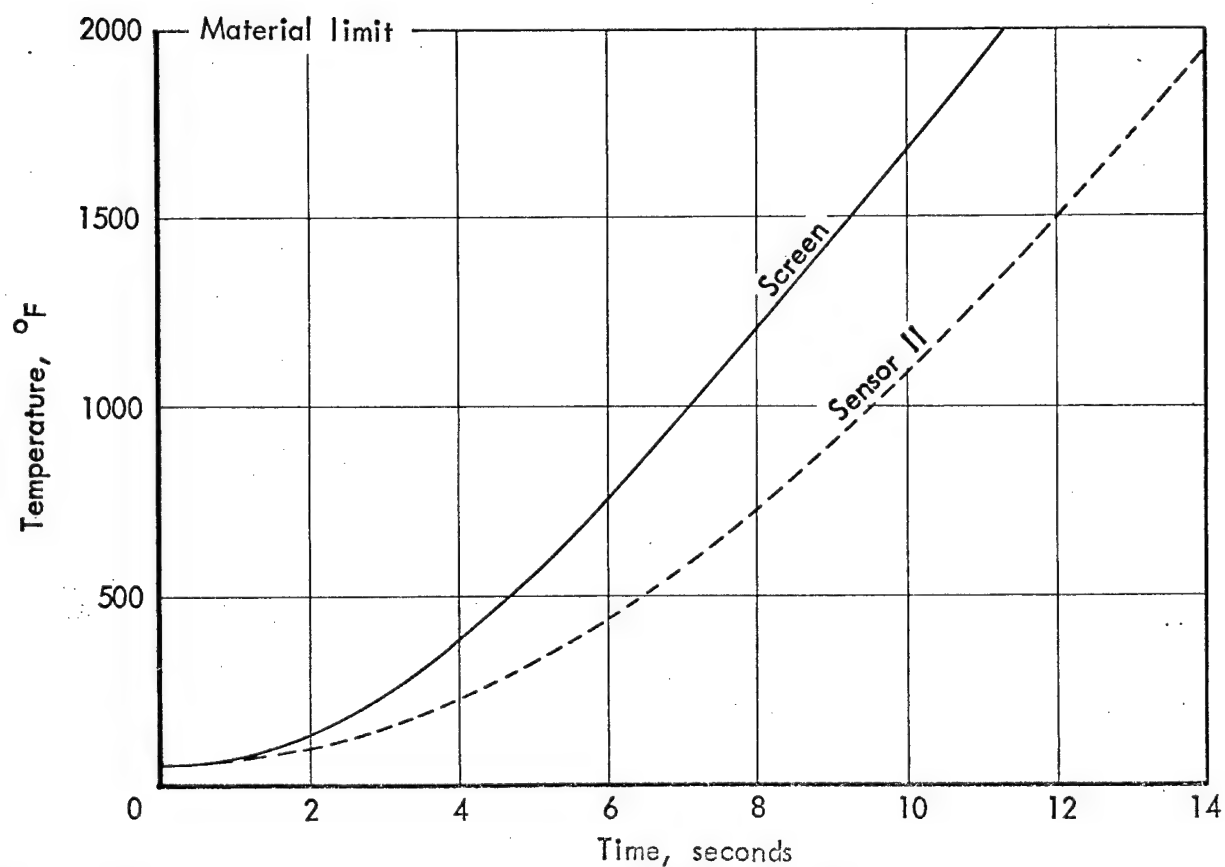
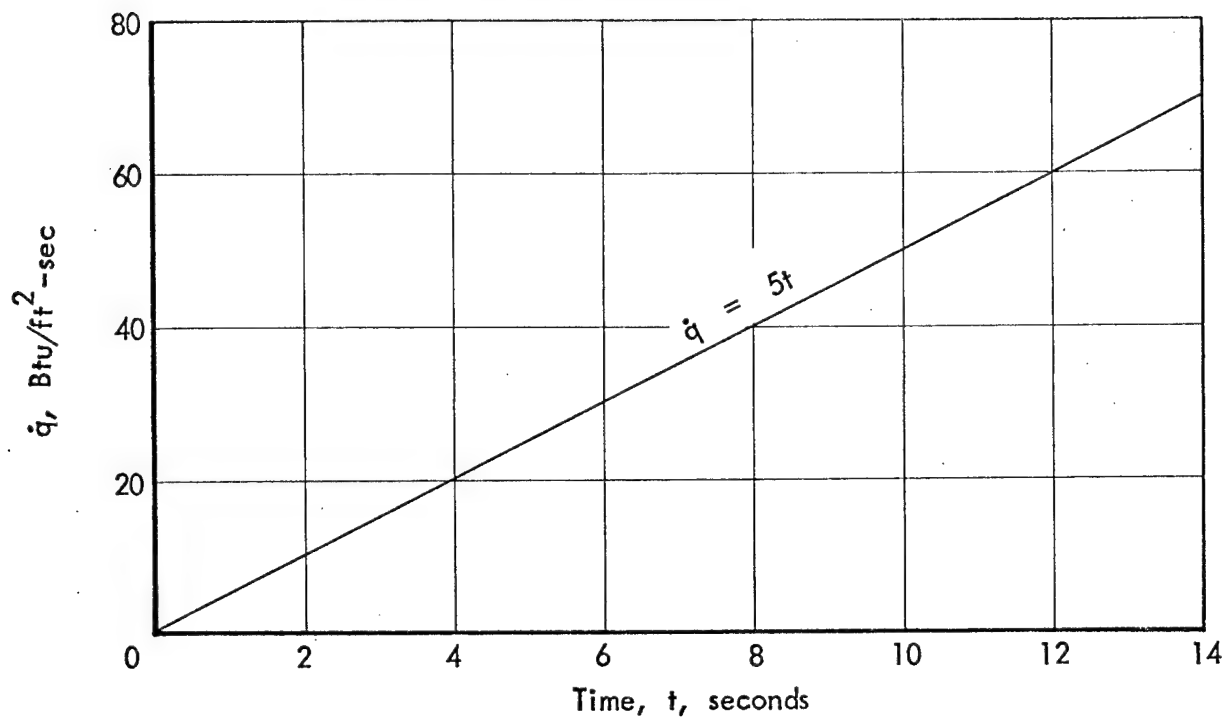


Figure 67.- Temperature history of .025" dia. 20-mesh Inconel screen and platinum resistance thermometer to a linear heating distribution.

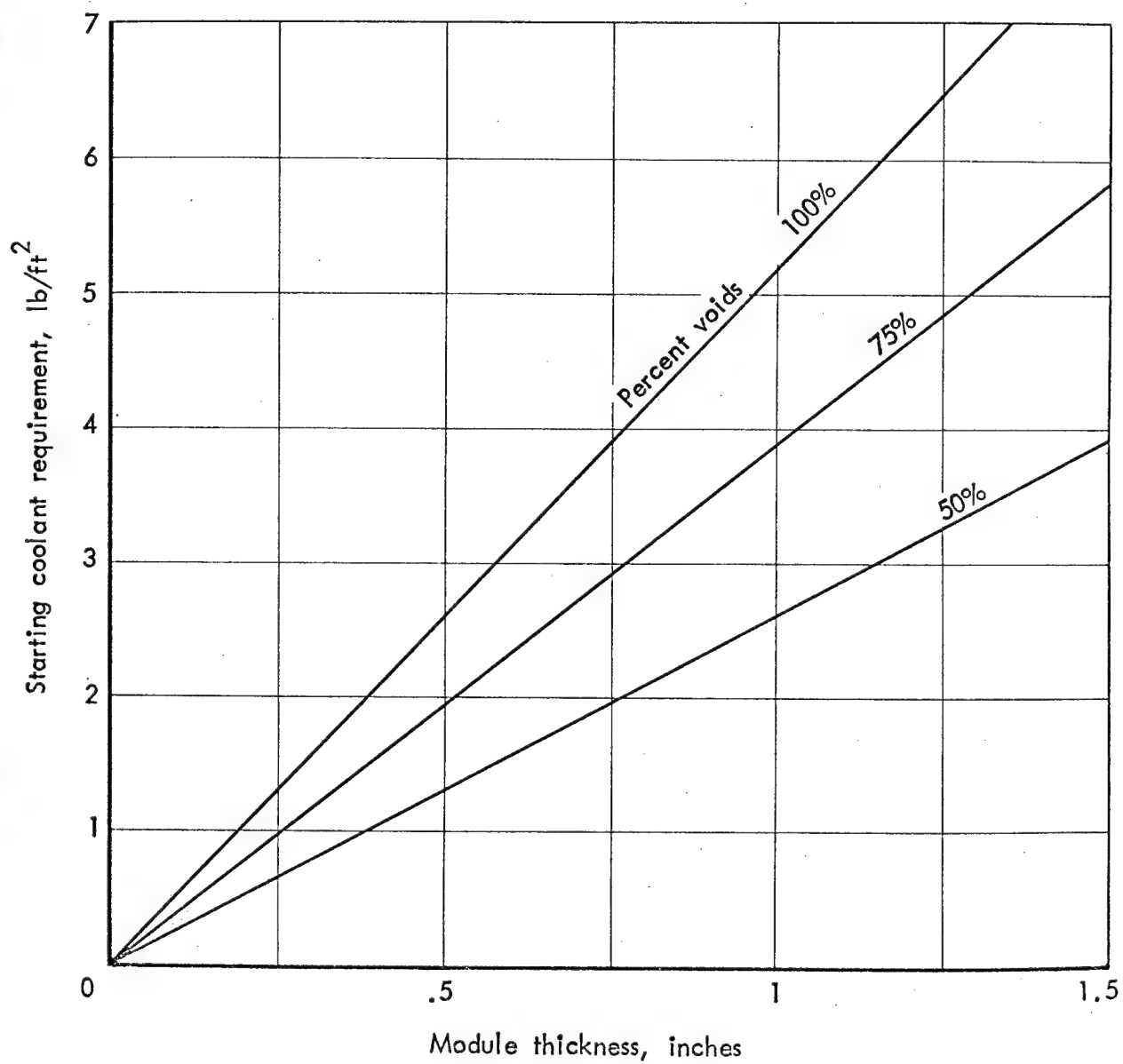
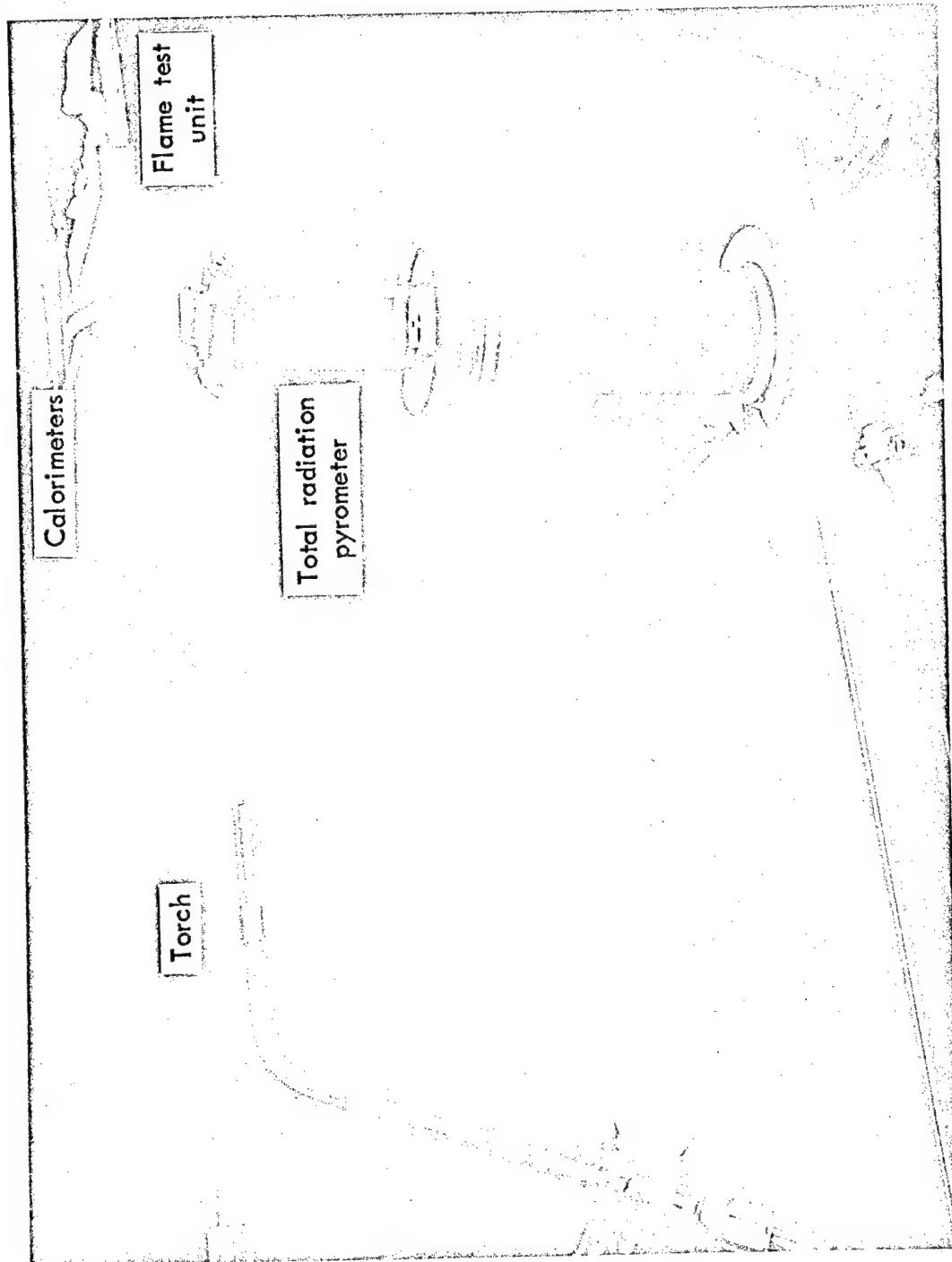
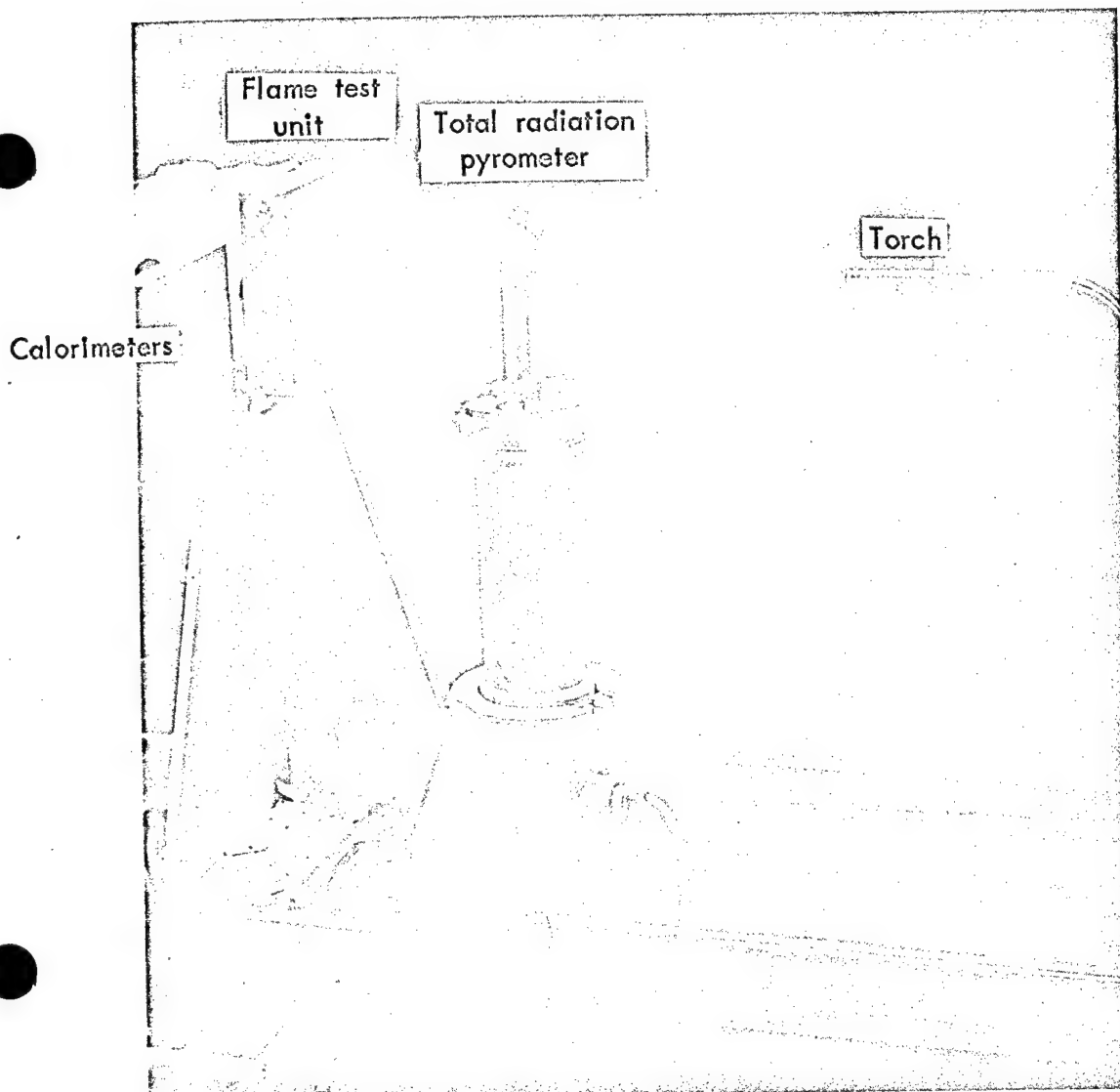


Figure 68.- The amount of coolant required to fully wet the dry module matrix.



a) Front view

Figure 69. - Flame test facility.



b) Back view

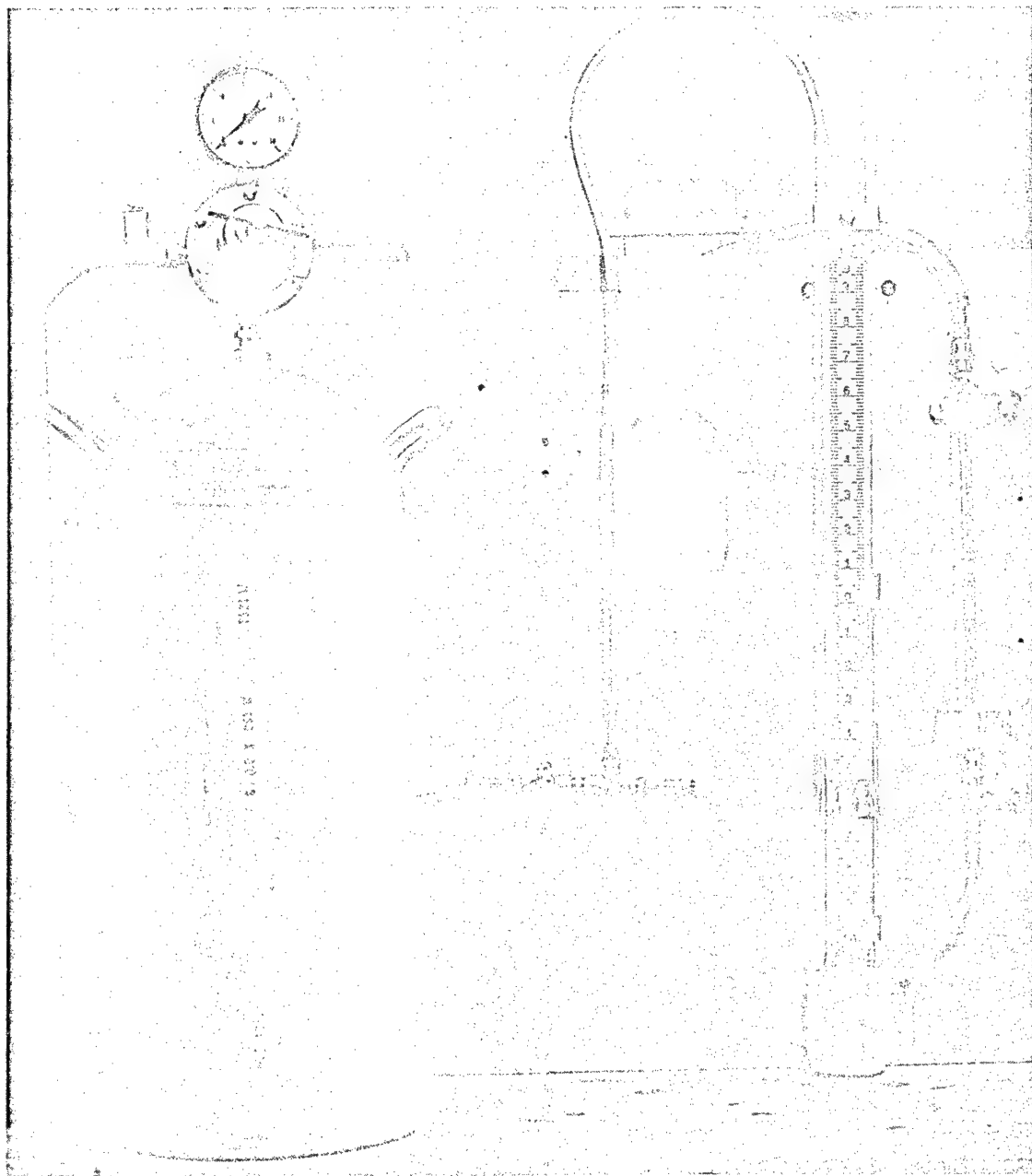


Figure 70.- Water storage tank, flowmeter, and manometer.

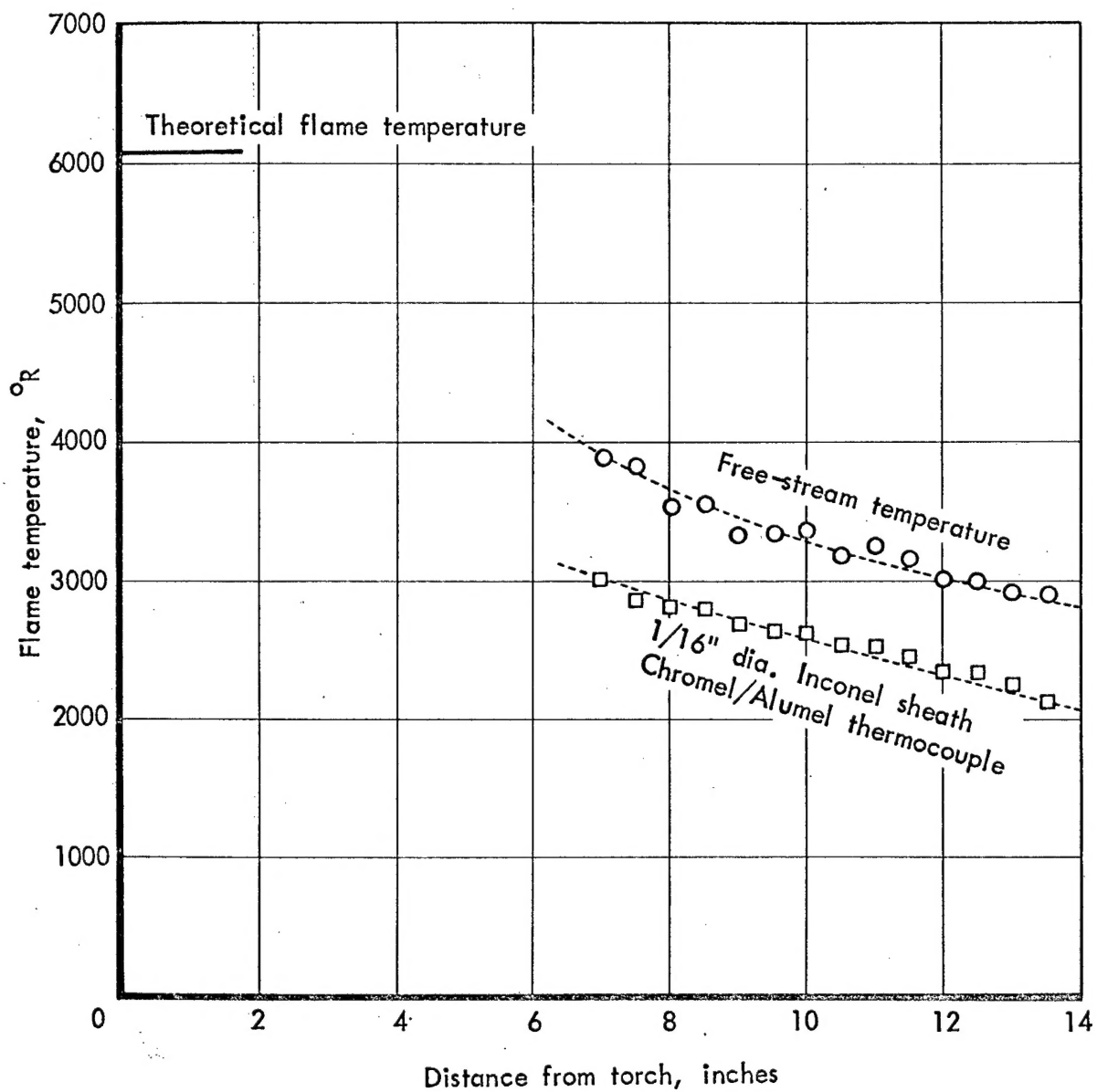


Figure 71.- Flame temperatures (#8 tip) with fixed $O_2 - C_2H_2$ flow rates.

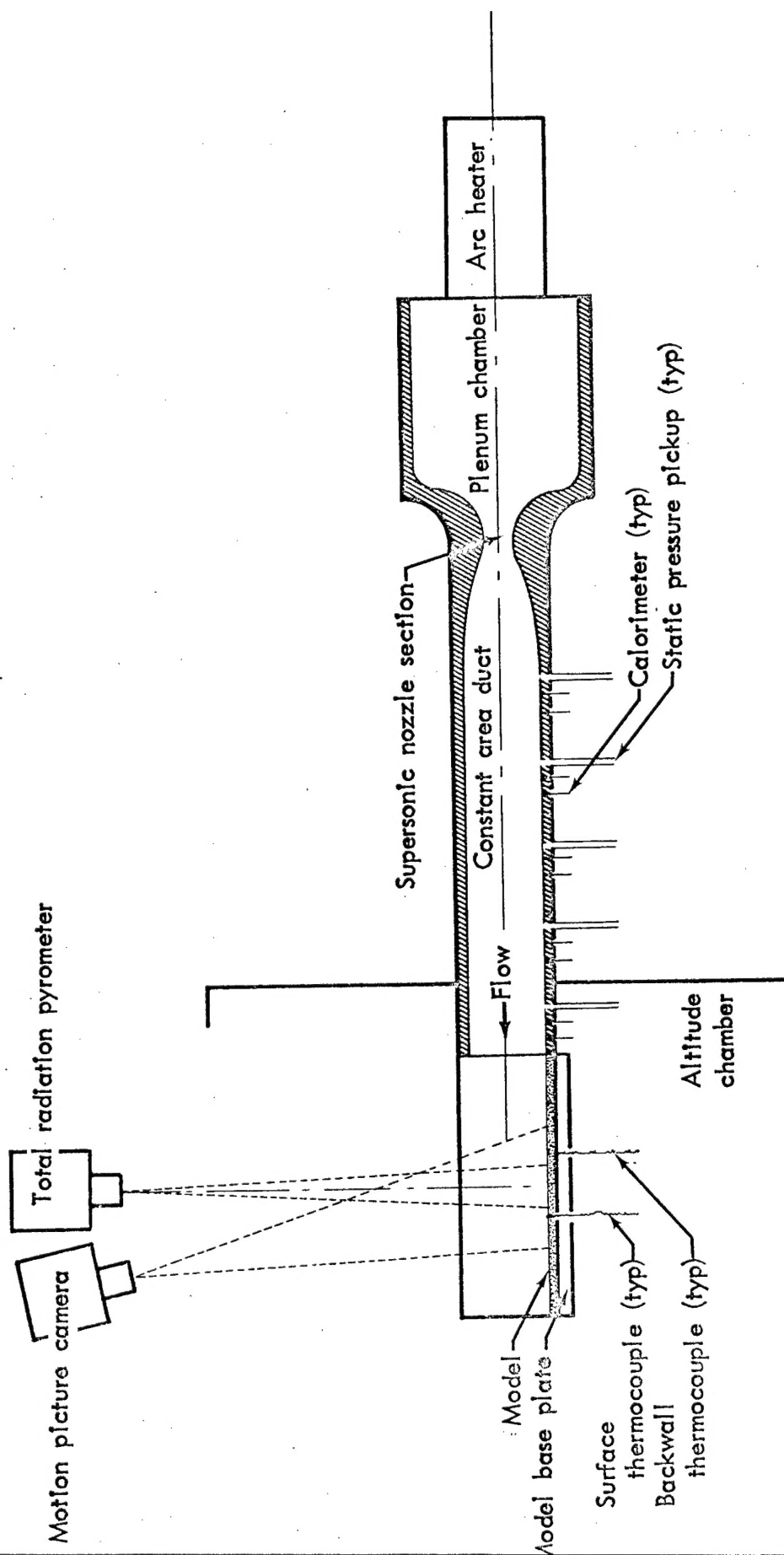


Figure 72.- Schematic of the turbulent flow duct in the Boeing arc plasma facility.

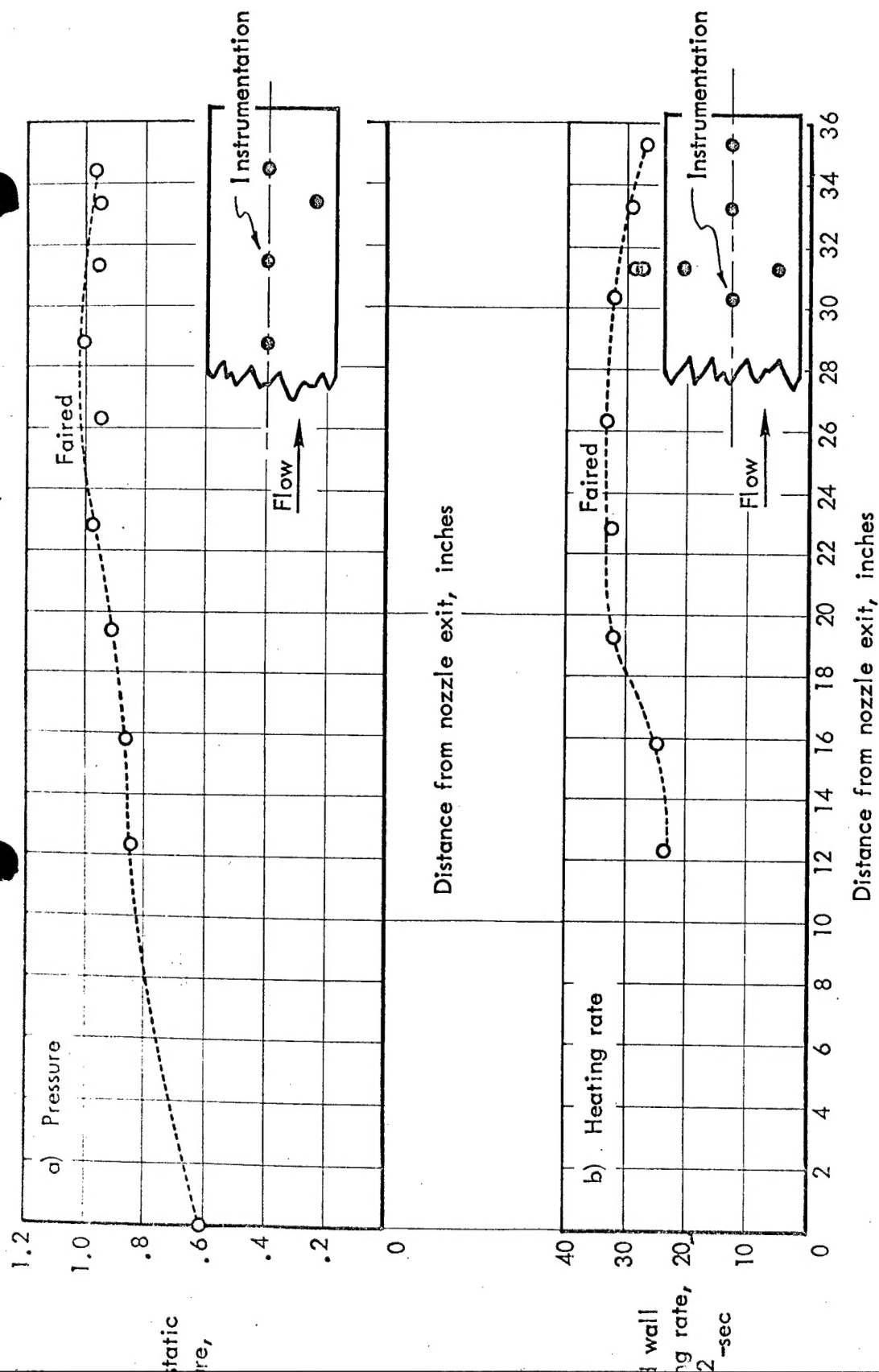


Figure 73. - Boeing plasma tunnel calibration for static pressure and heating rate.
 Atmosphere: reconstituted air; mass flow rate = 0.075 lb_m/sec; arc current = 1200 amps;
 test section total enthalpy = 2436 Btu/lb_m; and plenum chamber pressure = 9.03 psia.

REFERENCES

1. Nelson, B. E.; Johnson, H. E.; and Deriugin, V.: Transpiration Thermal Protection System Study for the M2-F2 Vehicle. Boeing Document D2-113373-1, September 1966.
2. Batiuk, W.; Goodwin, J.; Martin, D. W.; and Torgerson, R. T.: Fluidized Bed Techniques for Coating Refractory Metals. Air Force Technical Report AFML-TR-67-127, April 1967.
3. Belleman, Guy: Thermophysical Properties of Materials. Boeing Document D-16103-1, May 1961.
4. Torgerson, R. T.: Development of Columbium Alloys for Reentry Vehicle Structures. Boeing Document D2-35020, August 1962.
5. Wah Chang Bulletin: Columbium Alloys.
6. Woodruff, L. W.: Transpiration Effects on Heat Transfer. Boeing Document D2-22202, November 1962.
7. Tong, H.: Multicomponent Nonequilibrium Boundary Layer Program. Boeing Document D2-23929-1, September 1966.
8. Keenan, J. H.; and Keyes, F. G.: Thermodynamic Properties of Steam. John Wiley and Sons, 1936.
9. Evans, R. W.; and Noritake, C. S.: Development of Materials Combinations for Transpiration Cooling Systems. Boeing Document D2-20266-1, May 22, 1964.
10. McBride, B. J.; Heimel, S.; Ehlers, J. G.; and Gordon, S.: Thermodynamic Properties to 6000°K for 210 Substances Involving the First 18 Elements. NASA SP-3001, 1963.
11. Skinner Electric Company General Catalog V66.
12. Rosemount Engineering Co. Bulletin 1181 Rev. A, April 1966.
13. Rosemount Engineering Co. Bulletin 9612 Rev. B, 1962.
14. Eckert, E. R. G.; and Drake, R. M.: Heat and Mass Transfer. McGraw-Hill Book Company, Inc., 1959.
15. Gebhart, B.: Heat Transfer. McGraw-Hill Book Company, Inc., 1961.
16. Gaudette, R. S.; del Casal, E. P.; and Crowder, P. A.: Charring Ablation Performance in Turbulent Flow. Volume I - "Analytical and Experimental Studies". Boeing Document D2-114031-1, September 1967.